

**Adenylatcyclasen Rv2435c und Rv2212c aus
*Mycobacterium tuberculosis***

***Mycobacterium tuberculosis* adenylyl cyclases
Rv2435c and Rv2212c**

Dissertation

der Fakultät für Chemie und Pharmazie
der Eberhard-Karls-Universität Tübingen

zur Erlangung des Grades eines Doktors
der Naturwissenschaften

2006

vorgelegt von

Amira Abdel Motaal

Tag der mündlichen Prüfung:
Dekan:
Erster Berichterstatter:
Zweiter Berichterstatter:

11. Januar 2006
Prof. Dr. S. Laufer
Prof. Dr. J. E. Schultz
PD Dr. J. Linder

Der experimentelle Teil der vorliegenden Arbeit wurde zwischen Oktober 2002 und Juli 2005 am Institut für Pharmazeutische Chemie der Universität Tübingen unter der Leitung von Herrn Prof. Dr. J. E. Schultz angefertigt.

Herrn Prof. Dr. J. E. Schultz danke ich für das interessante Thema, Unterstützung, die allzeit offene Tür und dafür, dass er ein wirklich guter Doktorvater war.

Herrn PD Dr. J. Linder danke ich für die Übernahme des Zweitgutachten und die kompetente Rate, Hilfe und Diskussionen.

Herrn Prof. Dr. S. Laufer and Herrn Prof. Dr. P. Ruth danke ich für die Abnahme der Promotionsprüfung.

Der Deutscher Akademischer Austausch Dienst (DAAD) danke ich für die Unterstützung im Rahmen des Channel-Programms.

Ein besonderes Dankeschön geht an Frau Anita Schultz und Frau Ursula Kurz für die Hilfe mit der Klonierungsarbeit. Einen besonderen Dank hierzu möchte ich auch Frau Gertrud Kleefeld sagen.

Allen Mitgliedern der Arbeitsgruppe möchte ich für die gute Arbeitsatmosphäre und fachliche Hilfsbereitschaft Dank sagen aber vor allem danke ich diejenigen die mich emotionell unterstützt haben.

Contents

1	Introduction.....	1
1.1	Adenylyl cyclases.....	1
1.2	Class III adenylyl cyclases.....	2
1.3	Mycobacterium tuberculosis adenylyl cyclases.....	3
1.4	Aim of work.....	6
2	Materials.....	7
2.1	Chemicals and materials.....	7
2.2	Equipment.....	8
2.3	Buffers and solutions.....	9
2.4	Oligonucleotides.....	14
2.5	Plasmids.....	17
3	Methods.....	18
3.1	Methods of gene technology.....	18
3.1.1	Basic methods for analysis, processing and recombination of DNA.....	18
3.1.1.1	Extraction of DNA fragments from agarose-gels and buffer exchange of the DNA samples.....	18
3.1.1.2	Plasmid isolation from E.coli.....	18
3.1.1.3	Restriction of DNA molecules.....	18
3.1.1.4	DNA separation by agarose-gel electrophoresis.....	18
3.1.1.5	Blunting of DNA overhangs.....	19
3.1.1.6	5'-Phosphorylation of PCR products.....	19
3.1.1.7	5'-Dephosphorylation of linear plasmids.....	19
3.1.1.8	Ligation of DNA molecules.....	19
3.1.1.9	Polymerase chain reaction (PCR).....	19
3.1.1.10	DNA-sequencing.....	20
3.1.2	Transformation of recombinant DNA.....	21
3.1.2.1	Preparing competent E.coli bacterial cells for transformation.....	21
3.1.2.2	Standard transformation into E.coli cells.....	21
3.1.2.3	Preparation of bacterial stock cultures.....	22

Contents

3.2	Protein expression in E.coli.....	22
3.2.1	Pre-culture.....	22
3.2.2	Expression.....	22
3.2.3	Protein purification from E.coli BL 21 (DE3) [pREP4].....	22
3.3	Protein chemistry methods.....	23
3.3.1	Biorad protein determination (Bradford, 1976).....	23
3.3.2	Protein dialysis.....	23
3.3.3	Protein concentration and buffer exchange.....	24
3.3.4	Protein detection.....	24
3.3.4.1	SDS-PAGE.....	24
3.3.4.2	Western Blot.....	25
3.3.4.3	Dot Blot.....	26
3.3.5	Size-exclusion Chromatography (Gel filtration).....	26
3.3.6	Cyclase enzyme tests.....	27
3.3.6.1	Adenylyl cyclase test.....	27
3.3.6.2	Guanylyl cyclase test.....	28
3.3.7	Crystallization.....	28
3.4	Cloning	29
3.4.1	M. tuberculosis Rv2435c.....	29
3.4.1.1	Catalytic domain of Rv2435c.....	29
3.4.1.2	Holoenzyme of Rv2435c.....	30
3.4.2	M. tuberculosis Rv2212c.....	35
3.4.2.1	N-terminal domain (Rv2212c ₁₋₂₀₂).....	35
3.4.2.2	C-terminally His-tagged constructs of Rv2212c.....	37
3.4.2.3	C-terminally shortened Rv2212c ₂₁₂₋₃₈₈ N-His.....	37
3.4.2.4	Mutants of Rv2212c ₂₁₂₋₃₇₀	39
3.4.2.5	Shortening of Rv2212c ₂₁₂₋₃₇₀ at the N-terminus.....	39
4	Results.....	41
4.1	Expression and characterization of the adenylyl cyclase Rv2435c of M. tuberculosis.....	41
4.1.1	Sequence analysis of Rv2435c.....	41

4.1.2	Expression and characterization of adenylyl cyclase	
	Rv2435c ₅₁₁₋₇₃₀	44
4.1.2.1	Expression and purification.....	44
4.1.2.2	Adenylyl cyclase activity.....	44
4.1.2.3	Guanylyl cyclase activity.....	45
4.1.3	Expression and characterization of the adenylyl cyclase Rv2435c	
	holoenzymes.....	45
4.1.3.1	Expression of Rv2435c ₁₋₇₃₀	45
4.1.3.2	Expression of Rv2435c ₂₅₋₇₃₀ and Rv2435c ₄₁₋₇₃₀	46
4.1.3.3	Adenylyl cyclase activity.....	46
4.2	Expression and characterization of adenylyl cyclase Rv2212c of	
	<i>M. tuberculosis</i>	47
4.2.1	Sequence analysis of Rv2212c.....	47
4.2.2	Expression and characterization of adenylyl cyclase Rv2212c	
	N-terminal domain	50
4.2.2.1	Expression and purification.....	50
4.2.2.2	Crystallization of Rv2212c ₁₋₂₀₂	50
4.2.3	Expression and characterization of adenylyl cyclase Rv2212c	
	catalytic domain	52
4.2.3.1	Expression and purification.....	52
4.2.3.2	Protein dependence.....	53
4.2.3.3	Enzyme kinetics.....	54
4.2.3.4	Time dependence.....	55
4.2.3.5	pH dependence.....	55
4.2.3.6	Effect of phospholipids.....	56
4.2.3.7	Effect of fatty acids.....	56
4.2.3.8	pH dependence of linoleic acid effect	60
4.2.3.9	Effect of linoleic acid on the time dependence.....	60
4.2.3.10	Effect of detergents.....	61
4.2.3.11	Crystallization.....	63

Contents

4.2.4	Expression and characterization of C-terminally shortened constructs of Rv2212c ₂₁₂₋₃₈₈ (with N-terminal His-tag).....	63
4.2.4.1	Expression and purification.....	63
4.2.4.2	Enzyme kinetics.....	65
4.2.4.3	Crystallization of Rv2212c ₂₁₂₋₃₇₇ , Rv2212c ₂₁₂₋₃₇₄ and Rv2212c ₂₁₂₋₃₇₀	68
4.2.5	Expression and characterization of Rv2212c mutants L370V, L370A and L370G.....	68
4.2.5.1	Expression and purification.....	68
4.2.5.2	Adenylyl cyclase activity.....	69
4.2.6	Expression and characterization of N-terminally shortened constructs of Rv2212c ₂₁₂₋₃₇₀	69
4.2.6.1	Expression and purification.....	70
4.2.6.2	Enzyme kinetics.....	71
4.2.6.3	Protein dependence of Rv2212c ₂₁₃₋₃₇₀ and Rv2212c ₂₁₅₋₃₇₀	73
4.2.6.4	Gel filtration of Rv2212c ₂₁₃₋₃₇₀	74
4.2.6.5	Crystallization of Rv2212c ₂₁₃₋₃₇₀	76
4.2.7	Expression and characterization of adenylyl cyclase Rv2212c Holoenzyme.....	76
4.2.7.1	Expression and purification.....	76
4.2.7.2	Protein dependence.....	77
4.2.7.3	Time dependence.....	78
4.2.7.4	pH dependence.....	78
4.2.7.5	Effect of chemical compounds on AC activity.....	79
4.2.7.5.1	Effect of sugars.....	80
4.2.7.5.2	Effect of amino acids.....	81
4.2.7.5.3	Effect of salts and other miscellaneous compounds.....	81
4.2.7.5.4	Effect of phospholipids.....	82
4.2.7.5.5	Effect of fatty acids.....	83
4.2.7.5.6	pH dependence of fatty acids effect.....	87
4.2.7.5.7	Effect of linoleic acid on the time dependence.....	90
4.2.7.5.8	Effect of detergents.....	90
4.2.7.5.9	pH dependence of polidocanol effect.....	94
4.2.7.5.10	Effect of polidocanol on the time dependence.....	95

4.2.7.6	Crystallization of Rv2212c ₁₋₃₈₈	95
4.2.8	Expression and characterization of C-terminally His-tagged constructs of adenylyl cyclase Rv2212c	96
4.2.8.1	Expression and purification of Rv2212c ₁₋₂₀₂ C-His, Rv2212c ₂₁₂₋₃₈₈ C-His and Rv2212c ₁₋₃₈₈ C-His.....	96
4.2.8.2	Adenylyl cyclase activity.....	97
5	Discussion.....	98
5.1	Mycobacterial Rv2435c.....	98
5.2	Characterization of Rv2435c ₅₁₁₋₇₃₀	98
5.3	Characterization of Rv2435c holoenzyme.....	99
5.4	Mycobacterial Rv2212c.....	100
5.5	Rv2212c ₁₋₂₀₂	102
5.6	Rv2212c ₂₁₂₋₃₈₈	102
5.7	Rv2212c ₁₋₃₈₈	103
5.8	The effect of chemicals on Rv2212c activity.....	104
5.9	Outlook.....	107
6	Summary.....	108
7	Zusammenfassung.....	109
8	Appendix.....	110
8.1	DNA and protein sequences of Rv2435c.....	110
8.2	DNA and protein sequences of Rv2212c.....	113
8.3	Sequence alignment of Rv2435c with <i>Desulfovibrio vulgaris</i>	115
8.4	Fatty acids and detergents tested with Rv2212c.....	116
9	References.....	117

List of abbreviations

AA/Bis	Acrylamide/Bisacrylamide 37.5:1
ACs	Adenylyl cyclases
BSA	Bovine serum albumine
CHAPS	3-(3-Cholamidopropyl)-dimethylammonio-1-propane sulfonate
CS	Crystal Screen
C-His	C-terminal His-tag
CHD	Cyclase homology domain
dNTPs	Desoxynucleotide triphosphates
FA	Fatty acid
FAs	Fatty acids
IPTG	Isopropyl- β -D-thiogalactoside
Ni ²⁺ -NTA	Nickel-nitrilotriacetic acid-agarose
NAD	Nicotine amide dinucleotide
N-His	N-terminal His-tag
N-TD	N-terminal domain
PEG	Polyethylene glycol
RT	Room temperature
TEMED	N, N, N', N'- Tetramethylethylene diamine
X-Gal	5-bromo-4-chloro-3-indoyl- β -D-galactoside

1 Introduction

1.1 Adenylyl cyclases

Cyclic AMP (cAMP) is an important signalling molecule that controls a wide variety of cellular functions in many organisms, including virulence factors from a diverse range of pathogens (Botsford and Harman, 1992; D'Souza and Heitman, 2001; Gross *et al.*, 2003; Petersen and Young, 2002; Smith *et al.*, 2004; Wolfgang *et al.*, 2003). It is produced in cells by adenylyl cyclases (Peterkofsky *et al.*, 1993). This makes the modulation of AC activity the key step in regulating intracellular cAMP. ACs are subject to regulation by both extracellular and intracellular stimuli (Tang and Hurley, 1998). However the regulation and mechanism of action of cyclases can only be sufficiently understood by knowing the three-dimensional structure of the protein, which could be fulfilled through crystallization.

Currently the catalytic domains of ACs are grouped into five classes based on sequence similarity (Barzu and Danchin, 1994; Cotta *et al.*, 1998; Sismeiro *et al.*, 1998).

Class I ACs are present in many Gram-negative bacteria, best represented by the *Escherichia coli* AC. The amino-terminal moiety is responsible for catalytic activity, whereas the carboxy-terminal end confers glucose-mediated inhibition of activity. cAMP levels mirror the external presence and uptake of glucose, which is sensed through the phosphotransfer relay system (Barzu and Danchin, 1994).

Class II ACs are present in two taxonomically unrelated pathogens, *Bordetella pertussis* and *Bacillus anthracis*. These extracellularly released ACs serve as toxins. Upon entry into the host mammalian cells, they become activated by the mammalian calmodulin causing unregulated synthesis of cAMP and impairment of cellular functions. Whether class II ACs also have an intracellular function in those pathogens is unknown (Barzu and Danchin, 1994; Linder and Schultz, 2003).

Class III ACs include cyclases from eukaryotes as well as prokaryotes. Accordingly, intracellular physiological roles of cAMP seem to vary greatly among different organisms. Most mammalian ACs are monomeric integral membrane proteins which are catalytically active as pseudoheterodimers (Sunahara *et al.*, 1996; Taussig and Zimmermann, 1998), while prokaryotes and lower eukaryotes produce both soluble and membrane-bound nucleotidyl cyclases of variant domain compositions functioning as homodimers (Guo *et al.*, 2001; Linder

et al., 2002; Linder and Schultz, 2003). In eukaryotes, cAMP levels are modulated mostly in response to extracellular hormones via G-protein-coupled receptors (GPCR). Increase in cAMP usually then leads to activation of protein kinase A as the predominant cAMP-receptor. Therefore, cellular processes such as metabolism, secretion and proliferation are controlled via cAMP. On the other hand, GPCR-G-protein pathways are conspicuously absent in prokaryotes. Instead, the prokaryotic catalytic domain isoforms appear to be directly regulated by a variety of attached potential regulatory domains (Linder and Schultz, 2003; Sinha *et al.*, 2005).

Classes IV and V ACs are currently represented by only a single member each from *Aeromonas hydrophila* (class IV) and *Prevotella ruminicola* (class V) (Cotta *et al.*, 1998; Sismeiro *et al.*, 1998).

1.2 Class III adenylyl cyclases

The most wide spread class of cAMP-generating enzymes are the class III ACs, which are further subdivided into four subclasses IIIa-III d (Linder and Schultz, 2003). The catalytic domain of these ACs, also designated as the cyclase homology domain (CHD), is often linked to different protein domains which in many instances appear to impart peculiar regulatory features. As for example, GAF, BLUF, histidine kinase, receiver, PAS-associating and cation channel domains have been found in conjunction with the CHD of this class (Linder and Schultz, 2003). So far, all CHDs operate as dimers with mostly two catalytic centres positioned at the dimer interface, where catalysis is based on six highly conserved residues (Guo *et al.*, 2001; Sunahara *et al.*, 1998; Tesmer *et al.*, 1997). Two aspartate residues coordinate two metal cofactors (Mg^{2+} or Mn^{2+}), an asparagine and an arginine stabilize the transition-state and a lysine-aspartate couple specifies ATP as a substrate (Tesmer *et al.*, 1999; Tucker *et al.*, 1998; Yan *et al.*, 1997). However variations in all these six canonical catalytic residues do occur within the four subclasses IIIa-III d (Linder and Schultz, 2003), and the functional consequences of such changes are just beginning to be comprehended (Castro *et al.*, 2005; Sinha *et al.*, 2005).

Class IIIa ACs are pseudoheterodimeric in metazoans (Krupinski *et al.*, 1989) and homodimeric in bacteria (Guo *et al.*, 2001; Kasahara *et al.*, 2001). An (F/Y)XX(F/Y)D motif, which appears to participate in formation of the dimer interface (Tang *et al.*, 1995; Tesmer *et al.*, 1997), and an EK**IK** motif, containing the substrate defining lysine (bold), are two

signature motifs of this class. Besides, the arm region of class IIIa CHDs, thought to be an essential feature for dimerization, is conserved to 14 residues in length (Linder and Schultz, 2003).

Class IIIb ACs exist in both gram-negative and gram-positive bacteria as well as in mammals. A characteristic feature of this class is the replacement of the substrate-defining aspartate by a threonine or serine (Kanacher *et al.*, 2002), and a phosphate-binding arginine is frequently replaced by either a glycine or a serine. Here the arm region mentioned above consists of 15 residues (Linder and Schultz, 2003).

Class IIIc ACs are most frequently encountered in gram-positive bacteria but also in some gram-negative ones. In this class the arm region is shortened to only 7-11 residues. Also this class shows striking substitutions in the six canonical catalytic residues which calls for a plasticity of the catalytic mechanism within this subfamily (Linder and Schultz, 2003).

Class IIId ACs are present in protozoans, trypanosomatids and fungi. A VEVKT motif surrounding the substrate-defining lysine appears to be a prominent signature motif. The arm region is mostly 14 residues in length (Linder and Schultz, 2003).

1.3 Mycobacterium tuberculosis adenylyl cyclases

M. tuberculosis, the etiologic agent of tuberculosis, is a leading cause of death of approximately 2 million people each year. Nearly one-third of the world's population is latently infected with the *M. tuberculosis* bacillus, and 7 to 8 million new TB cases occur annually (Raviglione, 2003). So getting to know more about *M. tuberculosis* biochemistry, biology and gene regulation allows for a better understanding of the interaction of the tubercle bacillus with its environment, thus devising more effective treatments against TB.

Little is known about the role of cAMP in mycobacteria, although it is found in both pathogenic and non-pathogenic species (Padh and Venkitasubramanian, 1976 and 1977). A correlation between intracellular cAMP levels and phospholipid synthesis in *Mycobacterium smegmatis* has been reported (Kaur and Khuller, 1995). Elevated cAMP levels were correlated with reduced phagolysosome fusion during mycobacterial infection of macrophages (Lowrie *et al.*, 1979). A possible role for cAMP in persistence of *M. tuberculosis* infection by regulation of the glyoxylate shunt metabolism was reported (Gazdik and McDonough, 2005; McKinney *et al.*, 2000). Also a recent study provided the first

evidence that cAMP regulates gene expression in mycobacteria, and that this regulation occurs more often under low-oxygen, CO₂-enriched growth conditions suggesting that such conditions which the TB bacterium faces during its infection of a mammalian host, may provide a regulatory signal for the bacterium relayed by cAMP as a second messenger to effect regulation of genes that are required for its survival during intracellular growth (Gazdik and McDonough, 2005).

Pathogenesis of *M. tuberculosis* is not yet attributable to single or a few defined gene products, as is the case in *Bordetella pertussis* and *Bacillus anthrax* where AC plays a pivotal role in the onset of the disease (Reddy *et al.*, 2001; Khelef *et al.*, 1993; Gueirard *et al.*, 1998). For instance, a mycobacterial knockout strain illustrated that the AC Rv1625c alone is not a virulence factor in mice (Guo *et al.*, 2005). A recent study identified 15 putative cyclases in the *M. tuberculosis* genome using Bayesian computational methods, showing that both the number and diversity of functional ACs in this bacteria are extraordinary compared to other microorganisms (Linder *et al.*, 2004; McCue *et al.*, 2000). Therefore it is likely that each cyclase is associated with a distinct signalling pathway. It is expected that specific cyclases are activated to produce cAMP in response to different physiological conditions as for example hypoxia, intramacrophage environment (Gazdik and McDonough, 2005) or pH changes (Tews *et al.*, 2005). The selective availability of cAMP-binding effector molecules for each environmental condition would allow for different outcomes, especially in view of that *M. tuberculosis* encodes 10 putative cNMP-binding proteins with diverse functions that could fulfill this role (Gazdik and McDonough, 2005; McCue *et al.*, 2000).

Two of the *M. tuberculosis* 15 predicted ACs belong to class IIIa, four to class IIIb and nine to class IIIc. One predicted class IIIa and six predicted class IIIc cyclase genes possess variations at canonical positions of the catalytic centre, while the four IIIb cyclases contain the threonine variant mentioned above (Linder and Schultz, 2003). To date almost all mycobacterial ACs have been investigated [class IIIa: Rv1625c; class IIIb: Rv1318c, Rv1319c, Rv1320c, Rv3645; class IIIc: Rv1647, Rv1264, Rv1900c, Rv0386 (Castro *et al.*, 2005; Guo *et al.*, 2001; Linder *et al.*, 2002 and 2004; Reddy *et al.*, 2001; Shenoy *et al.*, 2005; Sinha *et al.*, 2005; Tews *et al.*, 2005)]. Rv2435c (class IIIa) and Rv2212c (class IIIc) are both investigated in this work.

Mycobacterial CHDs, being class III domains, are fused to different domains which appear to be regulators of the AC function (see section 1.2 above). These include membrane anchors, a

pH-sensing domain, AAA-ATPase domains, helix-turn-helix DNA-binding domains, an α/β -hydrolase domain and HAMP-domains (Linder *et al.*, 2004; Tews *et al.*, 2005). Despite the thorough investigations carried out in the past few years, still a lot is left to be known about these regulatory domains.

In Rv1625c, the membrane anchor consisting of six transmembrane spans has a prominent role in protein dimerization thus remarkably increasing its affinity towards the substrate ATP (Guo *et al.*, 2005).

The N-terminal domain of Rv1264 is a pH sensor. So Rv1264 is probably required by the *M. tuberculosis* to counteract acidification of phagolysosomes during host invasion for intracellular survival (Pethe *et al.*, 2004; Sturgill-Koszycki *et al.*, 1994; Tews *et al.*, 2005).

Rv1900c and Rv0386 are examples of unconventional cyclase genes of *M. tuberculosis*, possessing deviations in the six canonical residues, and displaying variations in substrate specificity and catalytic mechanism. The presence of a sequence similarity between the N-terminal domain of Rv1900c and α/β -hydrolases suggested that Rv1900c might possess lipase activity and hence was named 'lipJ' (Cole *et al.*, 1998), although consensus residues that confer esterase activity are absent (Shenoy *et al.*, 2004a). Whether regulation of the CHD activity is exerted by this uncharacterized N-terminal α/β -hydrolase domain in response to signals from unidentified ligands or protein partners, is still an open question (Sinha *et al.*, 2005).

Rv0386 cyclase homology domain is fused to an AAA-ATPase/NB-ARC domain, which is similar to the respective domains of several bacterial transcriptional regulators, and a helix-turn-helix DNA-binding domain suggesting that in Rv0386 an AC may be functionally linked with a transcriptional regulator (Castro *et al.*, 2005).

In mycobacterial class IIIb ACs, the HAMP domains appear to act directly as modulators of AC activity but without displaying a uniform regulatory input, instead each formed a distinct signalling unit with its adjoining CHD (Linder *et al.*, 2004).

1.4 Aim of work

Rv2435c is of particular interest because of its deviation in four of the six canonical residues participating in catalysis, and because of the presence of an N-terminal extracellular domain of unknown function. So the cloning and biochemical characterization of the so called class IIIa AC Rv2435c from *M. tuberculosis* is one of the aims of this work.

On the other hand, Rv2212c is similar to Rv1264 in having a catalytic AC domain, conserved in canonical residues, and a regulatory N-terminal domain. To understand AC regulation, 3D structures of the enzyme should be determined using X-ray crystallography. A comparison of the structures will show why these proteins have different regulatory functions, despite their conservation and common domain structure. This might give new clues to class III AC regulation.

2 Materials

2.1 Chemicals and materials

Amersham Pharmacia Biotech, Freiburg: ECL Plus Western Blot Detection System, Hyperfilm ECL, Thermo Sequenase Fluorescent Labelled Primer Cycle Sequencing Kit with 7-deaza-dGTP, Formamide, [2,8-³H]-cAMP and [8-³H]-cGMP

AppliChem, Darmstadt: HEPES, Acrylamide 4K-Solution, 30%

Appligene, Heidelberg: Taq DNA-Polymerase with 10x reaction buffer

BIO-RAD, München: Protein-Assay Dye Reagent

Biozym Diagnostik, Hess. Oldendorf: Sequagel XR, Sequagel Complete Buffer Reagent, Chill-Out 14 Liquid Wax from MJ Research

Canberra Packard, Taunusstein: Ultima Gold XR Scintillator

Dianova, Hamburg: Goat anti-mouse IgG-F_c horseradish peroxidase conjugated antibodies, goat anti-rabbit IgG-F_c horseradish peroxidase conjugated antibodies

Emerald BioStructures, Bainbridge Island, Washington (USA): Wizard I & II reagent kits for protein crystallization

Fluka, Basel: Sodiumdodecylsulfate, PEG, Nonidet P40

Hampton Research, Laguna Niguel (USA): Crystal Screen, Crystal Screen 2 and Crystal Screen Lite reagent kits for protein crystallization screening

Hartmann Analytik, Braunschweig: [α -³²P]-ATP and [α -³²P]-GTP

ICN Biomedicals, Eschwege: [α -³²P]-ATP

Macherey-Nagel, Düren: Nucleotrap Kit, Porablot PDVF-blotting membrane

Merck, Darmstadt: Glycerol 87%, ethanol, methanol, 2-mercaptoethanol, DMSO, imidazole, sodium chloride, amino acids, glyoxylic acid, linolenic acid, palmitic acid, stearic acid

MWG-Biotech, Ebersberg: Oligonucleotides

New England Biolabs, Schwalbach/Taunus: Restriction endonucleases, BSA for molecular biology, T4-Polynucleotide Kinase and 10x Kinase Buffer

Pall Corporation, Michigan (USA): Nanosep 10K OMEGA centrifugal devices

Peqlab, Erlangen: Agarose, peqGOLD Protein Marker

Promega, Madison (USA): Wizard Plus SV Plasmid Purification Kit (Minipreps)

Qiagen, Hilden: Ni²⁺-NTA Agarose, pQE-expression vectors, purified mouse

monoclonal RGS-His₄ antibody, Penta-His antibody, Tetra-His antibody

Roche (Boehringer), Mannheim: Restriction endonucleases, Klenow-Polymerase, Alkaline phosphatase, Rapid DNA Ligation Kit, dNTPs, Creatine kinase, Creatine phosphate

Roth, Karlsruhe: Glycin, ampicillin, kanamycin

Sartorius, Göttingen: Cellulose acetate filter (0.2 µm), polycarbonate filter holder

Schleicher & Schuell, Dassel: Whatmanpaper 3 MM, Protran BA 83 cellulosenitrate 0.2µm (200 x 200 mm) nucleic acid and protein transfer media

Serva, Heidelberg: Coomassie-Brilliant-Blue G250, visking dialysis tubing 8/32 (Ø 6 mm) and 27/32 (Ø 21 mm), Triton X-100

Sigma, Deisenhofen: Glycerol 99%, MOPS, TRIS, EDTA, X-Gal, IPTG, Tween 20, Ponceau S, TEMED, BSA, LB-agar powder, LB-broth powder, bromophenol blue, D-mannose, L-arabinose, L-rhamnose, D-galactose, polidocanol, oleic acid, linoleic acid, phospholipids

Stratagene, Heidelberg: pBluescript II SK(-), E.coli XL1-Blue MRF' cells

2.2 Equipment

Amersham Pharmacia Biotech, Freiburg: ÄKTA FPLC with fraction collector Frac- 950, pump P-920, monitor UPC-900, valve INV-907, mixer M-925 , software Unicorn version 4.11 , gel filtration columns Superose 12 HR 10/30 and Superdex 200

Bender & Hobein, Zurich: Vortex Genie 2TM

Biometra, Göttingen: TRIO-Thermoblock thermocycler

BIO-RAD, München: Trans-Blot SD Semi Dry Transfer Cell

Branson, Danbury, Connecticut (USA): Sonifier B-12, ultrasound bath Bransonic B12

Carl Zeiss, Göttingen: Microscope Axioskop 40/40 FL with fixed polarisator, Lambda plate, Canon Powershot G2 high quality digital camera with 4.0 M pixel, CCD sensor and 3x optical zoom

Eberhard-Karls-Universität, Tübingen: Gel electrophoresis chambers

Eppendorf, Hamburg: Table centrifuge 3200 and miniSpin, Thermostat 5320, Table centrifuges 5410 & 5414, Cooling centrifuge 5402, Biophotometer

Gilson: Pipets 1-20 µl, 10-100 µl, 100-1000 µl

Hampton Research, Laguna Niguel (USA): VDX 24 well polystyrene pre-greased plates,
22 mm siliconized glass square cover slides

Heraeus, Osterode: Megafuge 1.0 R (BS 4402/A), Biofuge A

Idaho Technologies, Idaho Falls (USA): Air Thermo Cycler 1605

Kontron-Hermle, Gosheim: Centrikon H401 & ZK401, Rotors A6.14 (SS34)
and A8.24 (GSA)

LTF Labortechnik, Wasserburg: Videoprinter Mitsubishi Video Copy Processor P91 with
Sony CCD video Camera Modul XC-ST500E, Thermopapers K65HM, Software BioCapt
Version 99.01s

Metrohm, Herisau (Switzerland): pH-Meter E 512

Millipore, Eschborn: Water purification apparatus MilliQ UF Plus

MWG-Biotech, Ebersberg: LI-COR DNA sequencer model 4000

Promega, Madison (USA): Vac-Man (vacuum for Wizard Plus SV Plasmid
Purification Kit)

Sartorius, Göttingen: Balance BP 2100 S, analytical balance Handy

Savant, Farmingdale (USA): Vacuum centrifuge speed vac concentrator SVC
100H

SLM Instruments, Urbana (USA): French Pressure Cell Press FA-078-E1

Vetter, Wiesloch: UV-Kontaktlampe Chroma 43

2.3 Buffers and solutions

MilliQ-H₂O was used, pH-values were adjusted at RT, unless indicated otherwise.

2.3.1 Molecular biology buffers and solutions

All solutions and buffers were either sterile-filtered or autoclaved for 20 min at 120°C (1 bar).

Buffers for DNA

TAE

40 mM TRIS/ acetate pH 8.0

1 mM EDTA

10x Klenow buffer

200 mM TRIS/HCl pH 7.5

60 mM MgCl₂

10 mM Dithiothreitol

Materials

TE-buffer

10 mM TRIS/ HCl pH 7.5

1 mM Na₂EDTA

10x TBE buffer

1000 mM TRIS

890 mM Boric acid

25 mM Na₂EDTA

4x Loading sample buffer (agarose gel)

0.05 % Bromophenol blue

0.05 % Xylenecyanol

50.0 % Glycerol

10x Dephosphorylation buffer

500 mM TRIS/HCl pH 8.5

1 mM Na₂EDTA

10x CM buffer

100 mM CaCl₂

100 mM MgCl₂

dNTPs

25 mM of each dNTP

Bacterial culture media

LB-broth

1 % Bacto Tryptone

0.5 % Yeast extract

1 % NaCl

LB-agar

1.5 % Agar in LB-broth

LB-ampicillin-agar plates

100 µg Ampicillin/ml LB-agar

2.3.2 Protein chemistry buffers and solutions

Protein purification with NiNTA-agarose

Pellet washing buffer

50 mM TRIS/HCl pH 8.0

1 mM EDTA

Cell lysis buffer

50 mM TRIS/HCl pH 8.0

0.02 % α-monothioglycerol

Washing buffer A

50 mM TRIS/HCl pH 8.0
0.02 % α -monothioglycerol
250 mM NaCl
15 mM Imidazole
5 mM MgCl₂

Washing buffer B

50 mM TRIS/HCl pH 8.0
0.02 % α -monothioglycerol
15 mM Imidazole
5 mM MgCl₂

Elution buffer

50 mM TRIS/HCl pH 8.0
0.02 % α -monothioglycerol
150 mM Imidazole
2 mM MgCl₂

Equilibration mixture for NiNTA-agarose

5 ml Cell lysis buffer
250 mM NaCl
15 mM Imidazole
5 mM MgCl₂

Dialysis buffer

50 mM TRIS/HCl pH 7.5
0.02 % α -monothioglycerol
20 % Glycerol

SDS-Polyacrylamide gel electrophoresis

Resolving gel buffer

1.5 M TRIS/HCl pH 8.8
0.4 % SDS

Stacking gel buffer

500 mM TRIS/HCl pH 6.8
0.4 % SDS

10x Running buffer

250 mM TRIS
1.92 M Glycin
1 % SDS

Coomassie staining solution

0.2 % Brilliant Blue
G-250
40 % Methanol
1 % Acetic acid

Materials

4x Sample buffer

130 mM TRIS/HCl pH6.8
10 % SDS
20 % Glycerol
0.06 % Bromophenol blue
10 % β -mercaptoethanol

Destaining solution

10 % Acetic acid
30 % Ethanol

Western blot

TBS buffer (TRIS Buffer Saline)

20 mM TRIS/HCl pH 7.5
150 mM NaCl

M-TBS

5 % Milk powder
in TBS buffer

TBS-T

0.1 % Tween 20
in TBS buffer

Towbin-Blot-buffer

25 mM TRIS/HCl
192 mM Glycin
20 % Methanol

Ponceau S staining solution

0.1 % (w/v) Ponceau S in
5 % (v/v) acetic acid

Cyclase enzyme tests

ATP or GTP stock solutions

10 mM pH 7.5 (adjusted
with NaOH)

cAMP or cGMP stock solutions

40 mM pH 7.5 (adjusted with
TRIS buffer)

10x AC-Start solution

5 mM ATP with
2.5-4x10⁶ Bq/ml
[α -³²P]-ATP

10x GC-Start solution

1 mM GTP with
2.5-4x10⁶ Bq/ml
[α -³²P]-GTP

2x AC-Cocktail

43.5 % Glycerol
 100 mM TRIS/HCl pH 7.5 or
 BIS/TRIS pH 6.5
 4 mM cAMP with
 2-4x10³ Bq/ml
 [2,8-³H]-cAMP
 0.23 mg * Creatine kinase
 6 mM * Creatine phosphate
 6-20 mM MnCl₂
 20 mM MgCl₂

2x GC-Cocktail

43.5 % Glycerol
 100 mM TRIS/HCl pH 7.5
 4 mM cAMP with
 2-4x10³ Bq/ml
 [2,8-³H]-cGMP
 6 mM MnCl₂

Creatine kinase

4 U/2.5 µl Creatine kinase in
 10 mM TRIS/HCl pH 7.5

Creatine phosphate

120 mM Creatine phosphate
 in 50 mM TRIS/HCl
 pH 7.5

AC-Stop buffer

3 mM cAMP/TRIS pH 7.5
 3 mM ATP
 1.5 % SDS

GC-Stop buffer

1.5 % SDS

Other buffers

FPLC buffer

50 mM TRIS/HCl pH 8.0
 0.015 % α-monothioglycerol
 2 mM MgCl₂
 250 mM NaCl
 10 % Glycerol

*As an ATP-regenerating system when impure protein samples were tested.

Materials

Crystallization buffer

The self-prepared crystallization buffers were prepared using deionized water (MilliQ) and were filtered through a 0.2 µm pore filter applying vacuum to a filter holder device.

2.4 Oligonucleotides

Restriction sites are underlined and mutations are in bold.

s = sense primer

as = antisense primer

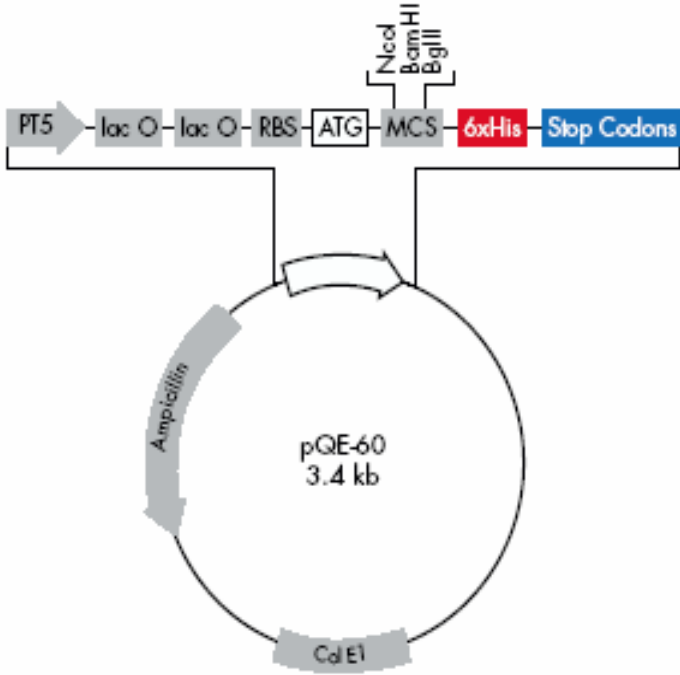
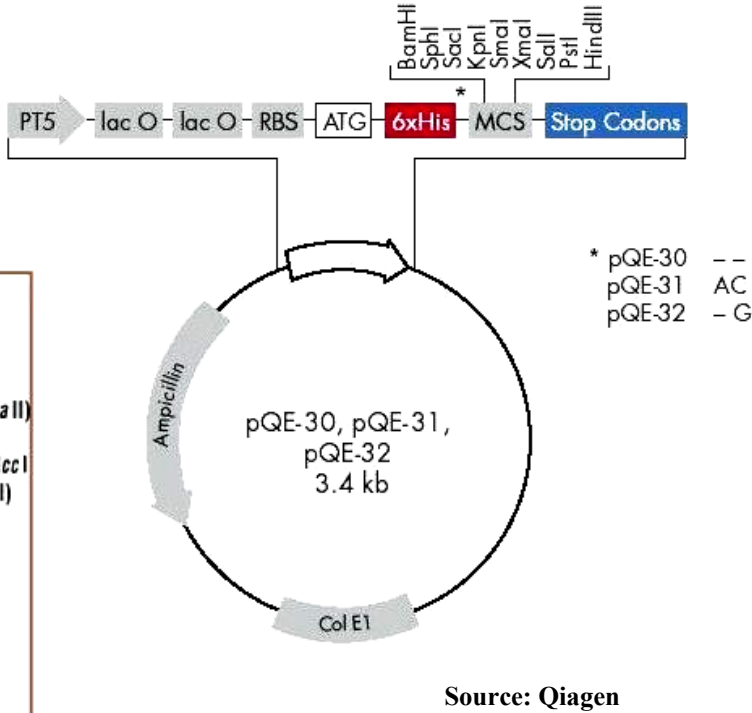
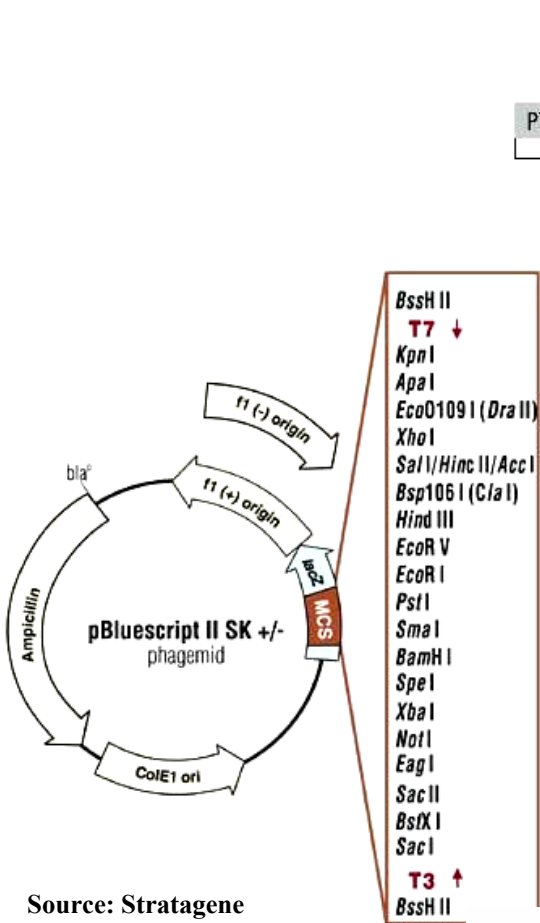
Name		Sequence (5'→3')	Position	Comments
Sequencing primers for plasmids				
T7	s	TAA TAC GAC TCA CTA TAG GG	625-646	universal for pBluescript II SK(-)
T3	as	AAT TAA CCC TCA CTA AAG GG	772-791	reverse for pBluescript II SK(-)
U- pQE	s	GAA TTC ATT AAA GAG GAG AAA	88-108	universal for pQE-30
R- pQE	as	CAT TAC TGG ATC TAT CAA CAG G	212-233	reverse for pQE-30
Cloning primers for Rv2435c AC catalytic domain and holoenzyme				
2435cs	s	AAA <u>GGA TCC</u> AAT CTG CAA ACC AAA GAG	1531-1548	BamHI
2435cas	as	AAA <u>AAG CTT</u> TCA TGA TCG CTC CGA CAA	2176-2193	HindIII
2435hAs	s	AAA <u>CCA TGG</u> GAA CGT CGG GTG AGG CAC TG	1-24	NcoI
2435hBs	s	AAA <u>CCA TGG</u> GAC TCC GGC GTC GGC CGC GT	73-96	NcoI
2435hCs	s	AAA <u>CCA TGG</u> TGC TGC TGC TGT TGA CG	121-141	NcoI
2435hDas	as	AAA <u>GGC GCC</u> CAA CGC TTT AAG GTA	760-777	SfoI

2435hEs	s	TTT <u>GGC GCC</u> AAC GCC GTC GAC TTT	788-795	SfoI
2435hFas	as	AAA <u>CTC GAG</u> CCG CCG GAT TGG CCG	1405-1424	XhoI
2435hGs	s	AAA <u>CTC GAG</u> GTT GGC ACC CAG AAG	1421-1440	XhoI
2435hHas	as	AAA <u>GGA TCC</u> TGA TCG CTC CGA CAA TCG GTA	2170-2190	BamHI
Cloning primers for Rv2212c N-terminal domain				
2212s1	s	AAA <u>GGA TCC</u> ATG GGC GTC CCT GCT GGC	1-18	BamHI
2212Nas	as	AAA <u>AGC TTC</u> TAG GTT CGT GCG CTG GCC AG	589-606	HindIII
Cloning primers for Rv2212c C-terminally His-tagged constructs				
2212s1	(see above)			
2212s3	s	AAA <u>GGA TCC</u> TCG GCA AGC GTG ACG TGC GG	634-653	BamHI
2212NasC-His	as	AAA <u>AGA TCT</u> GGT TCG TGC GCT GGC CAG	589-606	BglII
2212HasC-His	as	AAA <u>AGA TCT</u> ATC ACT GGC GGC GGG GCT	1147-1164	BglII
Cloning primers for Rv2212c C-terminally shortened catalytic domains				
2212s3	(see above)			
2212RARas	as	AAA <u>AGC TTC</u> TAC CTC GCA CGA GGG TTG	1116-1131	HindIII
2212DNPas	as	AAA <u>AGC TTC</u> TAA GGG TTG TCG TGC AGT	1107-1122	HindIII
2212HDNas	as	AAA <u>AGC TTC</u> TAG TTG TCG TGC AGT TCG	1104-1119	HindIII
2212LHDas	as	AAA <u>AGC TTC</u> TAG TCG TGC AGT TCG AAG	1101 -1116	HindIII
2212ELHas	as	AAA <u>AGC TTC</u> TAG TGC AGT TCG AAG GCC	1098-1113	HindIII
2212FELas	as	AAA <u>AGC TTC</u> TAC AGT TCG	1095-1110	HindIII

Materials

		AAG GCC ATC		
2212AFEas	as	AAA AGC TTC TAT TCG AAG GCC ATC ACC	1092-1107	HindIII
Cloning primers for Rv2212c mutants				
2212 s3	(see above)			
mut.FEVas	as	AAA AGC TTC TAC ACT TCG AAG GCC ATC	1095-1110	HindIII
mut.FEAas	as	AAA AGC TTC TAG GCT TCG AAG GCC ATC	1095-1110	HindIII
mut.FEGas	as	AAA AGC TTC TAC CCT TCG AAG GCC ATC	1095-1110	HindIII
Cloning primers for Rv2212c N-terminally shortened catalytic domains				
2212FELas	(see above)			
2212ASVs	s	AAA GGA TCC GCA AGC GTG ACG TGC GGT	637-654	BamHI
2212SVTs	s	AAA GGA TCC AGC GTG ACG TGC GGT ATC	640-657	BamHI
2212VTCs	s	AAA GGA TCC GTG ACG TGC GGT ATC GGC	643-660	BamHI
2212TCGs	s	AAA GGA TCC ACG TGC GGT ATC GGC TTT	646-663	BamHI
2212CGIs	s	AAA GGA TCC TGC GGT ATC GGC TTT GCG	649-666	BamHI

2.4 Plasmids



3 Methods

3.1 Methods of gene technology

3.1.1 Basic methods for analysis, processing and recombination of DNA

3.1.1.1 Extraction of DNA fragments from agarose-gels and buffer exchange of the DNA samples

DNA fragments separated through gel electrophoresis were excised from the agarose gel with a scalpel and extracted with the Nucleotrap-Gelextraction-Kit from Macherey-Nagel. The manufacturer's protocols were used for purification and desalting.

3.1.1.2 Plasmid isolation from E.coli

The *E.coli* culture was inoculated with 5 ml LB-medium in a glass tube and then shaken overnight at 37°C and 220 rpm. 3-5 ml of this culture were used for a miniprep using Wizard Plus SV Plasmid Purification Kit. The recombinant DNA was eluted with 50 µl of H₂O and was ready for restriction digest and/or DNA sequencing.

3.1.1.3 Restriction of DNA molecules

Restriction endonucleases were used according to the manufacturer's instructions. When a simultaneous digest was carried out using different enzymes, the most compatible buffer was used. Restriction digests contained 1 µg plasmid-DNA and 3-5 U enzyme. 0.5 µl purified BSA 100X from NEB was added to each incubation of 10 µl. Agarose-gel electrophoresis was used to analyse the digest.

3.1.1.4 DNA separation by agarose-gel electrophoresis

Agarose-gel electrophoresis was carried out in a horizontal electrophoresis apparatus. TAE-buffer was used for 1-1.5 % agarose (for 500-2000 bp DNA fragments). The gel was stained with ethidium bromide (0.01 mg/ml), the DNA band detected under a UV lamp (302 nm) and photographed. EcoRI-HindIII-restricted λ-DNA was used as a size standard (DNA marker).

3.1.1. Blunting of DNA overhangs (Klenow digestion)

The Klenow fragment of DNA polymerase I from *E. coli* was used to blunt DNA ends after a PCR or a restriction digest. The reaction mixture contained 6.7 μ l DNA (0.5-3 μ g), 0.5 μ l BSA 100X, 1 μ l 10x Klenow buffer and 0.8 U Klenow enzyme. After 10 min at 37°C, 1 μ l dNTPs was added and the mixture was incubated for 30 min at 37°C. It was then heated to 70°C for 10 min for enzyme denaturation.

3.1.1.6 5'-Phosphorylation of PCR products

PCR products were phosphorylated with T4-Polynucleotide Kinase. The reaction mixture contained in 10 μ l Klenow-treated DNA, 1 mM ATP, 10 U enzyme and 1x T4-PNK-buffer (incubation at 37°C for 1 hr).

3.1.1.7 5'-Dephosphorylation of linear plasmids

To prevent restricted plasmids from religation, they were incubated for 1hr at 37°C with 2 U alkaline phosphatase and 1x dephosphorylation buffer. The plasmid was then purified by gel electrophoresis.

3.1.1.8 Ligation of DNA molecules

The Rapid DNA Ligation Kit (Roche) was used for ligation according to the manufacturer's instructions. The molar ratio of vector to DNA insert was about 1:1.

3.1.1.9 Polymerase chain reaction (PCR)

All PCRs were carried out using specific primers to amplify DNA from plasmid or genomic DNA and for the introduction of endonuclease restriction sites and /or point mutations.

The reaction mixture contained (end concentrations):

- 1-10 ng plasmid-DNA
- 0.625 pmol/ μ l primer
- 250 μ M dNTPs
- 5 % DMSO
- 1 U Taq-polymerase
- 1x Incubation buffer (with 2 mM MgCl₂ added).

The following program was used:

Methods

Phase	Temperature	Time	Cycles
Pre-denaturation	95°C	1 min	
Denaturation	95°C	1 min	25-30
Primer annealing	T _a	1 min	
Extension	72°C	1 min	
Filling-up	72°C	10 min	

The annealing temperature (T_a in °C) was calculated from the following equation:

$$T_a = 4 \times (GC) + 2 \times (AT)$$

(GC): number of bases G and C in the primer sequence
(AT): number of bases A and T in the primer sequence

When the annealing temperatures of both primers differed, the lower one was applied.

The PCR reaction mixture was analysed on an agarose gel, the required band was excised and the DNA was extracted by Nucleotrap. After 5'-phosphorylation of the DNA fragments, they were ligated in the correspondingly restricted plasmids or in EcoRV-restricted and dephosphorylated pBluescriptII SK(-).

3.1.1.10 DNA-sequencing

DNA was sequenced with the Thermo Sequenase Fluorescent Labelled Primer Cycle Sequencing Kit. 8-10 µl (~130 ng/Kb) plasmid-DNA were mixed with 2 µl (2-3 pmol/µl) fluorescent-labelled primers, 3% DMSO and then the volume was completed to 18 µl with water. 4 µl of these mixtures were mixed each with 2 µl of the reaction mixture (see manufacturer's protocol), covered with a drop of Chill out Wax and then run in a Thermocycler according to the following program:

Phase	Temperature	Time	Cycles
Denaturation	95°C	2 min	
Denaturation	95°C	20 s	30
Primer annealing	T _a	20 s	
Extension	70°C	20 s	
Filling-up	4°C	∞	

An annealing temperature of 56°C was used for the primers T3 and T7 while for primers U-pQE and R-pQE a T_a of 54°C was used.

Afterwards the samples were mixed with 6 µl stop buffer and 1 µl was taken from each sample and loaded on a 6% polyacrylamide gel. Electrophoresis was carried out with TBE buffer at 50 W (1500 V, 37 mA, 50°C). The DNA fragments were detected through a laser beam at 700 nm with a Li-cor DNA Sequencer Model 4000 and were then analysed with the BaseImagIR V.4.0 software.

3.1.2 Transformation of recombinant DNA

3.1.2.1 Preparing competent E.coli bacterial cells for transformation

Competent *E.coli* cells were prepared with the CaCl_2 method (Cohen *et al.*, 1972). An overnight culture was inoculated in LB-medium in the ratio 1:100 and cultivated at 37°C and 220 rpm until it reached an OD_{600} of 0.4. After 10 min on ice, cells were centrifuged for 15 min at 4°C (1000x g). Pellets were suspended in 50 ml 100 mM CaCl_2 , left on ice for 20 min and after another centrifugation they were resuspended in 10 ml 100 mM CaCl_2 + 20% glycerol. The suspended cells were left for 2 hr on ice, divided into 100 µl aliquots and stored at -80°C.

3.1.2.2 Standard transformation into E.coli cells

Plasmid-DNA and 10 µl 10x CM-buffer were brought to 100 µl by addition of H_2O . After mixing with 100 µl competent bacterial cells by gentle agitation, the mixture was left for 20 min on ice and then heat shocked for exactly 1 min at 42°C. Afterwards the reaction mixture was left again for 20 min on ice. 500 µl LB-medium were added (45-60 min, 37°C, 220 rpm). 150-250 µl of this transformation reaction were spread on the appropriate antibiotic containing LB-agar plates which were incubated in an inverted position at 37°C for 12-16 hr. For transformation into pBluescript II SK (-), 40 µl of IPTG 0.1 M and 40 µl of X-Gal (2%) were spread on the LB agar plate prior to the bacterial culture in order to enable screening. Bacteria carrying the recombinant DNA formed white colonies, while those carrying empty plasmids formed blue colonies.

3.1.2.3 Preparation of bacterial stock cultures

1ml of an overnight culture was centrifuged and the pellets were resuspended in 750 μ l LB-broth/glycerol (4:1). The cultures could thus be stored at -80°C .

3.2 Protein expression in E.coli

All proteins were expressed in *E.coli* BL21(DE3)[pREP4] cells. These *E.coli* cells contain the low-copy plasmid pREP4 which confers kanamycin resistance and constitutively expresses the lac repressor protein which tightly regulates recombinant protein expression by a special "double operator" system in the pQE expression vectors.

3.2.1 Pre-culture

Cells were taken from the bacterial stock culture and inoculated in 10 ml LB-medium containing 50 $\mu\text{g/ml}$ kanamycin and 100 $\mu\text{g/ml}$ ampicillin. They were incubated overnight at 37°C and 220 rpm.

3.2.2 Expression

10 ml pre-culture were inoculated and left to grow in 200 ml LB broth containing 100 $\mu\text{g/ml}$ ampicillin and 25 $\mu\text{g/ml}$ kanamycin (30°C , 220 rpm) until an OD_{600} of 0.5-0.6 was reached. After induction with 60 μM IPTG, cells were incubated either at 22°C for 4-5 hr or at 16°C overnight and 220 rpm. They were harvested by centrifugation (15 min, 4000 x g, 4°C). Pellets were suspended in 40 ml pellet washing buffer and again centrifuged (15 min, 5500 x g, 4°C). Cell pellets were then shock-frozen in liquid nitrogen, stored at -80°C or were further worked upon (see protein purification).

3.2.3 Protein purification from E.coli BL 21 (DE3) [pREP4]

Protein purification was carried out through the C- or N- terminal hexa histidine residue (coded in pQE vectors, 6x His-tag). The 6x His-tag also enabled the immunochemical detection using anti-His antibodies as well as the affinity purification on Ni^{2+} -NTA agarose. The purification was carried out according to QIA expressionist protocol (Qiagen, Third Edition, 2001).

The bacterial pellets from 200-400 ml culture were left at RT for thawing and then suspended in 20 ml cell lysis buffer. The suspended cells were either sonicated on ice for 3 x 10 sec at step 4 (Branson Sonifier B-12) or pressed twice through a French Press and then centrifuged for 30 min at 16,000 x g (4°C). Sometimes lysozyme (0.2 mg/ml, 30 min on ice) and DNase I (0.02 mg/ml with 5 mM MgCl₂, 30 min on ice) were added after sonication prior to centrifugation.

The supernatant was then mixed with 250 mM NaCl and 15 mM imidazole and shaken on ice for 1-2 hr (or overnight) with 200 µl of Ni²⁺-NTA agarose. Samples were centrifuged at 2500 x g, 5 min. Ni²⁺-NTA agarose was suspended in 5 ml washing buffer A and transferred into a 10 ml syringe to which a Wizard mini-column was attached. The resin was successively washed with washing buffers A and B (5 ml each) before protein was eluted with 300 µl elution buffer. All steps were carried out on ice. All fractions of the procedure (pellets, supernatants, washing and elution samples) were analysed on SDS-PAGE. The purified protein was either directly tested for AC activity, concentrated and used for crystallization or stored at -20°C with 20 % glycerol (V/V).

3.3 Protein chemistry methods

3.3.1 Biorad protein determination (Bradford, 1976)

1-10 µg protein in 800 µl water were mixed with 200 µl Biorad reagent and mixed. Samples were measured at 595 nm and the protein concentration determined by means of a calibration curve. 0, 4, 6, 8 and 12 µg of BSA were used as standards.

3.3.2 Protein dialysis

The eluate of Ni²⁺-NTA-purification of the catalytic domain of Rv 2435c was dialysed overnight against 500 ml dialysis buffer in Visking Dialysis Tubing 8/32 (Ø 6 mm), to get rid of imidazole from the elution buffer which might affect the enzyme activity.

3.3.3 Protein concentration and buffer exchange

For crystallization purposes protein was concentrated by centrifugation, first to achieve the desired concentrations and second to change the elution buffer to the protein crystallization buffer (10 mM TRIS/HCl pH 7.5, 1 mM MgCl₂, 0.05 % α -monothioglycerol, 10 % glycerol). The Nanosep 10K Omega centrifugal devices were used, each filled with maximally 500 μ l of purified protein solution and centrifuged in an Eppendorf centrifuge (11,000 rpm, 4°C, 5-20 min) until a volume of 200 μ l. This was repeated several times until the required concentration was reached in a volume of 200 μ l. Protein crystallization buffer was added (5 x 200 μ l) until the concentration of the elution buffer was diluted to 3.125 %. Protein was kept at 4°C during preparation of the crystallization plates.

3.3.4 Protein detection

3.3.4.1 SDS-PAGE

Proteins were separated according to their molecular weights by discontinuous gel electrophoresis (Laemmli, 1970). Samples were mixed with SDS-PAGE 4x-sample buffer, heated for 5 min at 95°C and loaded on to the gel.

The following table shows the composition of the gels.

Stacking gel	4.5 %	Resolving gel	7.5 %	10 %	12.5 %	15 %
Stacking gel buffer	1 ml	Resolving gel buffer	3 ml	3 ml	3 ml	3 ml
Water	2.4 ml	Water	6 ml	5 ml	4 ml	3 ml
AA/Bis 37.5: 1	0.6 ml	AA/Bis 37.5: 1	3 ml	4 ml	5 ml	6 ml
10% APS	40 μ l	10% APS	80 μ l	80 μ l	80 μ l	80 μ l
TEMED	10 μ l	TEMED	10 μ l	10 μ l	10 μ l	10 μ l

These volumes are enough for 2 mini gels (Hoeffer, 10 cm x 8 cm, thickness: 1 mm). Electrophoresis was carried out in a vertical electrophoretic unit (Hoefel Mighty Small) at 20 mA per gel and a maximum of 200 V. Electrophoresis was stopped as soon as the blue sample buffer band quitted the gel. Staining was with Coomassie Brilliant Blue for at least 30 min and with the Coomassie-decolorizer bleached until the protein bands were clearly seen. The pepGold marker (14.4-116 kDa) was used as a protein standard, and below is a list of its components:

β -Galactosidase	116 kDa
Bovine Serum Albumin	66 kDa
Ovalbumin	45 kDa
Lactate dehydrogenase	35 kDa
RE Bsp981	25 kDa
β -Lactoglobulin	18.4 kDa
Lysozyme	14.4 kDa

The gels were photographed and filed by the Biocapt Software Version 99.01 .

3.3.4.2 Western Blot

For immuno-chemical detection proteins were transferred after SDS-PAGE to PVDF-membrane through Semi-Dry-Electrotransfer (Towbin *et al.*, 1979). The blot membrane was successively soaked in methanol, water and Towbin buffer each for 10 min. The following sandwich set-up was built up for the electric transfer:

- . Three Whatman 3 MM papers were soaked in Towbin buffer and layed on the anode plate.
- . Then comes the blot membrane over them, the gel and finally three soaked Whatman papers again on the side of the cathode plate.

Protein transfer was carried out for 2-3 hr at 20V and 2.5 mA/cm². The gel was stained in Coomassie Brilliant Blue to check transfer efficiency.

The membrane was stained in Ponceau S for about 5 min, then it was decolorized with deionized water until the protein bands were clear enough and the marker bands were then marked with a pencil. The membrane was blocked with M-TBS buffer for at least 1 hr at RT or overnight at 4°C and washed with TBS-T buffer (2 x 10 sec, 2 x 5 min). It was then incubated with the primary antibody (mouse monoclonal RGS-His₄ antibody 1:2000, Penta-His antibody 1:1000 or Tetra-His antibody 1:1000 diluted in M-TBS) for 1 hr. After washing (TBS-T, 1 x 15 min, 2 x 5 min) it was incubated with the secondary antibody (goat anti-mouse IgG-F_c or goat anti-rabbit IgG-F_c horseradish peroxidase conjugated antibodies 1:5000 diluted in M-TBS) for 1 hr and then washed as above with TBS-T.

The chemiluminescent reaction with the ECL Plus Western Blotting Detection Kit (Amersham) was carried out according to the manufacturer's instructions and it was detected on Hyperfilm-ECL after its exposure to the detection reaction (from 10 sec to 15 min).

3.3.4.3 Dot Blot

This was used to detect the expression of the C-terminal His-tagged constructs of Rv2212c as a preliminary step before a Western Blot. A set of serial dilutions of the purified protein (concentrations of 0.05-0.35 µg per spot) were applied directly to a Protran BA83 nitrocellulose membrane. The membrane was then incubated in M-TBS buffer for 1 hr, after washing it was incubated with primary (Tetra-His antibody) and secondary (Goat anti-mouse) antibodies and developed as described for the Western Blot.

3.3.5 Size-exclusion Chromatography (Gel filtration)

Rv2212c wild type catalytic domain and Rv2212c₂₁₃₋₃₇₀ were chromatographed on an ÄKTA FPLC at 4°C. Buffers used were prepared in MilliQ water, filtered through a microfilter (0.2 µm) and degassed. Proteins were detected at 280 nm. All fractions were tested for AC activity. The column (Superose 12 HR 10/30) was first washed with the FPLC-buffer, then calibrated using the following calibration proteins (each 1 mg in 250 µl injection volume). This 1 mg protein was dissolved in elution buffer + 20% glycerol + 250 mM NaCl, to reflect the same conditions as the tested protein.

Calibration Protein	kDa
Cytochrome C	12,5
Chymotrypsinogen A	25
Ovalbumin	45
Bovine Serum Albumin	66

200 µg of the wild type catalytic domain or 530 µg of Rv2212c₂₁₃₋₃₇₀ (in 250 µl) were injected into the column. The column volume was 23.56 ml and the flow rate was 0.5 ml/min. Fractionation (500 µl) started after the first 7 ml and 65 fractions were collected.

Larger amounts of Rv2212c₂₁₃₋₃₇₀ (4.7 mg) were purified in three runs (same conditions as above). Fractions corresponding to the wanted peak were tested for activity, analysed on SDS-PAGE, united and concentrated using the Nanosep 10K Omega centrifugal devices.

3.3.6 Cyclase enzyme tests

They were carried out after Salomon *et al.*, 1974.

3.3.6.1 Adenylyl cyclase test

AC activity was measured by conversion of [α - ^{32}P]-ATP into [^{32}P]-cAMP. [2,8- ^3H]-cAMP was used as an internal standard. The standard test reaction mixture was composed of: 40 μl protein sample, 50 μl AC-Cocktail and 10 μl AC-Start solution. The protein sample and the cocktail were mixed in 1.5 ml epicups on ice, the reaction was started with ATP. Each sample was incubated at 37°C for 10 min (unless indicated otherwise). The reaction was stopped with 150 μl AC-Stop buffer, returned on ice and 750 μl of water were added to each sample. Duplicates were routinely carried out. A blank sample contained only water. For separating the ATP from the cAMP the samples were applied onto Dowex columns (glass columns filled with 1.2 g Dowex-50WX4), washed with 3 ml water and eluted with 5 ml water on Al_2O_3 columns (plastic columns filled with 1 g neutral, active Al_2O_3 90). They were eluted with 4.5 ml 0.1 M TRIS/HCl pH 7.5 into scintillation vials, mixed with 4 ml Ultima Gold XR scintillator and counted in a Liquid Scintillation Counter. The specific activity A ($\text{pmol}\cdot\text{mg}^{-1}\cdot\text{min}^{-1}$) was calculated using the following formula:

$$A = \frac{\text{Substrate } (\mu\text{M}) \times 100 \mu\text{l}}{\text{Time (min)}} \times \frac{1000}{\text{Protein } (\mu\text{g})}$$

$$\times \frac{\text{cpm } [^3\text{H}]_{\text{total}}}{\text{cpm } [^3\text{H}]_{\text{sample}} - 3\% [^{32}\text{P}]_{\text{sample}}} \times \frac{\text{cpm } [^{32}\text{P}]_{\text{sample}} - \text{cpm } [^{32}\text{P}]_{\text{blank}}}{\text{cpm } [^{32}\text{P}]_{\text{total}}}$$

The subtraction of 3% of the ^{32}P -counts from the corresponding ^3H -counts was made because of the spillover of ^{32}P into the ^3H channels. Activities lower than double the background (in cpm) were considered as zero activity. Columns were regenerated as follows:

Methods

- Dowex columns: 5 ml 2 N HCl, 1x 10 ml then 1 x 5 ml water
- Al₂O₃ columns: 2 x 5 ml 0.1 M TRIS/HCl pH 7.5

3.3.6.2 Guanylyl cyclase test

The same protocol used for AC tests was followed for GC tests using GC-Cocktail, GC-Start solution and GC-Stop solution instead. Also the elution from the Dowex columns was in this case with 2 ml of water, after a washing step with 3 ml of water, and from the Al₂O₃ columns with 4 ml 0.1 M TRIS/HCl pH 7.5. The Dowex columns were filled with 4 g while the Al₂O₃ columns with 0.8 g. Calculation of the enzymatic activity and regeneration of the columns were carried out as stated above.

3.3.7 Crystallization

The hanging drop vapour diffusion technique (fig. 3.1) was used using the 24 well polystyrene pre-greased plates and 22 mm siliconized glass square slide covers from Hampton Research. The reagent kits Crystal Screen (CS), Crystal Screen 2 (CS 2) and Crystal Screen Lite from Hampton Research and Wizard I & II from deCODE genetics were used for crystallization.

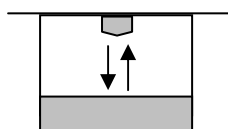


Fig. 3.1: Scheme showing the hanging drop technique where the hanging drop was prepared on a siliconized slide cover by mixing the protein sample and the crystallization buffer in a ratio 1:1. The slide cover was then inverted over a well (reservoir) containing 500 μ l of the crystallization buffer.

Protein was either purified with Ni²⁺-NTA only or was further purified by gel filtration (in case of Rv2212c₂₁₃₋₃₇₀ only). Proteins were assayed for stability in the crystallization solution and storage temperature. Crystallization trials were done within the scope of this work using different proteins under different crystallization conditions.

Buffers of the mentioned crystallization reagent kits were examined with the proteins as a first screening step. Different crystallization variables were examined as; protein concentration, incubation temperature and presence of glycerol in the protein crystallization solution. Also incubation of Rv2212c₂₁₂₋₃₇₄ with ATP (substrate) overnight before setting the plates for crystallization was examined with buffers : CS # 3,11 ; Wizard I # 8, 9, 13, 16, 20, 27, 34, 43; Wizard II # 9, 10, 19, 3, 35, 41, 45, 46, 47, 48. Crystals were inspected under a polarization microscope every day for the first week and then once every week. After obtaining crystals the components of the corresponding precipitating buffer were varied to optimize size and form of the crystals.

3.4 Cloning

M. tuberculosis genomic DNA was provided by Prof. Dr. Boettger (University of Zürich, Medical School). Generally all constructs were cloned into the MCS of pBluescriptII SK(-) as a first cloning step and for sequencing. They were then cloned into pQE-30 or pQE-60 for expression. As a result, all proteins ended up with an N-terminal MRGSH₆GS or a C-terminal RSH₆ extension, respectively.

3.4.1 *M. tuberculosis* Rv2435c

3.4.1.1 Catalytic domain of Rv2435c

Rv2435c₅₁₁₋₇₃₀ was amplified from *M. tuberculosis* genomic DNA by PCR using primers 2435cs and 2435cas with insertion of 5'- BamHI and 3'- HindIII restriction sites. The PCR fragment was then ligated into a dephosphorylated EcoRV restricted pBluescript II SK(-), after Klenow treatment, transformed into E.coli XL1 blue MRF' and sequenced (fig. 3.2).

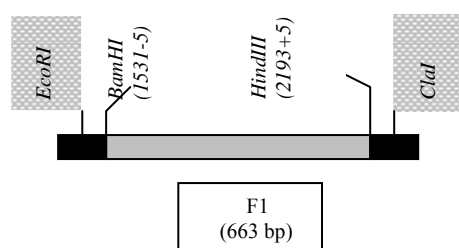


Fig. 3.2: Chart showing the orientation of the insert in pBluescript II SK(-). F1(grey rectangle coding for Rv2435c₅₁₁₋₇₃₀). The MCS of pBluescript II SK(-) is shown as a black beam.

F1 was then cloned into a dephosphorylated BamHI /HindIII digested pQE-30 (fig. 3.3).

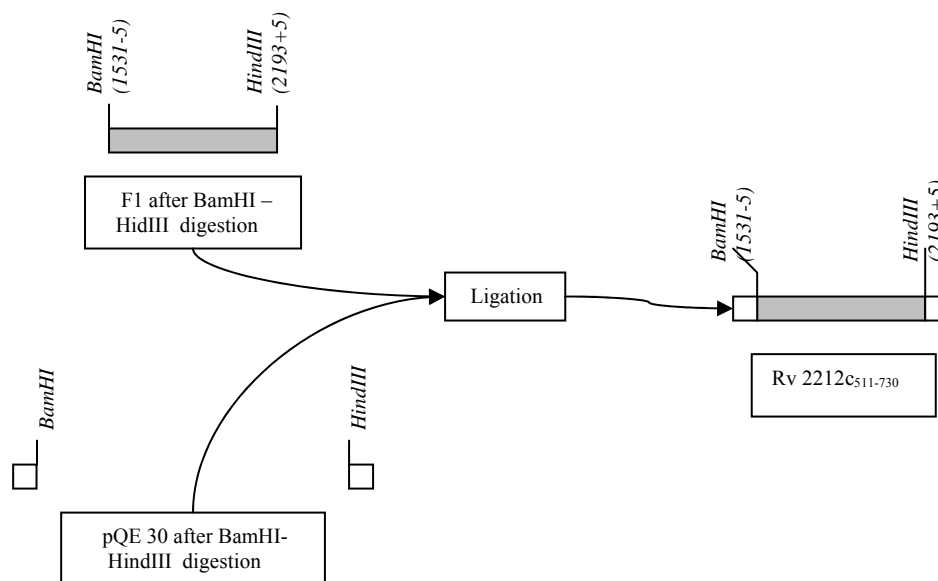


Fig. 3.3 : Cloning scheme for Rv2435c₅₁₁₋₇₃₀

3.4.1.2 Holoenzyme of Rv2435c

In a trial to determine the actual start of the holoenzyme sequence, three different constructs were cloned each having a different start; Rv2435c₁₋₇₃₀ starting with L₁, Rv2435c₂₅₋₇₃₀ with V₂₅ and Rv2435c₄₁₋₇₃₀ with M₄₁.

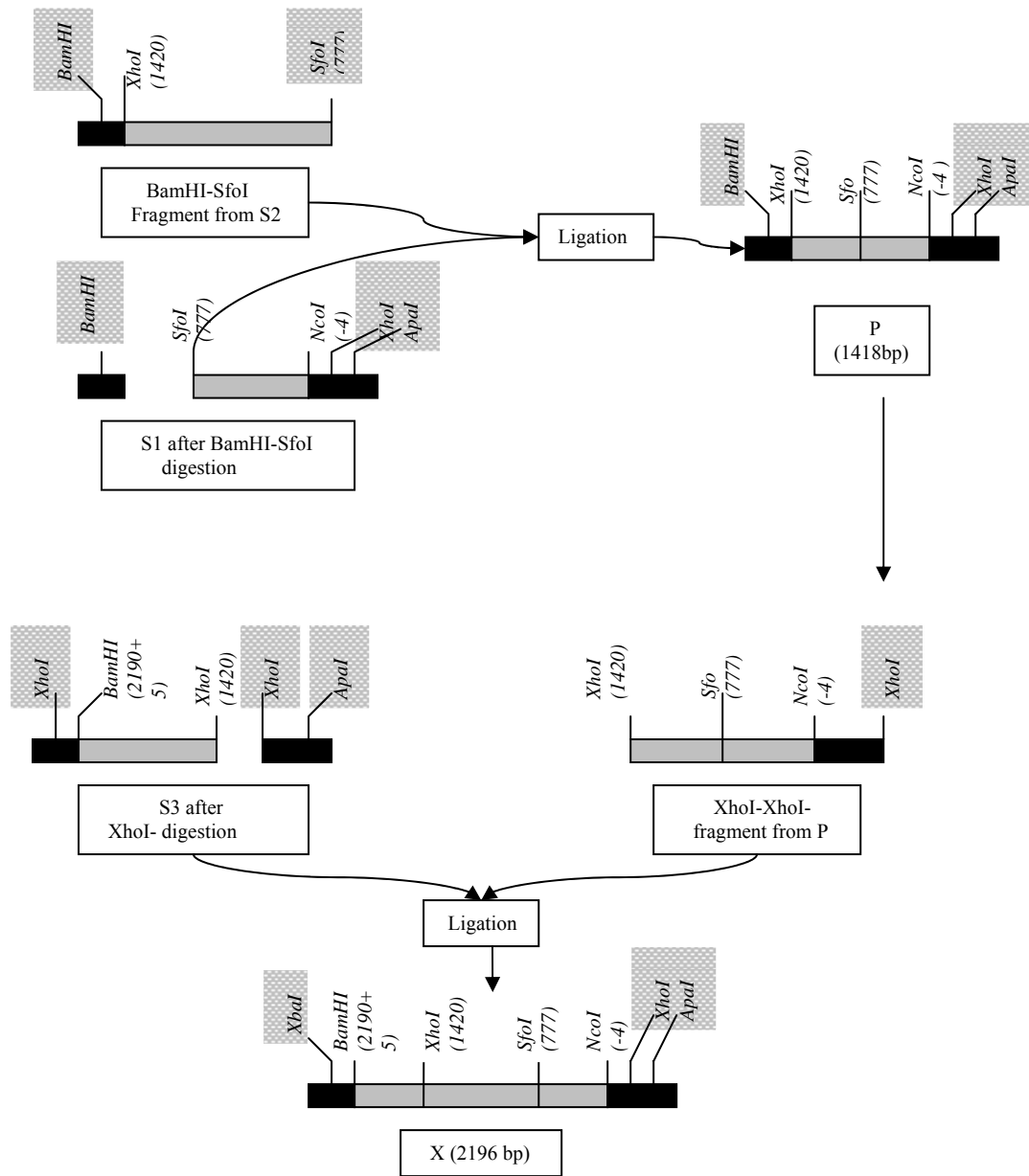
a- Rv2435c₁₋₇₃₀

The holoenzyme was amplified in three separate fragments from *M. tuberculosis* genomic DNA by 3 PCR reactions, thus covering the entire ORF (2190 bp), using primers (2435hAs, 2435hDas, 2435hEs, 2435hFas, 2435hGs and 2435hHas; see table 3.1 for scheme). An ATG start codon was inserted instead of TTG coding for L₁ followed by a glycine. S1 and S2 were ligated into a dephosphorylated EcoRV restricted pBluescript II SK(-), after treatment with Klenow, transformed into E.coli XL1 blue MRF' and sequenced. The third PCR fragment (S3) was ligated into a dephosphorylated BamHI/XhoI restricted pBluescript II SK(-), transformed into E.coli XL1 blue MRF' and sequenced (see table 3.1).

Clone	Primer	Length (bp/AA)	Orientation of insert in pBluescript II SK(-)
S1	2435hAs 2435hDas	778 L ₁ -G ₂₅₉	
S2	2435hEs 2435hFas	640 A ₂₆₀ -R ₄₇₃	
S3	2435hGs 2435hHas	772 L ₄₇₄ -S ₇₃₀	

Table 3.1: Subclones for Rv2435c₁₋₇₃₀ are represented by grey rectangles. The MCS of pBluescript II SK(-) is represented by a black beam.

The three clones (S1, S2 and S3) were then ligated and inserted into a dephosphorylated NcoI/BamHI digested pQE-60 thus adding a GSRSH₆ tag C-terminally (fig. 3.4).



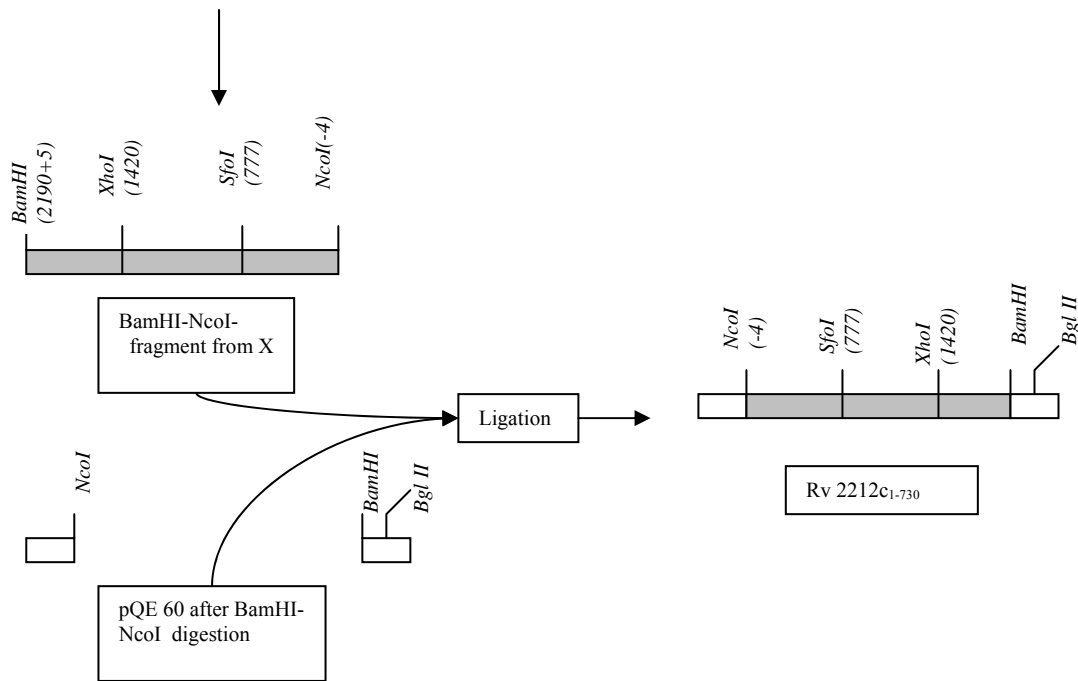


Fig. 3.4 : Cloning scheme for Rv2435c₁₋₇₃₀ . Labels and shading are as in Fig. 3.2 and table 3.1.

b- Rv2435c₂₅₋₇₃₀ and Rv2435c₄₁₋₇₃₀

The 5'-terminal fragments of these two holoenzymes were amplified by PCR using primers (2435hBs, 2435hDas) and (2435hCs, 2435hDas) for Rv2435c₂₅₋₇₃₀ and Rv2435c₄₁₋₇₃₀ respectively, and S1 (table 3.1) as template. A 5'-NcoI restriction site was also inserted. In Rv2435c₂₅₋₇₃₀ an ATG start codon was inserted instead of GTG coding for V₂₅ followed by a glycine. S4 and S5 were ligated into a dephosphorylated EcoRV restricted pBluescript II SK(-), transformed into E.coli XL1blue MRF⁺ and sequenced (table 3.2).

Clone	Primer	Length (bp/AA)	Orientation of insert in pBluescript II SK(-)
S4	2435hBs 2435hDas	708 V ₂₅ – G ₂₅₉	<p style="text-align: center;">S4</p>
S5	2435hCs 2435hDas	657 M ₄₁ – G ₂₅₉	<p style="text-align: center;">S5</p>

Table 3.2 : Subclones for Rv2435_{c25-730} and Rv2435_{c41-730}. Labels and Shading as in table 3.1.

S4 and S5 were restricted with SfoI and NcoI and ligated with the fragment obtained after digestion of Rv2212_{c1-730} with SfoI and NcoI (fig. 3.5).

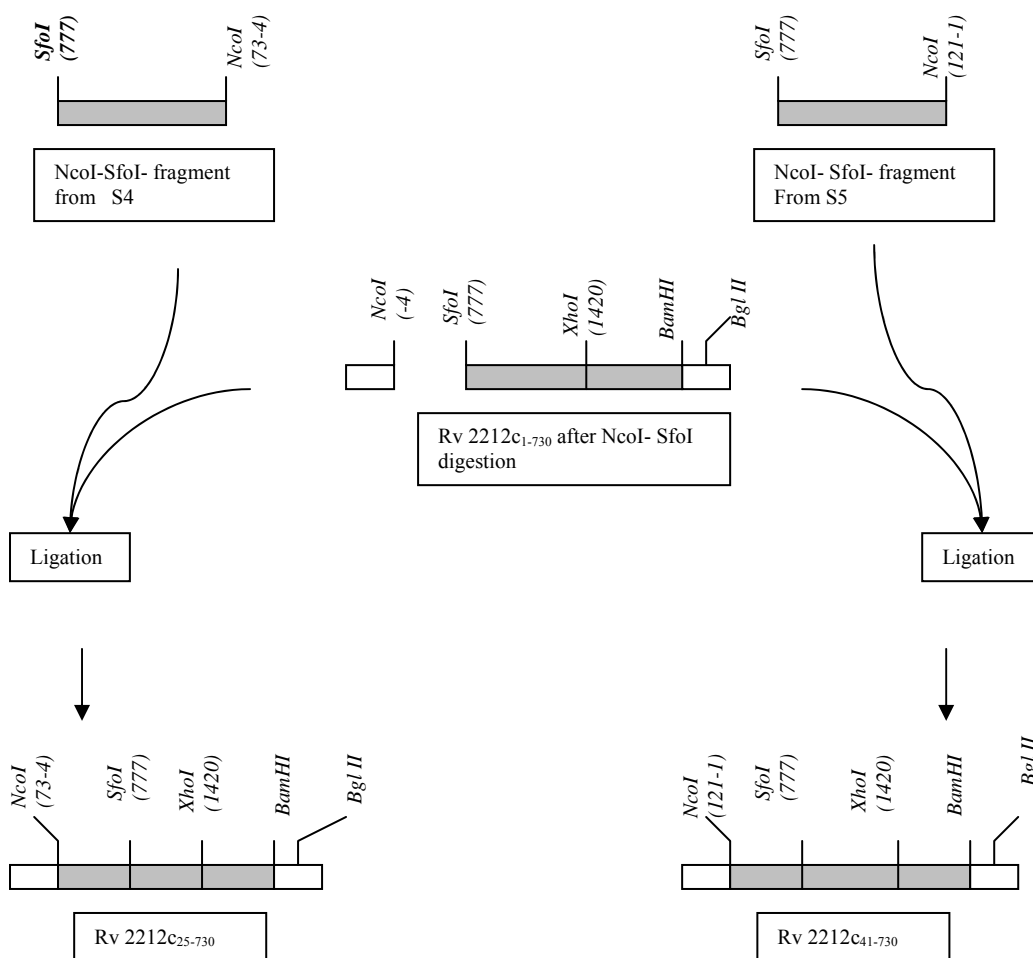


Fig. 3.5 : Cloning scheme for Rv2435c₂₅₋₇₃₀ and Rv2435c₄₁₋₇₃₀

3.4.2 *M. tuberculosis* Rv2212c

3.4.2.1 N-terminal domain (Rv2212c₁₋₂₀₂)

Rv2212c₁₋₂₀₂ was amplified by PCR using the recombinant DNA of the Rv2212c₁₋₃₈₈ in pBluescript II SK (-) (cloned by S. Zeibig, 2003) as a template. Primers 2212s1 and 2212Nas were used with the insertion of 5'-BamHI and 3'-HindIII restriction sites. The PCR fragment was ligated into a dephosphorylated EcoRV restricted pBluescript II SK(-), after Klenow treatment, transformed into *E. coli* XL1 blue MRF' and sequenced (fig. 3.6).

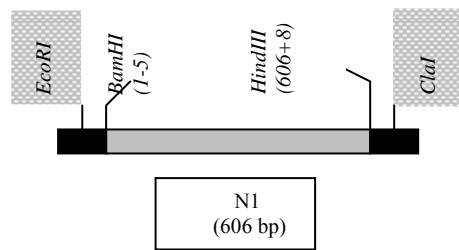


Fig. 3.6 : Chart showing the orientation of the insert in pBluescript II SK(-). N1(grey rectangle coding for Rv2212c₁₋₂₀₂). The MCS of pBluescript II SK(-) is shown as a black beam.

N1 was cloned into a dephosphorylated BamHI /HindIII digested pQE-30 (fig. 3.7).

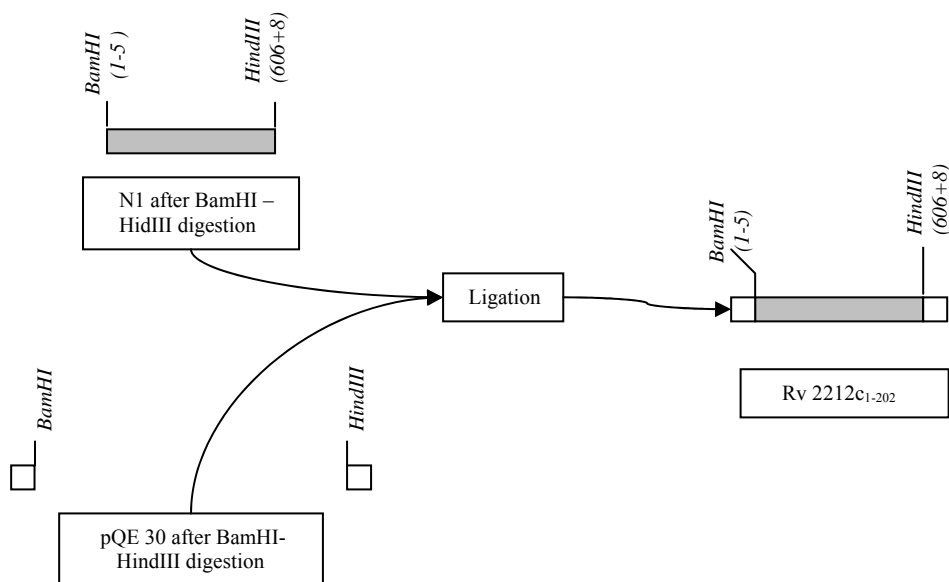


Fig. 3.7 : Cloning scheme for Rv2212c₁₋₂₀₂

3.4.2.2 C-terminally His-tagged constructs of Rv2212c

The N-terminal domain (Rv2212c₁₋₂₀₂ C-His), the catalytic domain (Rv2212c₂₁₂₋₃₈₈ C-His) and the holoenzyme (Rv2212c₁₋₃₈₈ C-His) were amplified by PCR using the recombinant DNA of Rv2212c₁₋₃₈₈ in pBluescript II SK (-) (cloned by S. Zeibig, 2003) as a template. 5'-BamHI and 3'-BglII restriction sites were inserted in each construct introduced by the different primers used.

a- Rv2212c₁₋₂₀₂ C-His

It was amplified using primers 2212s1 and 2212NasC-His. The PCR fragment (618 bp) was ligated into a dephosphorylated EcoRV restricted pBluescript II SK(-), after Klenow treatment, transformed in E.coli XL1 blue MRF' and sequenced. The correct clone was digested with BamHI/BglII and cloned into a dephosphorylated BamHI/BglII digested pQE-60.

b- Rv2212c₂₁₂₋₃₈₈ C-His

Primers 2212s3 and 2212HasC-His were used. The PCR fragment (543 bp) was ligated into a dephosphorylated EcoRV restricted pBluescript II SK(-), after Klenow treatment, transformed into E.coli XL1 blue MRF' and sequenced. The correct clone was digested with BamHI/BglII and cloned into a dephosphorylated BamHI /BglII digested pQE-60.

c- Rv2212c₁₋₃₈₈ C-His

It was amplified using primers 2212s1 and 2212HasC-His. The PCR fragment (1176 bp) was ligated into a dephosphorylated EcoRV restricted pBluescript II SK(-), after Klenow treatment, transformed into E.coli XL1 blue MRF' and sequenced. The correct clone was digested with BamHI/BglII and cloned into a dephosphorylated BamHI /BglII digested pQE-60.

3.4.2.3 C-terminally shortened Rv2212c₂₁₂₋₃₈₈ (with N-terminal His-tag)

Rv2212c₂₁₂₋₃₈₈ (N-His) had already been cloned by S. Zeibig. Successive C-terminal truncations were carried out in order to achieve the shortest possible active catalytic centre of Rv2212c₂₁₂₋₃₈₈. Seven truncations were made and each time the AC activity was tested until the construct (Rv2212c₂₁₂₋₃₆₉) having very poor activity was reached. The recombinant DNA of Rv2212c₁₋₃₈₈ in pBluescript II SK(-) was used as a template and primer 2212s3 was used as

the sense primer for these constructs introducing a 5'-BamHI restriction site. The following antisense primers were used introducing a 3'-HindIII restriction site in each corresponding construct:

Rv2212c ₂₁₂₋₃₇₇ :	2212RARas
Rv2212c ₂₁₂₋₃₇₄ :	2212DNPas
Rv2212c ₂₁₂₋₃₇₃ :	2212HDNas
Rv2212c ₂₁₂₋₃₇₂ :	2212LHDas
Rv2212c ₂₁₂₋₃₇₁ :	2212ELHas
Rv2212c ₂₁₂₋₃₇₀ :	2212FELas
Rv2212c ₂₁₂₋₃₆₉ :	2212AFEas

The PCR fragments were ligated into a dephosphorylated EcoRV restricted pBluescript II SK(-), after Klenow treatment, transformed into E.coli XL1 blue MRF' and sequenced. The correct clones were digested with BamHI/HindIII and cloned into a dephosphorylated BamHI/HindIII digested pQE-30 (fig. 3.8).

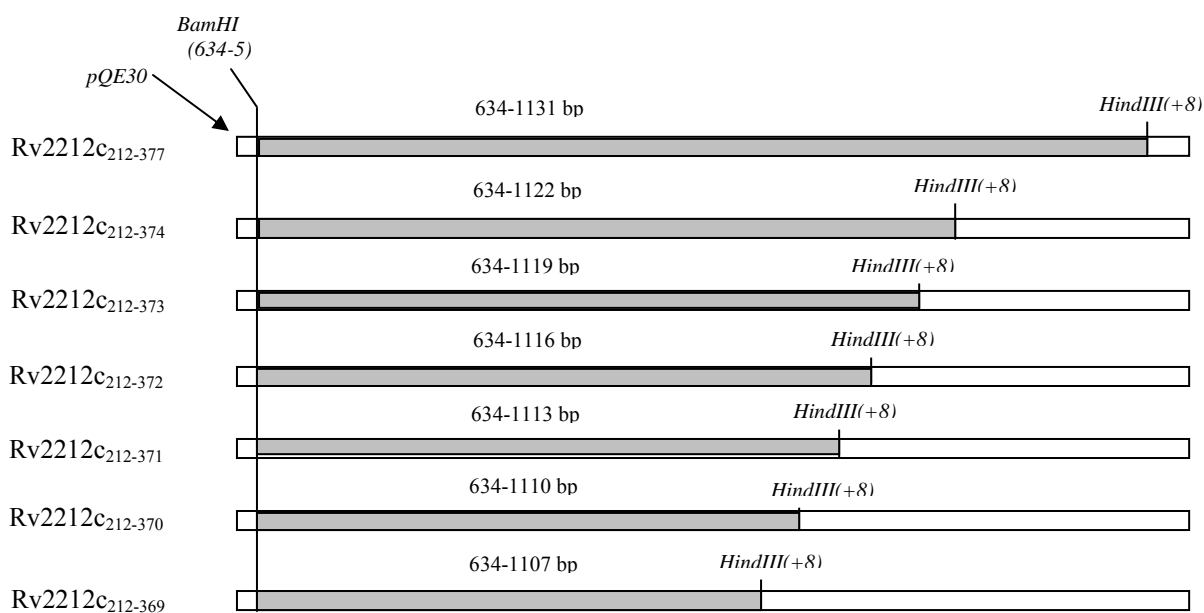


Fig. 3.8 : Cloning scheme for the C-terminally shortened Rv2212c₂₁₂₋₃₈₈ N-His constructs. The grey rectangles represent the constructs having different lengths. Base pair numbers are written above each rectangle. They are cloned into the same restriction site in pQE-30 (white rectangle).

3.4.2.4 Mutants of Rv2212c₂₁₂₋₃₇₀

Three different point mutations were introduced into Rv2212c₂₁₂₋₃₇₀ changing L₃₇₀ once to V, A or G. The recombinant DNA of Rv2212c₁₋₃₈₈ in pBluescript II SK(-) was used as a template and primer 2212s3 was used as the sense primer for the three mutants introducing a 5'-BamHI restriction site. The antisense primers used were mut.FEVas, mut.FEAAs and mut.FEGas for the mutants L370V, L370A and L370G respectively introducing a 3'-HindIII restriction site in each .

Each PCR fragment (492 bp) was ligated into a dephosphorylated EcoRV restricted pBluescript II SK(-), after Klenow treatment, transformed into E.coli XL1 blue MRF' and sequenced. The correct clones were digested with BamHI/HindIII and cloned into a dephosphorylated BamHI /HindIII digested pQE-30.

3.4.2.5 Shortening of Rv2212c₂₁₂₋₃₇₀ at the N-terminus

Successive N-terminal truncations were carried out in Rv2212c₂₁₂₋₃₇₀ in order to achieve the shortest possible active catalytic centre. Five truncations were made and each time the AC activity was tested until the construct having no activity was reached. The recombinant DNA of Rv2212c₁₋₃₈₈ in pBluescript II SK(-) was used as a template and primer 2212FELas was used as the antisense primer for these constructs introducing a 3'-HindIII restriction site. The following sense primers were used introducing a 5'-BamHI restriction site in each corresponding construct:

Rv2212c ₂₁₃₋₃₇₀ :	2212ASVs
Rv2212c ₂₁₄₋₃₇₀ :	2212SVTs
Rv2212c ₂₁₅₋₃₇₀ :	2212VTCs
Rv2212c ₂₁₆₋₃₇₀ :	2212TCGs
Rv2212c ₂₁₇₋₃₇₀ :	2212CGIs

The PCR fragments were ligated into a dephosphorylated EcoRV restricted pBluescript II SK(-), after Klenow treatment, transformed into E.coli XL1 blue MRF' and sequenced. The correct clones were then digested with BamHI/HindIII and cloned into a dephosphorylated BamHI/HindIII digested pQE-30 (fig. 3.9).

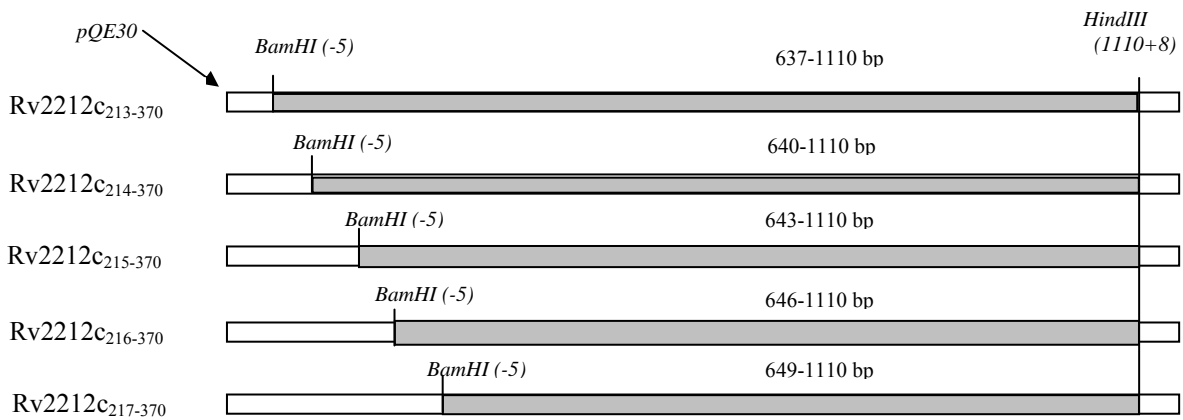


Fig. 3.9 : Cloning scheme for the N-terminally shortened constructs of Rv2212c₂₁₂₋₃₇₀. The grey rectangles represent the constructs having different lengths. Base pair numbers are written above each rectangle. They are cloned into the same restriction site in pQE-30 (white rectangle).

4 Results

4.1 Expression and characterization of the adenylyl cyclase Rv2435c of

M. tuberculosis

4.1.1 Sequence analysis of Rv2435c

At the TubercuList website, the *M. tuberculosis* Rv2435c gene product (GenBank accession number BX842577) is predicted to be a probable cyclase (adenylyl- or guanylyl-). It is topologically predicted as a membrane protein composed of an extracellular domain, two transmembrane helices as a membrane anchor and a C-terminal catalytic domain (fig. 4.1, SOSUI). It was classified together with Rv1625c with the eukaryotic ACs (McCue *et al.*, 2000), although it possesses four exchanges in the six canonical amino acids in-register that have been identified as participating in catalysis (Tesmer *et al.*, 1999; Yan *et al.*, 1997; Sunahara *et al.* 1998). One of the aspartate residues which is supposed to coordinate the metal cofactor, is exchanged for an asparagine, the substrate-defining lysine for an arginine and the transition state stabilizing asparagine and arginine for a serine and a glutamine respectively (fig. 4.2). Later, it was classified as a class IIIa AC (Linder and Schultz, 2003) as the arm region of class IIIa cyclase homology domains which is thought to be an essential feature for dimerization (Tesmer *et al.*, 1997), is conserved in length (14 residues between a conserved glycine and the substrate-defining aspartate, fig. 4.2). Other typical signature motifs of class IIIa adenylyl cyclases as the (F/Y)X₂(F/Y)D motif, which appears to participate in formation of the dimer interface (Tesmer *et al.*, 1997; Tang *et al.* 1995), shows up as a VX₂FD in Rv2435c and the EKIK motif as an ERIR (Linder and Schultz, 2003). The extracellular domain of this protein was reported to have homology to the ligand binding N-terminal domain of a chemotaxis receptor H (DcrH) in the anaerobic, sulphate-reducing bacteria *Desulfovibrio vulgaris* (Deckers and Voordouw 1996) (see appendix section 8.3). The deduced amino acid sequence of DcrH protein indicated a structural similarity to that of other methyl-accepting chemotaxis proteins (MCPs) (Deckers and Voordouw 1996; McCue *et al.*, 2000). Also the Protein-Protein BLAST search program at NCBI (Aug-26-2005; <http://www.ncbi.nlm.nih.gov/BLAST/> ; Altschul *et al.*, 1997) showed similarity of this domain to the MCPs in *Vibrio vulnificus*. An alignment of the Rv2435c catalytic domain with that of Rv1625c, rat type IIC2 and canine type VC1 ACs revealed extensive similarities (fig. 4.2). The identity to Rv1625c CHD was 32% and the similarity 55%. Similar values were obtained with C₂ from rat AC type II and C_{1a} from canine AC type V; an identity of 30% and 26%, and a similarity of 49% and 48%, respectively.

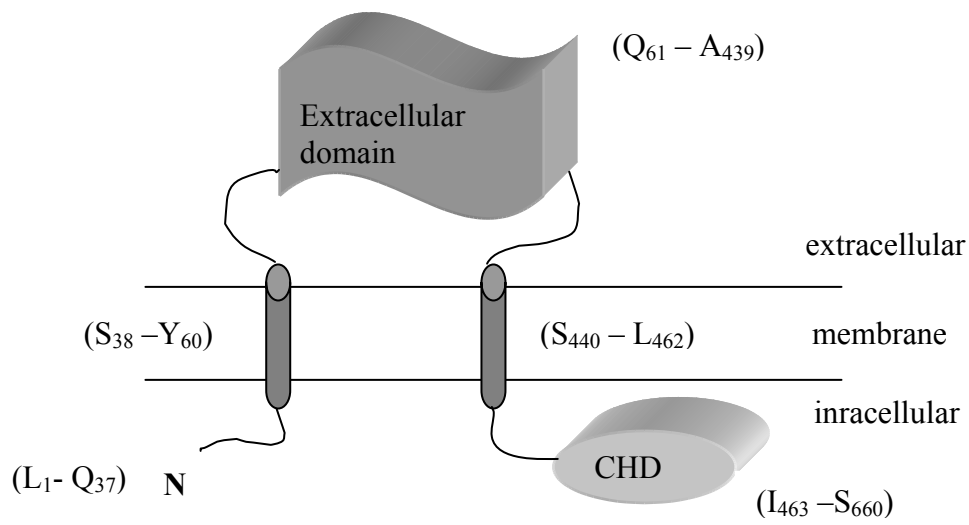


Fig. 4.1: Topological prediction of Rv2435c from *M. tuberculosis* (SOSUI-prediction of transmembrane regions; http://sosui.proteome.bio.tuat.ac.jp/cgi-bin/adv_sosui.cgi). Amino acid residues for each domain are in brackets.

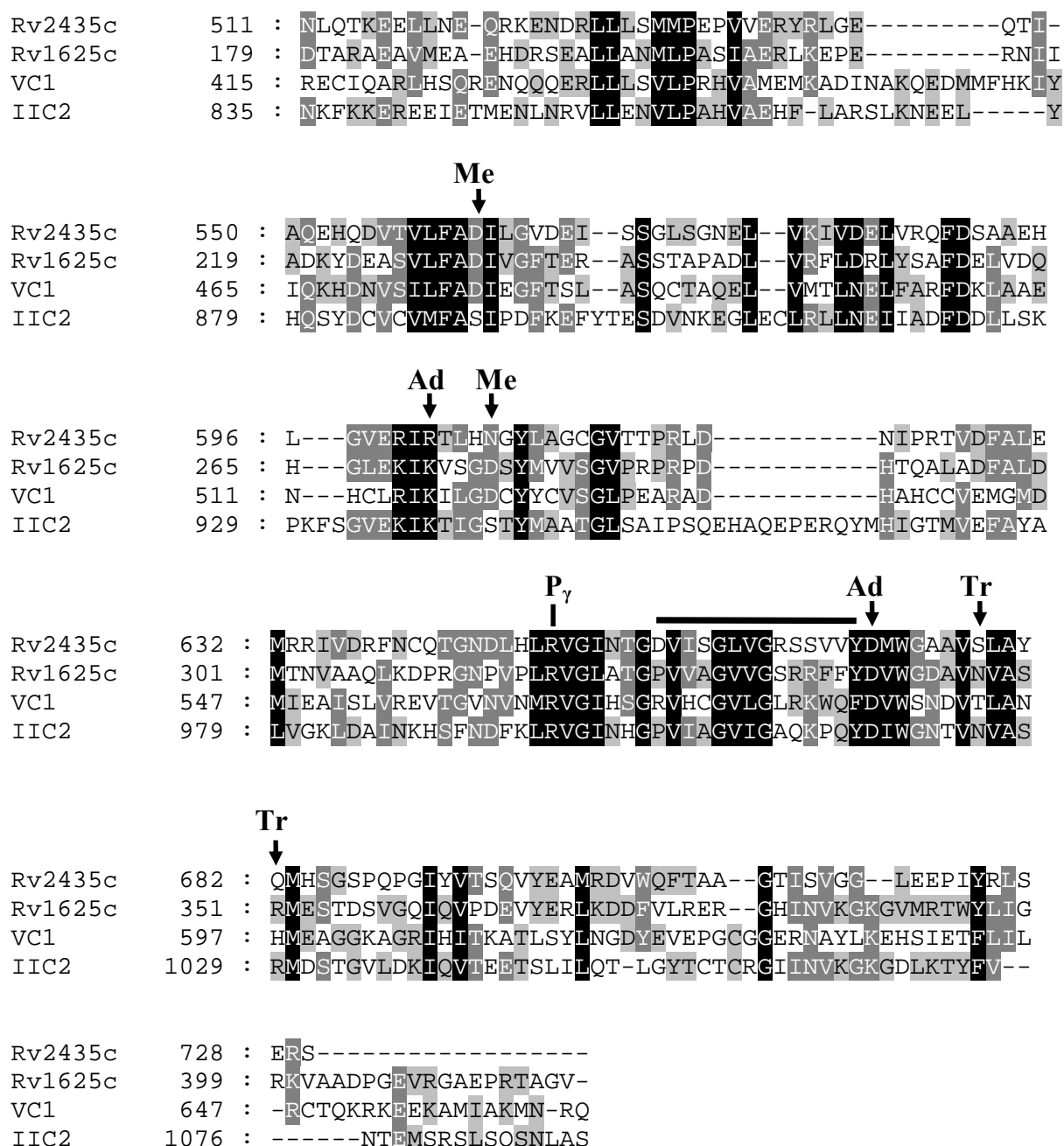


Fig. 4.2 : Alignment of the CHDs of Rv2435c and Rv1625c from *M. tuberculosis* with C₁-domain from canine type V (VC₁) and C₂-domain from rat type II (IIC₂) ACs. These two mammalian domains were chosen because of the available X-ray structures (Tesmer *et al.*, 1997, 1999; Zhang *et al.*, 1997). The six canonical residues involved in catalysis are marked (Me: metal-cofactor, Ad: adenine/purine specifying, Tr: transition-state stabilizing). Note that the position of the γ -phosphate binding Arg (P _{γ}) is also indicated. The top bar specifies the so called arm region.

4.1.2 Expression and characterization of adenylyl cyclase Rv2435c₅₁₁₋₇₃₀

4.1.2.1 Expression and purification

The protein Rv2435c₅₁₁₋₇₃₀ has a calculated MW of 25,19 kDa (including the N-terminal His₆-tag) and an isoelectric point of 4.8. It was expressed in E.coli for 5 hours with 60 μ M IPTG at 22°C. Cells were lysed by sonication and the protein was purified to homogeneity after absorption to Ni²⁺-NTA agarose for 60 min. The yield was 114 μ g/200 ml. Expression overnight yielded 450 μ g/200 ml. The protein was either stored at -20 °C with 20% glycerol, or dialyzed overnight to remove imidazole and tested immediately.

All fractions were analyzed by SDS-PAGE (fig. 4.3).

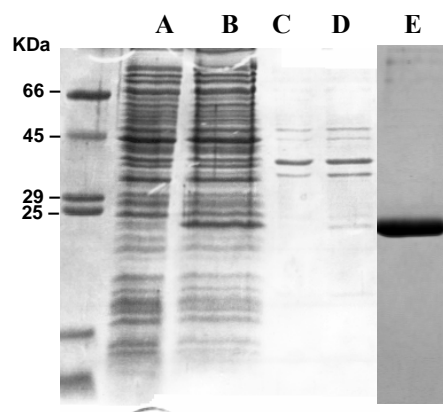


Fig.4.3: 15% SDS-PAGE. Supernatant and pellet of empty pQE-30 in BL21 cells as a control (lanes **A** and **C**), and (lanes **B** and **D**) from cells expressing homogenate of Rv2212c₅₁₁₋₇₃₀. 2 μ g of purified Rv2212c₅₁₁₋₇₃₀ (lane **E**). The majority of the protein can be seen in the supernatant at 25 kDa indicating the solubility of the protein.

1 ml of the expression culture was taken after 2 hours of expression, centrifuged, pellets washed with pellet washing buffer, centrifuged, resuspended in cell lysis buffer and centrifuged once again (Eppendorf Kühl 15 min/14000 rpm/4°C) after sonication. 15 μ l of the supernatant were mixed with 5 μ l SDS-buffer and 15 μ l were then loaded on the gel. The pellets (about 20 mg) were suspended in 50 μ l H₂O, mixed with 50 μ l SDS-buffer and after centrifugation 5 μ l from the supernatant were loaded on the gel.

4.1.2.2 Adenylyl cyclase activity

AC tests were carried out to assay for AC-activity. The following tests were done and all showed no activity:

- 40 μ l of each of the supernatant and pellet (fig. 4.3 lanes B and D) were tested with 75 μ M ATP for 10 min at 37°C, pH 7.5 (TRIS/HCl) and 3 mM MnCl₂.
- 3.8 and 7.6 μ g of the purified Rv 2212c₅₁₁₋₇₃₀ (fig. 4.3 lane E) were tested with 75 μ M ATP for 10 min at 37°C, pH 7.5 (TRIS/HCl), using 3 mM MnCl₂ or 10 mM MgCl₂.
- 9.6 μ g of the purified Rv 2212c₅₁₁₋₇₃₀ were tested with 500 μ M ATP for 10 min at 37°C at different pH values; acetic acid (4.5), MOPS/TRIS (6.4) and TRIS/HCl (7.5 & 9), using 3 mM MnCl₂ or 5 mM MgCl₂.
- 9.6 μ g of the purified Rv 2212c₅₁₁₋₇₃₀ were also tested with 500 μ M ATP for 10 min at 37°C, pH 7.5 (TRIS/HCl), 3 mM MnCl₂ and 100 μ M NAD⁺.
- 10 and 20 μ g of dialyzed Rv 2212c₅₁₁₋₇₃₀ were tested with 100 μ M ATP for 15 min at 37°C, pH 7.5 (TRIS/HCl), using 3 mM MnCl₂ or 10 mM MgCl₂.

4.1.2.3 Guanylyl cyclase activity

GC activity of 10 and 20 μ g of the dialyzed protein was tested with 100 μ M GTP for 15 min at 37°C, pH 7.5 (TRIS/HCl), using 3 mM MnCl₂ or 10 mM MgCl₂. No GC activity was detected.

4.1.3 Expression and characterization of the adenylyl cyclase Rv2435c

holoenzymes

4.1.3.1 Expression of Rv2435c₁₋₇₃₀

The protein has a calculated MW of 80.3 kDa and an isoelectric point of 5.5. It was first expressed in E.coli with 60 μ M IPTG at 22°C overnight. No expression was detected in the supernatant or pellet as assayed by a 10 % SDS-PAGE or by Western blotting (exposure time up to 3 min). Thus expression was carried using different concentrations of IPTG (30, 120 and 500 μ M) at 16°C overnight. Protein was not detectable in the supernatants or pellets on a 10 % SDS-PAGE, but it was faintly detected on a Western blot (fig. 4.4, a). A more pronounced band was visible at about 25 kDa which demonstrated degradation. This band appeared more prominent in the supernatant. Induction with three different concentrations of IPTG did not seem to have remarkable effects. No purification was attempted with the protein.

Results

4.1.3.2 Expression of Rv2435c₂₅₋₇₃₀ and Rv2435c₄₁₋₇₃₀

Rv2212c₂₅₋₇₃₀ and Rv2212c₄₁₋₇₃₀ have MWs of 77.55 and 75.79 kDa, respectively. Both proteins were expressed in E.coli with 60 μ M IPTG at 22°C overnight. Again no clear band at approximately 80 kDa could be detected in the supernatants and pellets by a 10 % SDS-PAGE or by a Western blot (exposure time up to 3 min). So expression was carried out again with different concentrations of IPTG (120 and 500 μ M) at 16°C overnight. Both proteins were not detected in the supernatants and pellets on a 10 % SDS-PAGE, but were detected on Western blots (fig. 4.4, b and c).

Rv 2212c₂₅₋₇₃₀ appeared as a faint band at about 80 kDa and was more apparent in pellets than in the supernatant. A strong band was detected at about 25 kDa which shows that most of the protein was degraded (fig. 4.4, b). Rv 2212c₄₁₋₇₃₀ was detected only as a thick band at about 25 kDa indicating that all of the protein was degraded (fig. 4.4, c). Attempts for further purification of both proteins were not carried out.

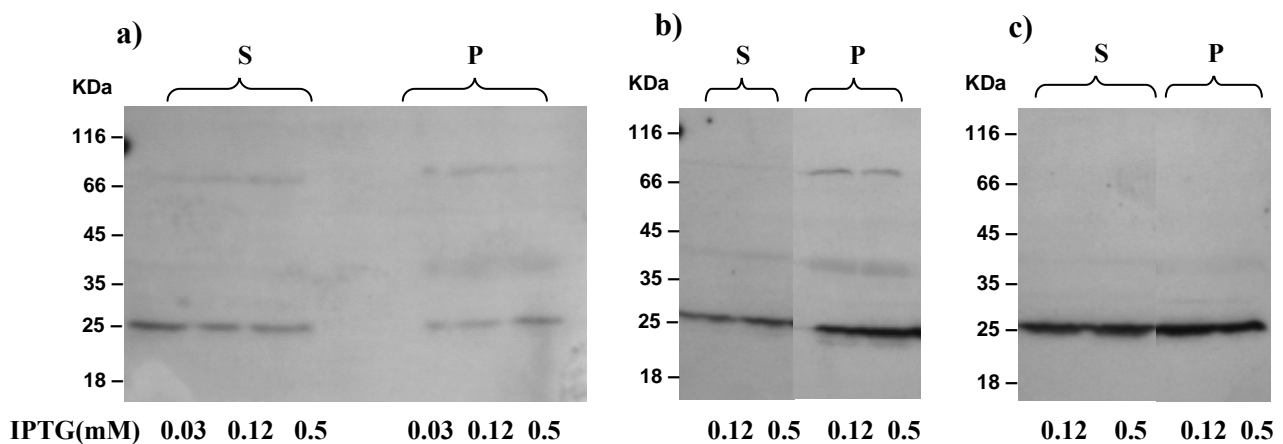


Fig. 4.4: Western blot from 10 % SDS-PAGE using the Penta-His antibody as the primary antibody. (a) Rv2212c₁₋₇₃₀; about 30 and 15 μ g protein were applied in each lane from the supernatants and pellets resp. (b) Rv2212c₂₅₋₇₃₀; 23.7 and 14.7 μ g protein were applied in each lane from the supernatants and pellets resp. (c) Rv2212c₄₁₋₇₃₀; 19.3 and 48 μ g protein were applied in each lane from the supernatants and pellets, respectively. S = supernatant, P = pellet.

4.1.3.3 Adenylyl cyclase activity

An AC-test was carried out to test whether any of the three constructs had AC activity. The supernatants (78.4, 63.2 and 51.6 μ g protein) as well as the pellets (75.6, 73.6 and 240 μ g

protein) of each construct were tested with 100 μ M ATP for 10 min at 37°C, pH 7.5 (TRIS/HCl) and 3 mM $MnCl_2$. No activity was measurable. Because of this general failure we discontinued work with gene product of Rv2435c and continued with gene Rv2212c, another of the 15 predicted mycobacterial ACs.

4.2 Expression and characterization of adenylyl cyclase Rv2212c of

M. tuberculosis

4.2.1 Sequence analysis of Rv2212c

Gene Rv2212c (GenBank accession number BX842576) codes for a soluble protein which is predicted to be composed of two distinct domains; a C-terminal catalytic domain (cyclase homology domain; CHD) and an N-terminal domain which represents a novel protein domain possessing sequence similarities to the N-termini of other bacterial ACs as its homolog from *M. smegmatis*, Rv1264 from *M. tuberculosis* and its homolog from *M. smegmatis*, one from *B. liquefaciens* (GeneBank accession number X57541), one from *Streptomyces coelicolor* (GeneBank accession number AL512667) and one from *S. griseus* (GeneBank accession number AB018557) (Linder *et al.*, 2002). An alignment of Rv2212c CHD with the mammalian C_{1a} catalytic segment from canine type V and the C₂ segment from rat type II revealed considerable similarities and the conservation of the six amino acids annotated to be participating in catalysis (fig. 4.5). This unequivocally classifies the protein as a class III AC, probably operating as a homodimer. Recently, it was identified as a class IIIc AC catalyst which have a considerably shortened arm region (only 7 instead of 15 amino acids between the conserved glycine and the substrate defining aspartate outlined in fig. 4.5) (Linder and Schultz, 2003; Tesmer *et al.*, 1997).

Rv2212c and Rv1264, another class IIIc mycobacterial AC, share significant sequence similarity in their N-terminal domains (21% identity and 31% similarity) as well as catalytic domains (29% identity and 41% similarity) (fig. 4.6). These common features support the hypothesis of a similarity in AC regulation. Therefore attempts to crystallize Rv2212c were made for comparison with the known structure of Rv1264. Furthermore, the potential regulation of Rv2212c AC was analyzed.

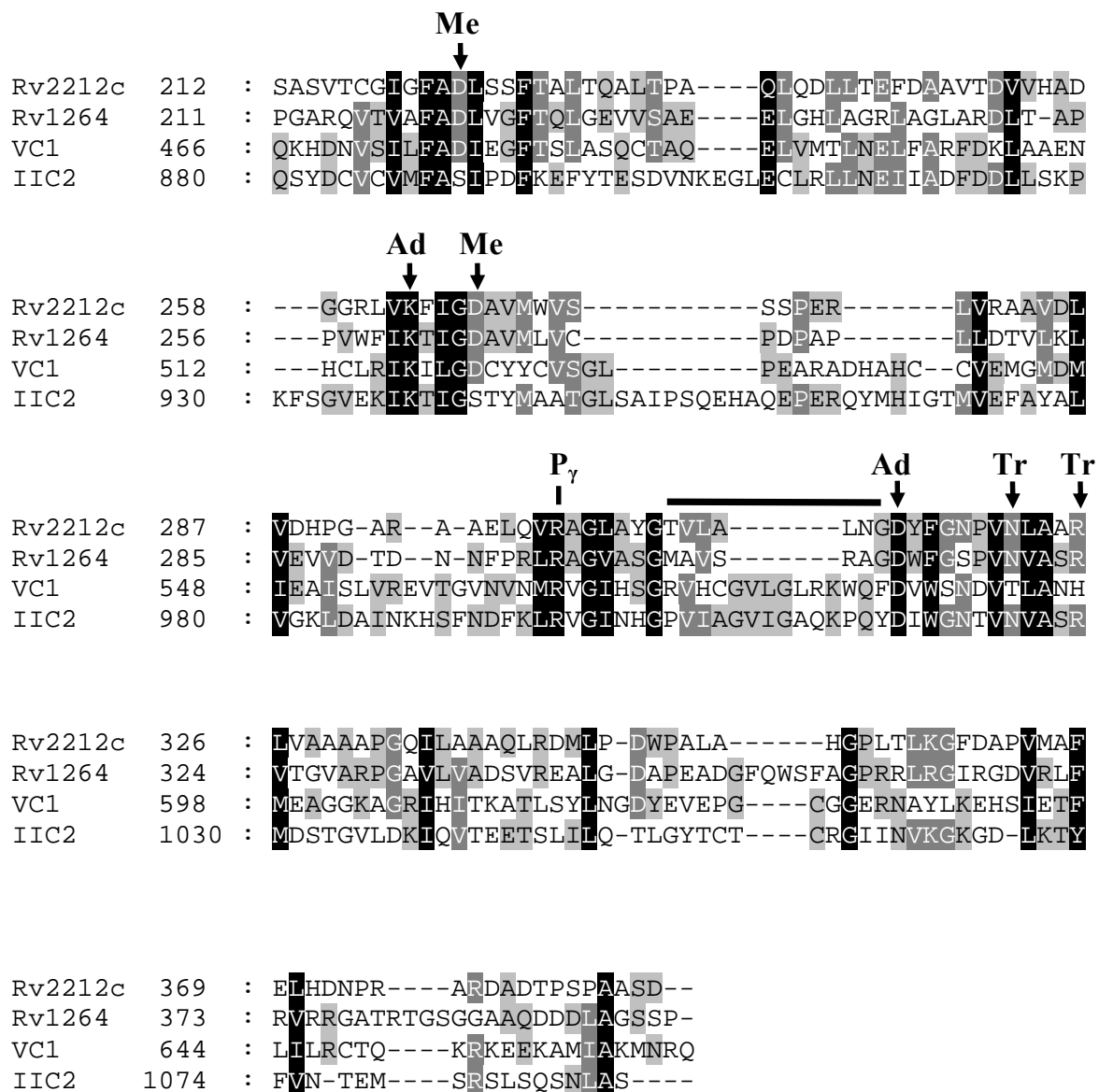


Fig. 4.5: Alignment of the CHDs of Rv2212c and Rv1264 from *M. tuberculosis* with C₁-domain from canine type V (VC₁) and C₂-domain from rat type II (IIC₂) adenylyl cyclases. These two mammalian domains were chosen because of the available X-ray structures (Tesmer *et al.*, 1997, 1999; Zhang *et al.*, 1997). The six canonical residues involved in catalysis are marked (Me: metal-cofactor, Ad: adenine/purine specifying, Tr: transition-state stabilizing). The position of the γ -phosphate binding Arg (P _{γ}) is also indicated. The top bar specifies the so called arm region. VC₁ and IIC₂ show an identity of 19% and 18%, and a similarity of 31% and 34% to Rv2212c CHD, respectively.

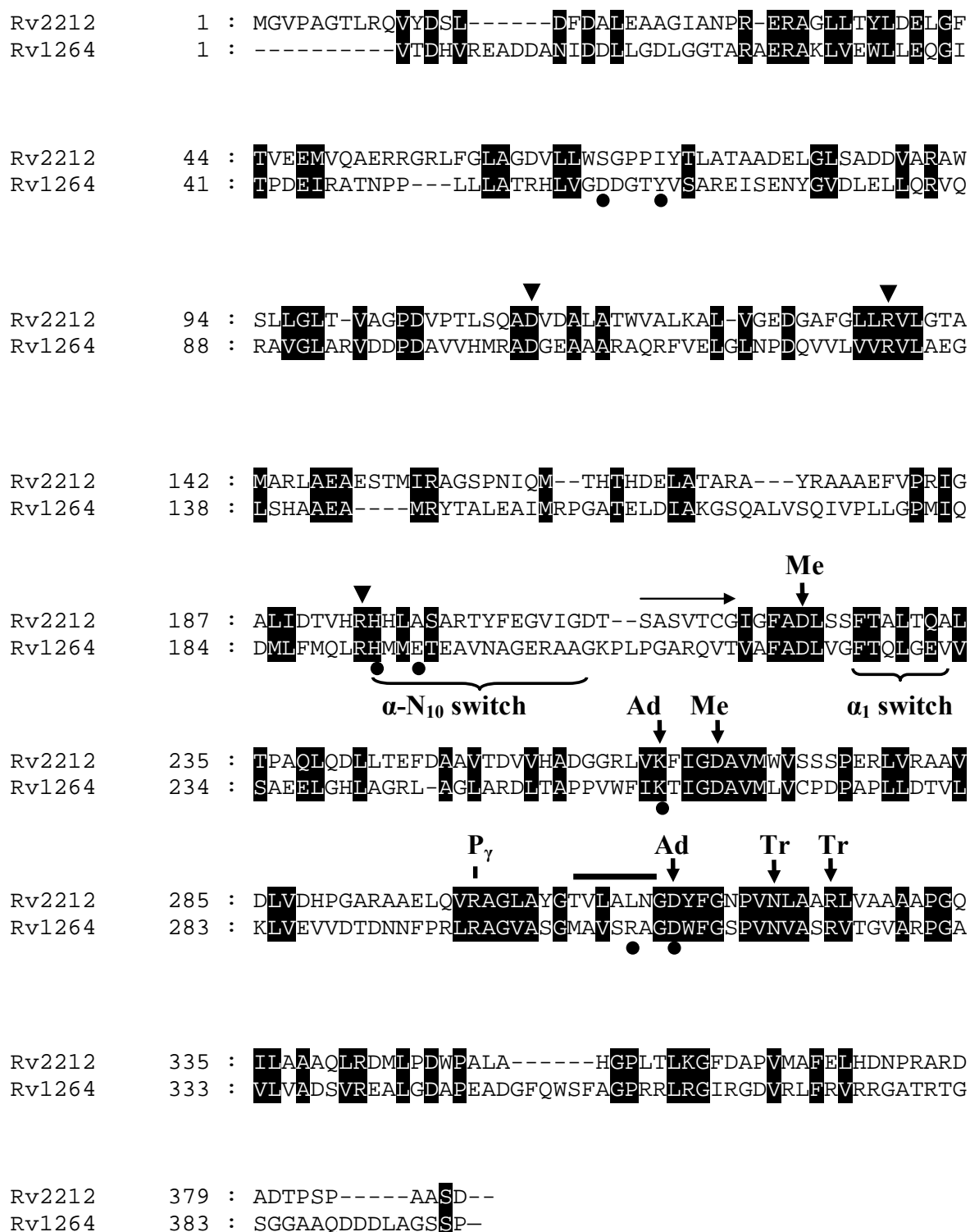


Fig. 4.6: Alignment of Rv2212c and Rv1264 holoenzymes from *M. tuberculosis*. The start of the CHD is marked with a horizontal arrow pointing to the right. Three inverted triangles mark the three polar residues shown to be conserved in the N-terminal domains of seven other Gram-positive bacteria (Linder *et al.*, 2002). The six canonical amino acids are marked by arrows and the γ -phosphate binding (P_γ) Arg is indicated by a vertical line. The top bar specifies the so called arm region. Ad, adenine ring binding; Me, metal-cofactor binding; Tr, transition state stabilizing. Residues identified by mutagenesis to be important for the interaction between the regulatory and catalytic domains in Rv1264 are indicated by black dots beneath them, also the α -N₁₀ switch and the α_1 switch are clearly determined (Tews *et al.*, 2005).

4.2.2 Expression and characterization of adenylyl cyclase Rv2212c

N-terminal domain

Rv2212c₁₋₂₀₂ was expressed and purified for crystallization purposes.

4.2.2.1 Expression and purification

Rv2212c₁₋₂₀₂ has a calculated MW of 23.43 kDa (including the N-terminal His₆-tag). It was expressed in E.coli for 5 hours with 60 μ M IPTG at 22°C. Cells were lysed by sonication, treated with lysozyme and DNaseI and the protein was purified to homogeneity by affinity chromatography on Ni²⁺-NTA. The purified protein yield was 2.6 mg/400 ml culture. The protein was either stored at -20 °C with 20% glycerol or concentrated for crystallization (see section 3.3.3) and stored at 4°C. The supernatants, pellets and purified Rv2212c₁₋₂₀₂ were analyzed on SDS-PAGE (fig. 4.7).

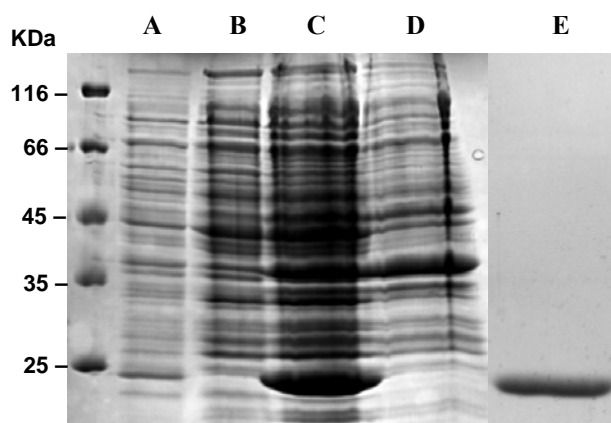


Fig. 4.7: 12.5% SDS-PAGE showing supernatants and pellets of empty pQE-30 in BL21 cells as a control (lanes **B** and **D**), supernatants and pellets of the construct (lanes **A** and **C**). 15% SDS-PAGE with 1.7 μ g of Ni²⁺-NTA purified Rv2212c₁₋₂₀₂ (lane **E**). 1 ml of the expression culture was taken after 2 1/2 hours of expression (see legend of fig. 4.3 for details).

4.2.2.2 Crystallization of Rv2212c₁₋₂₀₂

The first crystals were obtained with buffer CS#19 from the Hampton research kit. Variation of the crystallization conditions and buffer concentrations were carried out to optimize the size and quality of the crystals (table 4.1, fig. 4.8).

Crystallization buffer	Protein solution	Protein concentration	Crystal form	Remarks
30% isopropanol, 0.1 M TRIS/HCl pH 8.5, 0.2 M CH ₃ COO NH ₄ (CS#19)	10 mM TRIS/HCl, pH 7.5, 1mM MgCl ₂ , 0.05% α -monothioglycerol	19.7 mg/ml	Tiny prisms (see fig. 4.8, a)	After 4 days at 16°C, and 7 days at 12°C
Optimization based on buffer CS#19 (0.1 M TRIS/HCl, pH 8.5 constant)				
30% isopropanol, 0.17 M CH ₃ COO NH ₄	10 mM TRIS/HCl, pH 7.5, 1mM MgCl ₂ , 0.05% α -monothioglycerol	19.7 mg/ml	Styloid prisms 25×50 μ	After 7 days at 16°C
30% isopropanol, 0.2 M CH ₃ COO NH ₄			Styloid prisms 10×20 μ	After 7 days at 16°C
30% isopropanol, 0.22 M CH ₃ COO NH ₄			Styloid prisms 50×100 μ (see fig. 4.8,b)	After 7 days at 16°C
31% isopropanol, 0.2 M CH ₃ COO NH ₄			Styloid prisms 15×20 μ	After 7 days at 16°C
32% isopropanol, 0.17 M CH ₃ COO NH ₄			Styloid prisms 25×50 μ (see fig. 4.8, c)	After 7 days at 16°C

Table 4.1: Brief summary of the conditions in which crystals of Rv2212_{c1-202} were grown. (CS#19 = Crystal Screen buffer no.19 ; the numbering is according to the Hampton research kit).

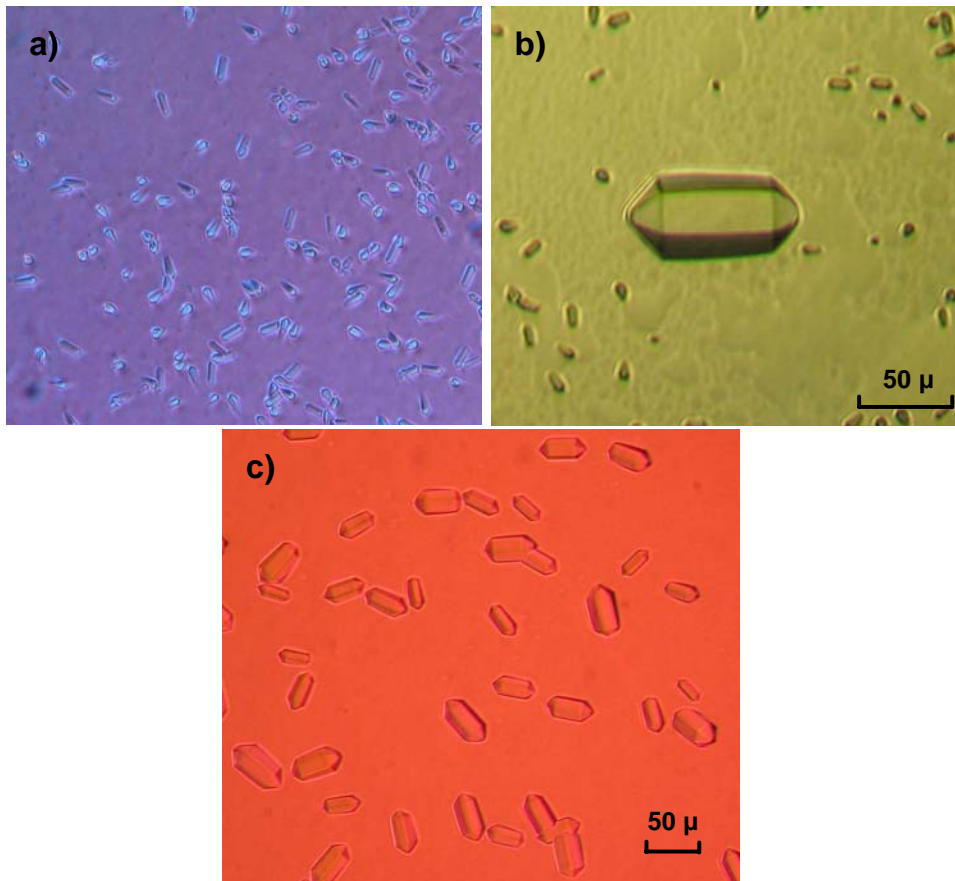


Fig. 4.8: Crystals of Ni²⁺-NTA purified Rv2212c₁₋₂₀₂ as outlined in table 4.1. The crystals did not diffract (Dr. Ivo Tews, BZH, Universität-Heidelberg).

4.2.3 Expression and characterization of adenylyl cyclase Rv2212c catalytic domain (Rv2212c₂₁₂₋₃₈₈)

4.2.3.1 Expression and purification

The clone for this protein was from S. Zeibig (2003) in pQE-30 in BL21 cells. It was expressed in E.coli with 60 μM IPTG at 22°C for 4 hours. Cells were lysed by sonication and treated with lysozyme and DNaseI. The protein was purified to homogeneity by affinity chromatography on Ni²⁺-NTA (fig. 4.9). The yield was 360 μg/200 ml culture. The protein yield was not improved upon overnight expression at 16 °C. Protein was stored at -20 °C with 20% glycerol.

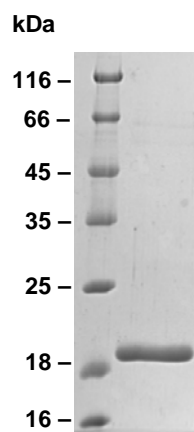


Fig. 4.9: 15% SDS-PAGE of Rv2212_{c212-388}. 2.3 μg of Ni^{2+} -NTA purified protein was applied. MW = 20.46 kDa, pI = 4.4.

4.2.3.2 Protein dependence

A protein range from 5 to 140 nM (10 to 280 ng) was tested. The specific activity increased linearly up to 50 nM. Further protein increments resulted in decrease in specific activity (fig. 4.10) suggesting formation of inactive oligomers at high protein concentrations. Half maximal activity was attained at 20 nM protein, indicating a high affinity of the catalytic domains for each other.

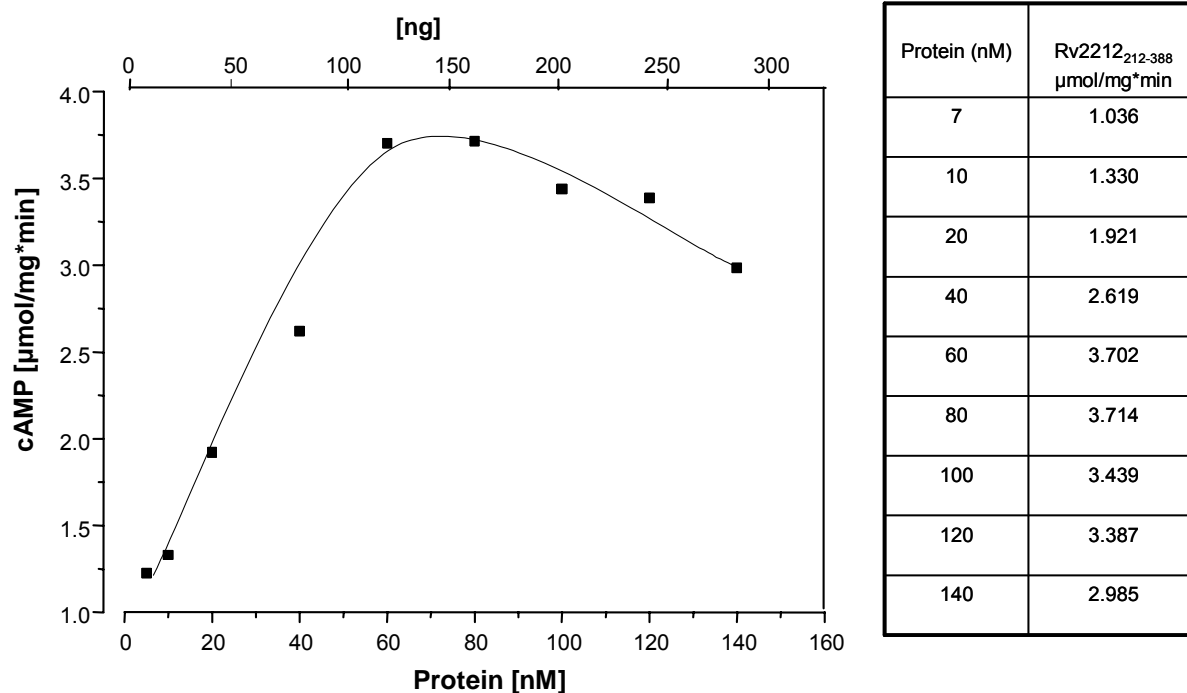


Fig. 4.10: Protein dependence of Rv2212_{c212-388}. Assay conditions: 500 μM ATP, 3 mM Mn^{2+} , BIS-TRIS/HCl, pH 6.5, 37°C, 10 min.

4.2.3.3 Enzyme kinetics

The kinetic properties of the catalytic domain were investigated. The V_{\max} and K_m values were calculated from a Hill-Plot, as a calculation after Lineweaver-Burk was not possible due to cooperativity, as indicated by a sigmoidal Michaelis-Menten curve (fig. 4.11). The V_{\max} was $26 \pm 0.5 \mu\text{mol}/\text{mg}\cdot\text{min}$ which is high compared to catalytic domains of other mycobacterial ACs. Also the K_m value of $2.1 \pm 0.01 \text{ mM}$ ATP, is higher than the K_m of the other mycobacterial ACs indicating a rather low ATP affinity. (Castro *et al.*, 2005; Guo *et al.*, 2001; Linder *et al.*, 2002, 2004; Sinha *et al.*, 2005; Tang and Hurley, 1998). The Hill-coefficient of 1.4 ± 0.02 indicated cooperativity ($n = 2$).

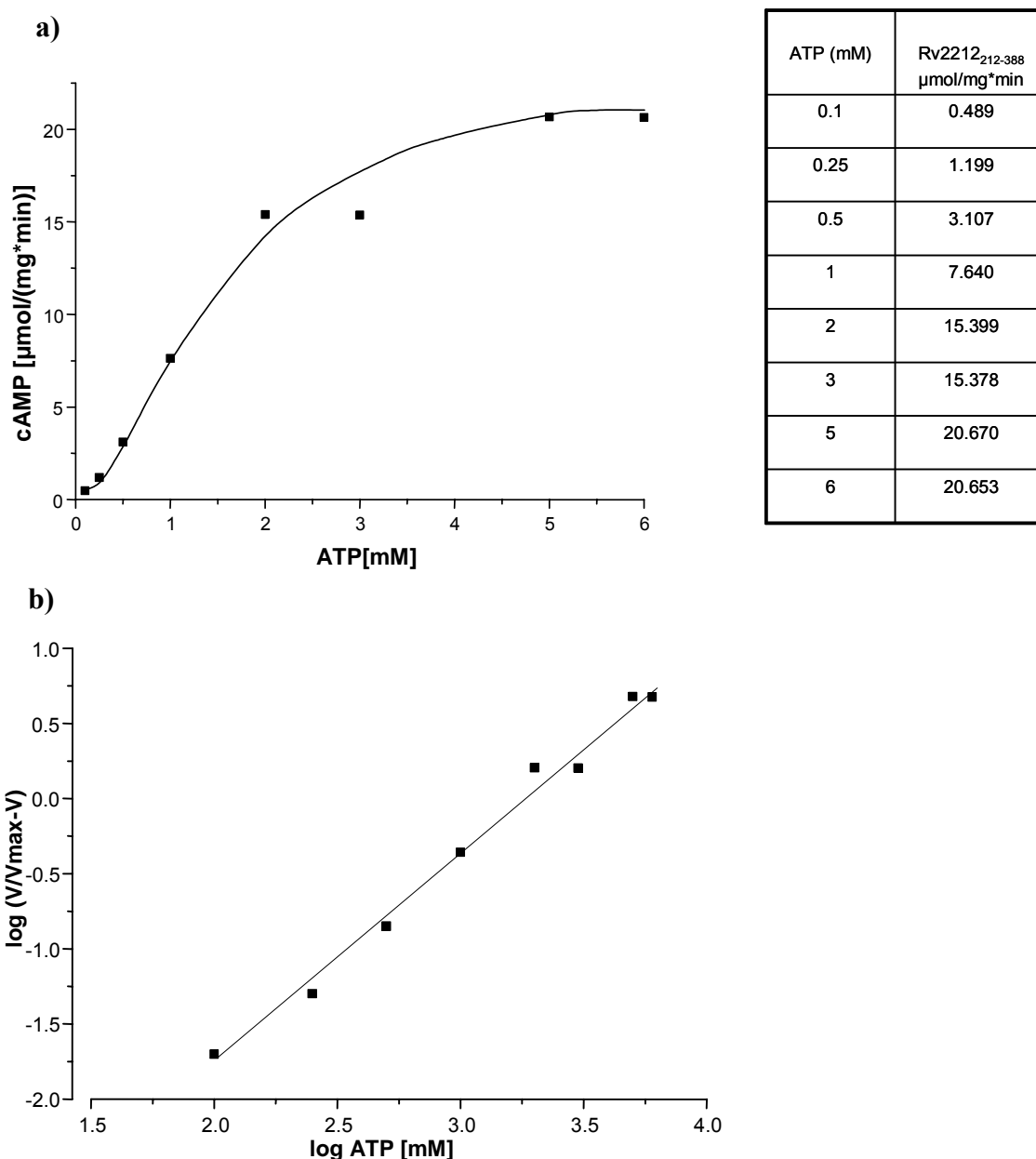


Fig. 4.11: a) Michaelis-Menten curve of Rv2212₂₁₂₋₃₈₈. The assay was conducted at 0.15 μg (75nM) protein, BIS-TRIS/HCl buffer pH 6.5, 10 mM Mn^{2+} at 37°C and for 10 min. b) Corresponding Hill-Plot ($y = 1.405x - 4.5815$; $R^2 = 0.9904$).

4.2.3.4 Time dependence

The curve (fig. 4.12) shows a linearity of cAMP formation for up to 16 min.

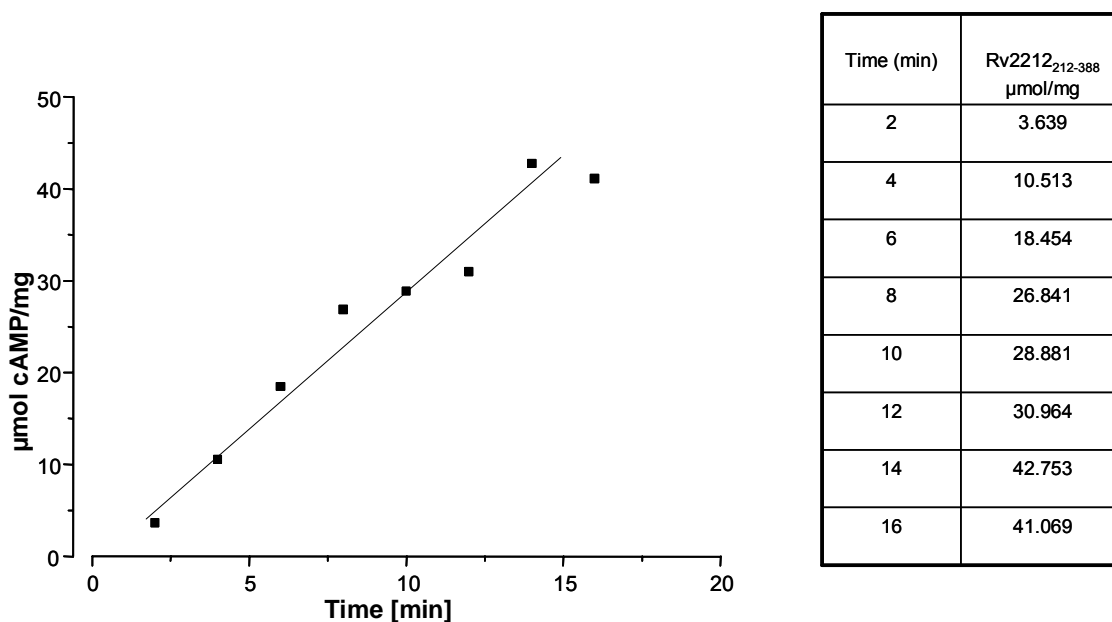


Fig. 4.12: Time dependence of Rv2212c₂₁₂₋₃₈₈. Assay conditions: 100 nM protein, 500 µM ATP, 3 mM Mn²⁺, BIS-TRIS/HCl pH 6.5, 37°C.

4.2.3.5 pH dependence

Different pH values strongly influenced AC activity. Protein was tested at different pH values (4.9-8.0) using 3 different buffer systems (fig. 4.13). An overlap in the pH values when changing the buffer system was intended to show the effect of buffer substance on enzyme activity. The pH optimum was at pH 6.5 (BIS-TRIS/HCl), therefore it was used in all subsequent assays. At pH 8, the activity increases clearly once again to 0.545 ± 0.01 µmol/mg*min (n = 6).

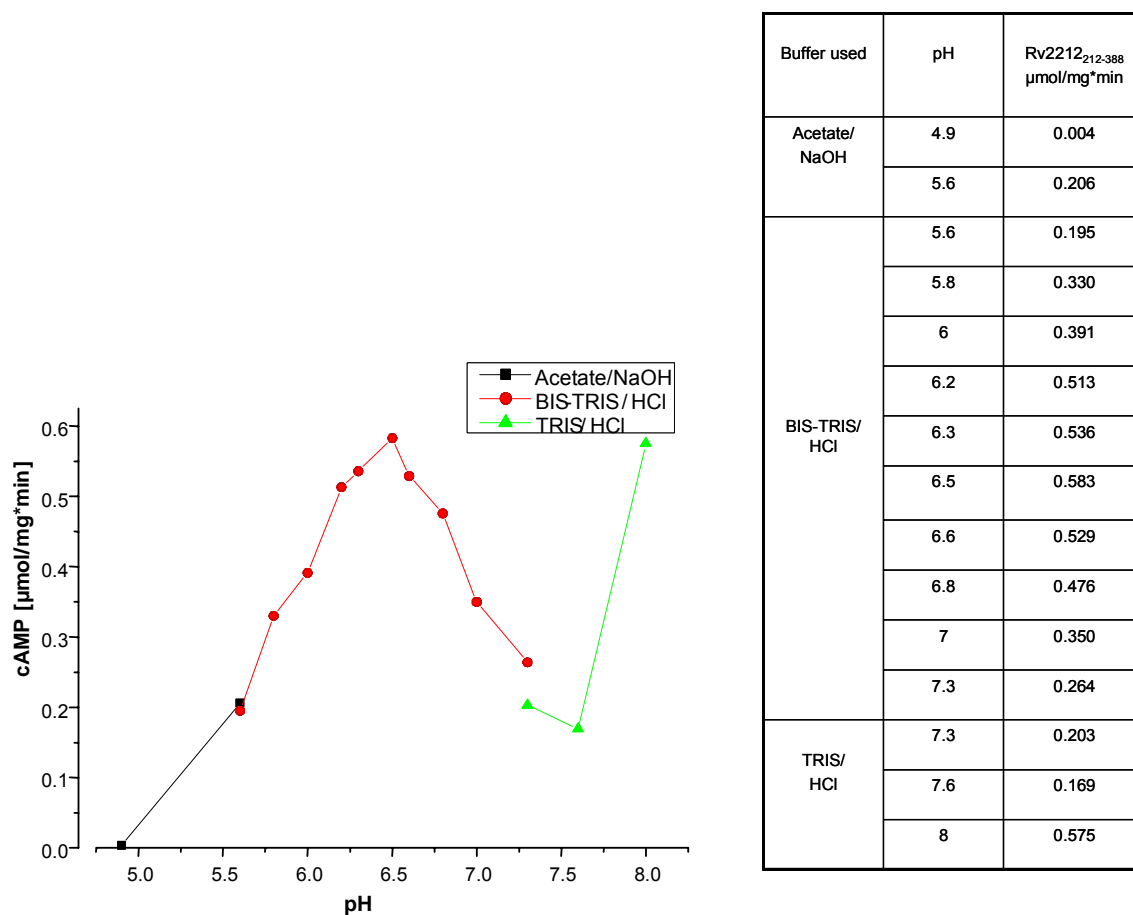


Fig. 4.13: pH dependence of Rv2212c₂₁₂₋₃₈₈. Assay conditions were 200 nM (0.4 µg) protein, 500 µM ATP, 3 mM Mn²⁺, 37°C, 10 min.

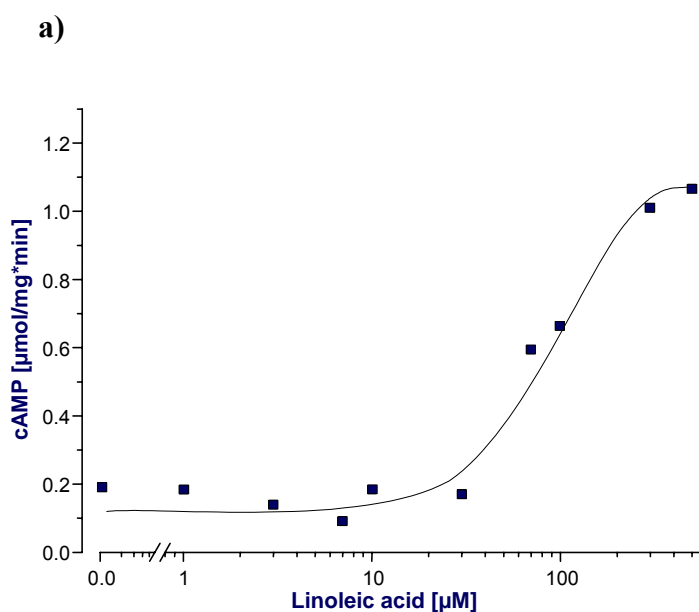
4.2.3.6 Effect of phospholipids

As 70 µM of each of phosphatidyl ethanolamine and phosphatidyl choline inhibited the activity of Rv2212c holoenzyme (see section 4.2.7.5.4), it was worth testing the corresponding effect on the Rv2212c₂₁₂₋₃₈₈. Both phospholipids were prepared as stated beneath 4.2.7.5.4 and tested with 100 nM Rv2212c₂₁₂₋₃₈₈ using 500 µM ATP, 3 mM Mn²⁺, BIS-TRIS/HCl pH 6.5 at 37°C for 10 min. 70 µM phosphatidyl ethanolamine caused 50% reduction in activity while 1 mM phosphatidyl choline induced about 30% inhibition.

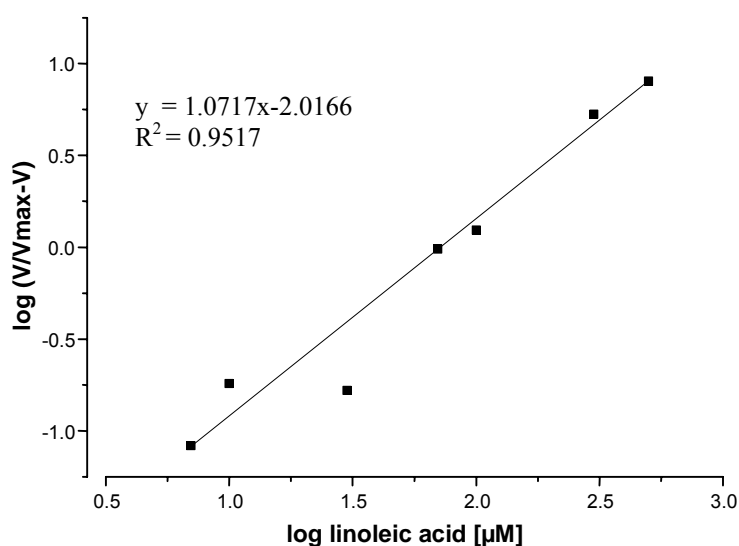
4.2.3.7 Effect of fatty acids

Fatty acids which turned out to stimulate holoenzyme activity (see section 4.2.7.5.5), were tested with Rv2212c₂₁₂₋₃₈₈ to determine whether these stimulatory effects were mediated by the regulatory N-terminal domain. Fatty acid solutions were prepared as stated in 4.2.7.5.5 and a concentration range 1-500 µM was tested. Linoleic acid (500 µM) stimulated the CHD

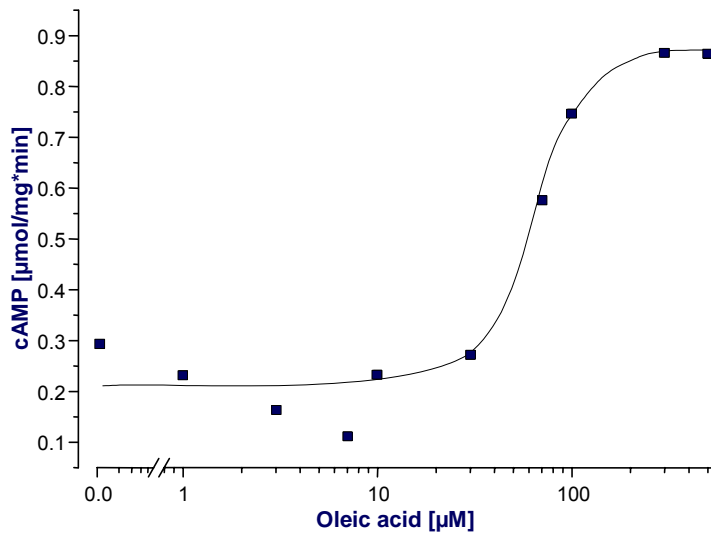
activity 5-fold while oleic and arachidonic acid (300 μM and 70 μM , respectively) caused a 3-fold increase in activity (fig. 4.14). The Hill coefficient of 1.0 denoted no cooperativity (table 4.2). Arachidonic acid stimulated Rv2212_{c212-388} with an EC_{50} of $10 \pm 0.05 \mu\text{M}$ (table 4.2). Linolenic and palmitic acids did not stimulate up to 500 μM . V_{max} and the Hill coefficient of Rv2212_{c212-388} were unaffected in the presence of 100 μM linoleic acid, while K_m decreased slightly (table 4.3).



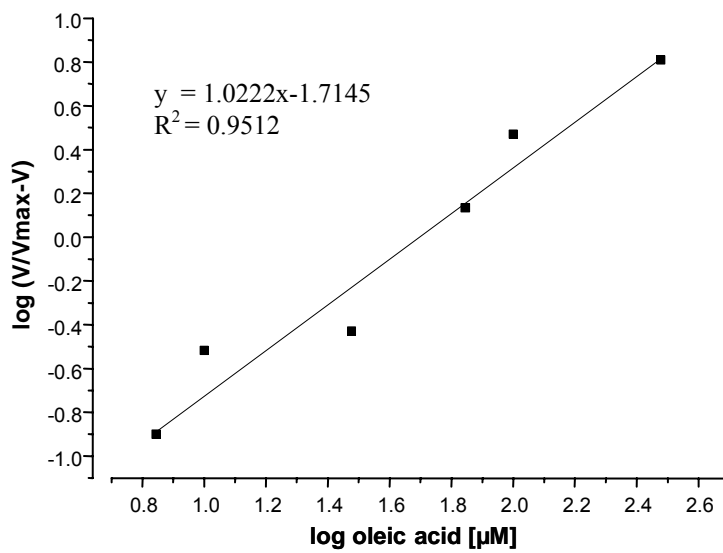
Linoleic acid (μM)	Rv2212 _{c212-388} ($\mu\text{mol/mg*min}$)
0	0.204
1	0.184
3	0.140
7	0.092
10	0.184
30	0.171
70	0.594
100	0.664
300	1.010
500	1.067



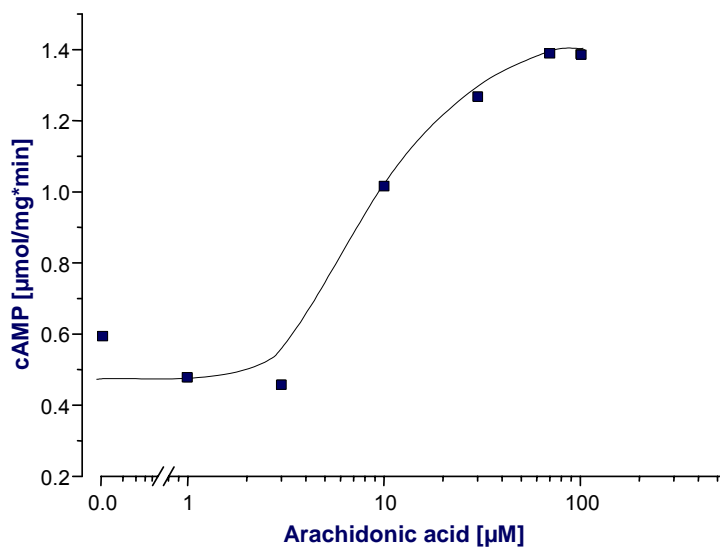
b)



Oleic acid (µM)	Rv2212 ₂₁₂₋₃₈₈ µmol/mg*min
0	0.333
1	0.232
3	0.164
7	0.112
10	0.233
30	0.272
70	0.577
100	0.747
300	0.866
500	0.864



c)



Arachidonic acid (µM)	Rv2212 ₂₁₂₋₃₈₈ µmol/mg*min
0	0.601
1	0.478
3	0.458
10	1.016
30	1.268
70	1.391
100	1.387

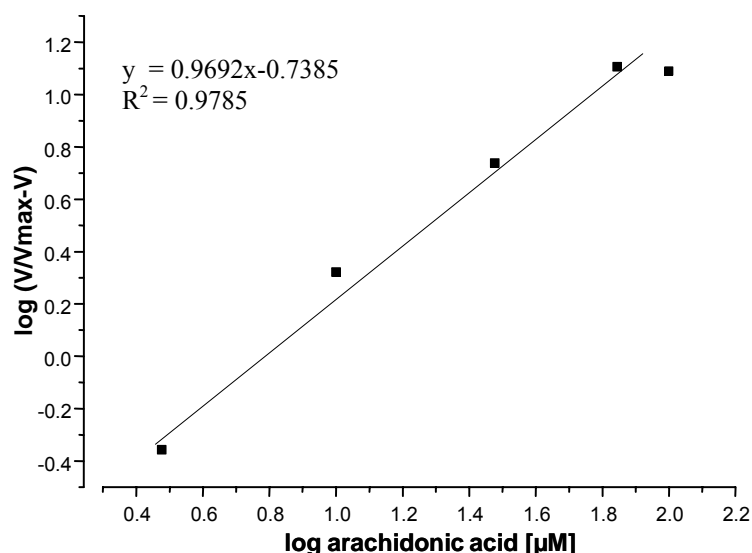


Fig. 4.14: Dose–response curves of linoleic, oleic and arachidonic acid stimulation of Rv2212c₂₁₂₋₃₈₈ and the corresponding Hill plots (**a**, **b** and **c**) Assay conditions were 200 nM protein, 500 μM ATP, 3 mM Mn^{2+} , BIS-TRIS/HCl pH 6.5, 37°C, 10 min. For each fatty acid dilution, a control sample consisting of the solvent system free from FA was tested to exclude solvent effect.

Fatty acid	EC ₅₀ [μM]	Hill coefficient
Linoleic	78 \pm 1.7 (4)	1.0 \pm 0.01 (4)
Oleic	65 \pm 0.3 (2)	1.0 \pm 0.02 (2)
Arachidonic	10 \pm 0.05 (2)	1.0 \pm 0.01 (2)

Table 4.2: EC₅₀ and Hill coefficients for fatty acids stimulation of Rv2212c₂₁₂₋₃₈₈. EC₅₀ values were derived by Origin 6.0 program and the Hill coefficients from the Hill plots above (fig. 4.14). Standard errors of the mean are shown (number of experiments in brackets).

Kinetic parameter	Rv2212c ₂₁₂₋₃₈₈	Rv2212c ₂₁₂₋₃₈₈ + 100 μM linoleic
V _{max} ($\mu\text{mol}/\text{mg}\cdot\text{min}$)	7.5 \pm 0.04 (6)	7.6 \pm 0.1 (4)
K _m (mM)	3.3 \pm 0.08 (6)	2.5 \pm 0.2 (4)
Hill coefficient	1.8 \pm 0.0 (6)	1.7 \pm 0.0 (4)

Table 4.3 : Kinetic characterization of Rv2212c₂₁₂₋₃₈₈ \pm 100 μM linoleic acid. Assay conditions were 10 mM Mn^{2+} , BIS-TRIS/HCl buffer pH 6.5 at 37°C for 10 min. An ATP range of 0.1–6 mM was used. Standard errors of the mean are shown (number of experiments in brackets).

4.2.3.8 pH dependence of linoleic acid effect

100 μM linoleic acid was tested with Rv2212c₂₁₂₋₃₈₈ at a pH range 5-9. As apparent from fig. 4.15, linoleic acid did not substantially affect the pH dependence (compare with fig. 4.13). There was an increase in the enzyme activity by 100 μM linoleic acid.

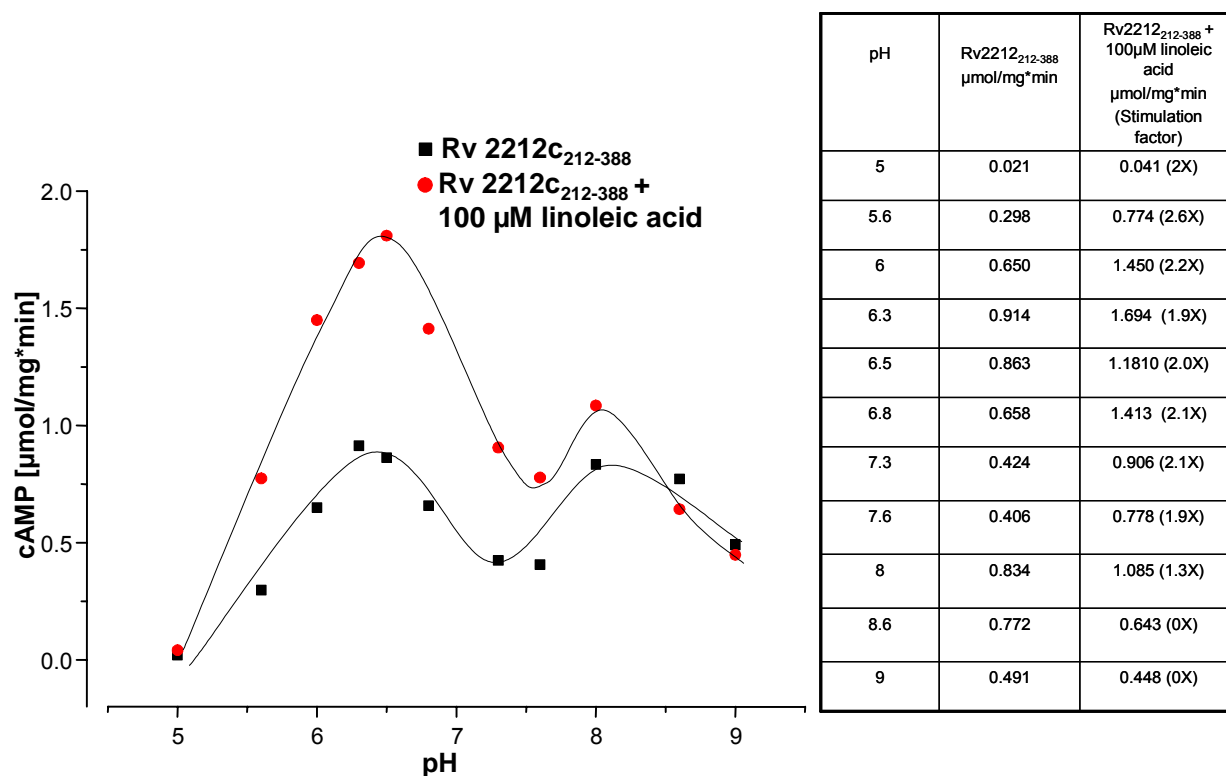


Fig. 4.15: pH dependence of Rv2212c₂₁₂₋₃₈₈ \pm 100 μM linoleic acid. Assay conditions were 200 nM protein, 500 μM ATP, 3 mM Mn^{2+} , 37°C, 10 min. Buffer systems used: Acetate/NaOH (pH 5 and 5.6), BIS-TRIS/HCl (pH 5.6-7.3) and TRIS/HCl (pH 7.3-9).

4.2.3.9 Effect of linoleic acid on the time dependence

The activity of Rv2212c₂₁₂₋₃₈₈ was tested in the presence of 100 μM linoleic acid at 2 min. time intervals (fig. 4.16). Linearity was observed up to 12 min \pm 100 μM linoleic acid. The stimulation factor of linoleic acid decreased gradually over time.

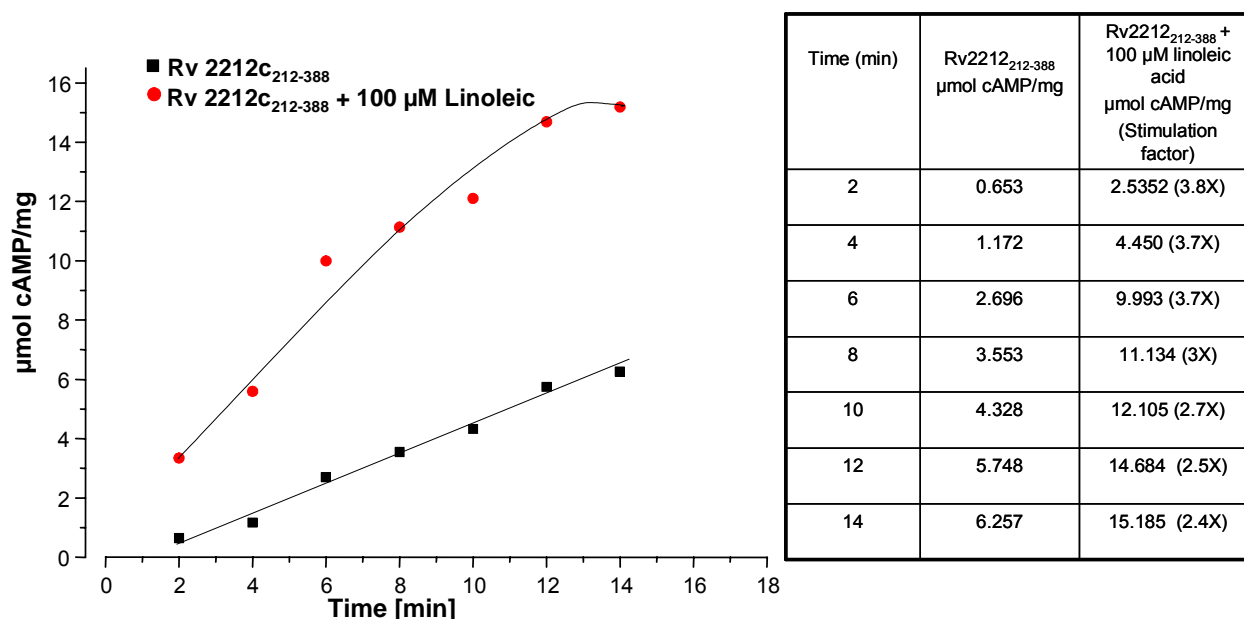
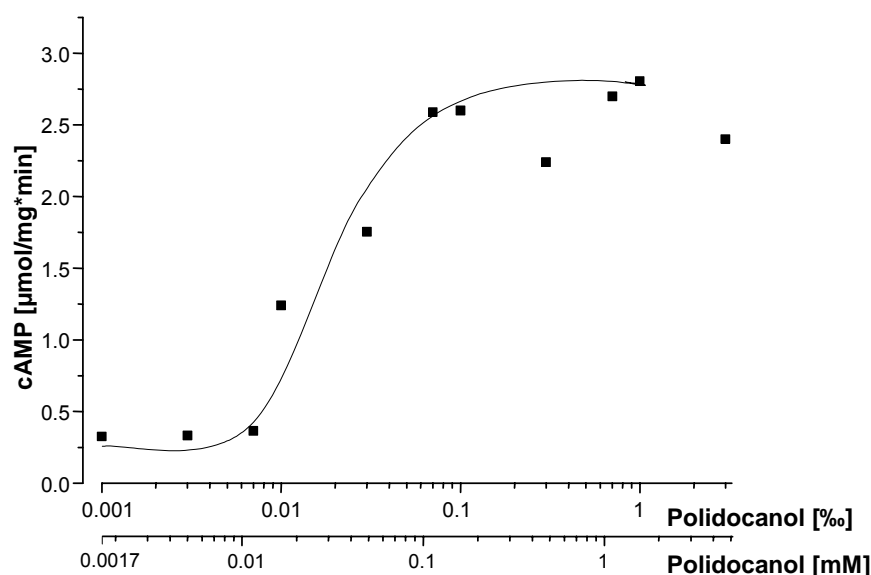


Fig. 4.16: Time dependence of Rv2212c₂₁₂₋₃₈₈ ± 100 µM linoleic acid. Assay conditions were 200 nM protein, 500 µM ATP, 3 mM Mn²⁺, BIS-TRIS/HCl, pH 6.5, 37°C.

4.2.3.10 Effect of detergents

Only detergents which had a significant effect on the Rv2212c holoenzyme activity were tested with the CHD (see section 4.2.7.5.8). Detergents were prepared as stated in section 4.2.7.5.8 and a concentration range of (0.2 – 4 ‰) was tested. Triton X-100 and Nonidet P40 did not show a significant effect, CHAPS (2‰) stimulated 2-fold, while Polidocanol stimulated 7-fold. A dose-response curve for Polidocanol from 0.001‰ (1.7 µM) – 3‰ (5.1 mM) showed an 8-fold increase in activity at 1‰ (1.7 mM) with an EC₅₀ of 30 ± 2 µM (fig. 4.17). The Hill coefficient was 1.3 ± 0.05 (n = 2) indicating cooperative binding of the detergent to the CHD (fig. 4.17). Kinetic characterization showed a slight increase in V_{max}, decrease in the Hill coefficient while K_m remained unchanged in presence of 0.1‰ Polidocanol (table 4.4).

Results



Polidocanol (mM)	Rv2212 ₂₁₂₋₃₈₈ μmol/mg*min
0	0.372
0.0017	0.326
0.0051	0.334
0.0119	0.366
0.017	1.241
0.051	1.756
0.19	2.589
0.17	2.601
0.51	2.240
1.19	2.699
1.7	2.806
5.1	2.401

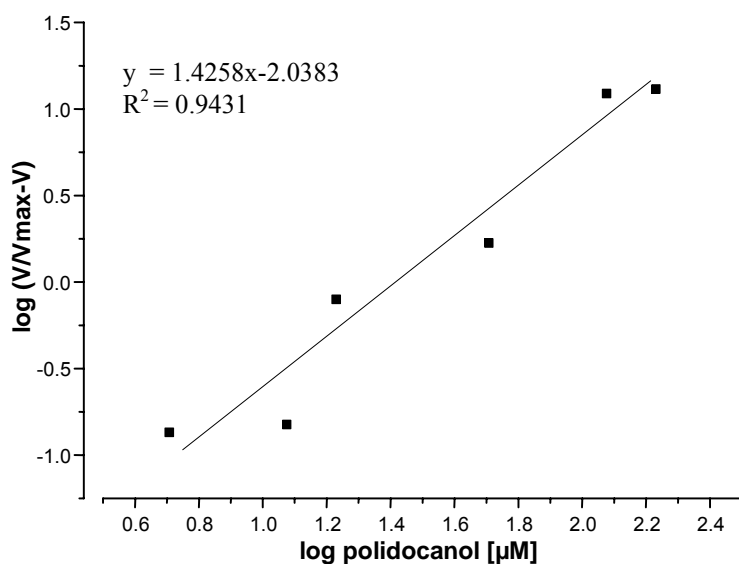


Fig. 4.17: Dose–response curve of Polidocanol stimulation of Rv2212c₂₁₂₋₃₈₈ and the corresponding Hill plot. Assay conditions were 200 nM protein, 500 μM ATP, 3 mM Mn²⁺, BIS-TRIS/HCl pH 6.5, 37°C, 10 min.

Kinetic parameter	Rv 2212c ₂₁₂₋₃₈₈	Rv 2212c ₂₁₂₋₃₈₈ + 0.1% Polidocanol
V _{max} (μmol/mg*min)	7.5 ± 0.04 (6)	16 ± 0.2 (2)
K _m (mM)	3.3 ± 0.08 (6)	3.4 ± 0.2 (2)
Hill coefficient	1.8 ± 0.0 (6)	1.3 ± 0.005 (2)

Table 4.4: Kinetic characterization of Rv2212c₂₁₂₋₃₈₈ ± 0.1% (170μM) Polidocanol. Assay conditions were 200 nM protein, 10 mM Mn²⁺, BIS-TRIS/HCl pH 6.5, 37°C, 10 min. An ATP range of 0.1-7 mM was used.

4.2.3.11 Crystallization

Rv2212c₂₁₂₋₃₈₈ did not crystallize at 7.6 mg/ml using CS and CS2. The plates were initially incubated at 16°C and after 14 days transferred to 12°C. No further experiments were carried out.

4.2.4 Expression and characterization of C-terminally shortened constructs

of Rv2212c₂₁₂₋₃₈₈ (with N-terminal His₆-tag)

Useful structural data have been obtained from systems that are hard to crystallize by removing regions that interfere with crystal growth (Ducruix and Giegé, 1999). Flexible parts in proteins are generally good substrates for proteases and have to be eliminated because a residual proteolytic activity present in the sample could easily generate heterogeneity, as illustrated by the crystallization of the interferon γ receptor (Windsor *et al.*, 1996), which required the deletion of eight amino-terminal residues. Also a flexible extremity might be responsible for the poor diffraction quality of crystals (Zhang *et al.*, 1997; Ducruix and Giegé, 1999). Here, seven successively C-terminal truncated constructs were made to determine the shortest possible active catalytic centre of Rv 2212c₂₁₂₋₃₈₈ (fig. 4.18).

```

Rv2212    353 : HGPLTLKGFDAPVMAFELHDNPRRARDADTPSP-----AASD
Rv1264    357 : AGPRRLRGIRGDVRLEFRVRRGATRTGSGGAAQDDDLAGSSP

```

Fig. 4.18: Alignment of the C-terminal ends of the CHDs of Rv2212c and Rv1264. Sites of C-terminal truncations in Rv 2212c are indicated by dotted lines.

4.2.4.1 Expression and purification

The constructs were expressed in E.coli with 60 μ M IPTG at 16°C overnight, cells were lysed with a French Press and the protein was purified by Ni²⁺-NTA affinity chromatography. Purified protein yield and MW of each construct are tabulated in table 4.5. Proteins were either stored at -20 °C with 20% glycerol or concentrated to be used for crystallization and stored at 4°C. They were analyzed by SDS-PAGE where all showed a single band except for Rv2212c₂₁₂₋₃₆₉ which was further analyzed on a Western blot to confirm its expression (fig. 4.19).

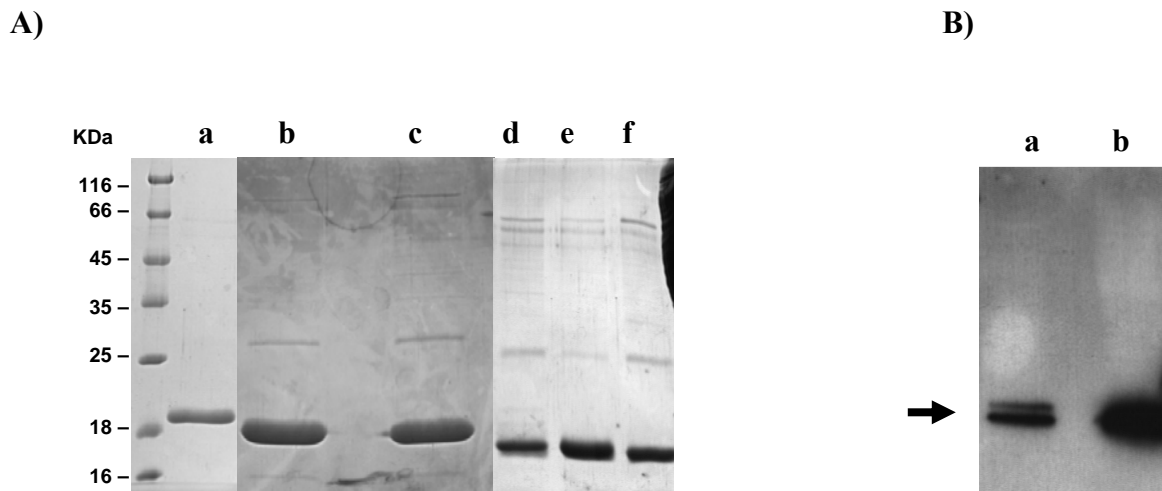


Fig. 4.19: **A)** 15% SDS-PAGE showing Ni^{2+} -NTA purified proteins of: 3 μg Rv2212c₂₁₂₋₃₇₇ (**a**) 5.1 μg Rv2212c₂₁₂₋₃₇₄ (**b**) 4.5 μg Rv2212c₂₁₂₋₃₇₃ (**c**) 1.2 μg Rv2212c₂₁₂₋₃₇₂ (**d**) 2.4 μg Rv2212c₂₁₂₋₃₇₁ (**e**) 2.4 μg Rv2212c₂₁₂₋₃₇₀ (**f**). **B)** Western blot from a 15 % SDS-PAGE using the RGS-His₄ antibody as primary antibody and goat anti-mouse IgG-F_c peroxidase conjugated antibody as secondary antibody. 2 μg of purified Rv2212c₂₁₂₋₃₆₉ were applied on lane (**a**) and 15 μl of the impure supernatant on lane (**b**). Exposure time of the film is 4 min. Note that in lane (**a**) the purified protein shows 2 bands at about 18 kDa (\rightarrow) which probably means that part of the protein was degraded during purification.

Construct	MW (kDa)	Protein yield /400 ml culture
Rv2212c ₂₁₂₋₃₇₇	19.25	900 μg
Rv2212c ₂₁₂₋₃₇₄	18.92	612 μg
Rv2212c ₂₁₂₋₃₇₃	18.81	561 μg
Rv2212c ₂₁₂₋₃₇₂	18.7	390 μg
Rv2212c ₂₁₂₋₃₇₁	18.59	360 μg
Rv2212c ₂₁₂₋₃₇₀	18.48	195 μg
Rv2212c ₂₁₂₋₃₆₉	18.37	120 μg

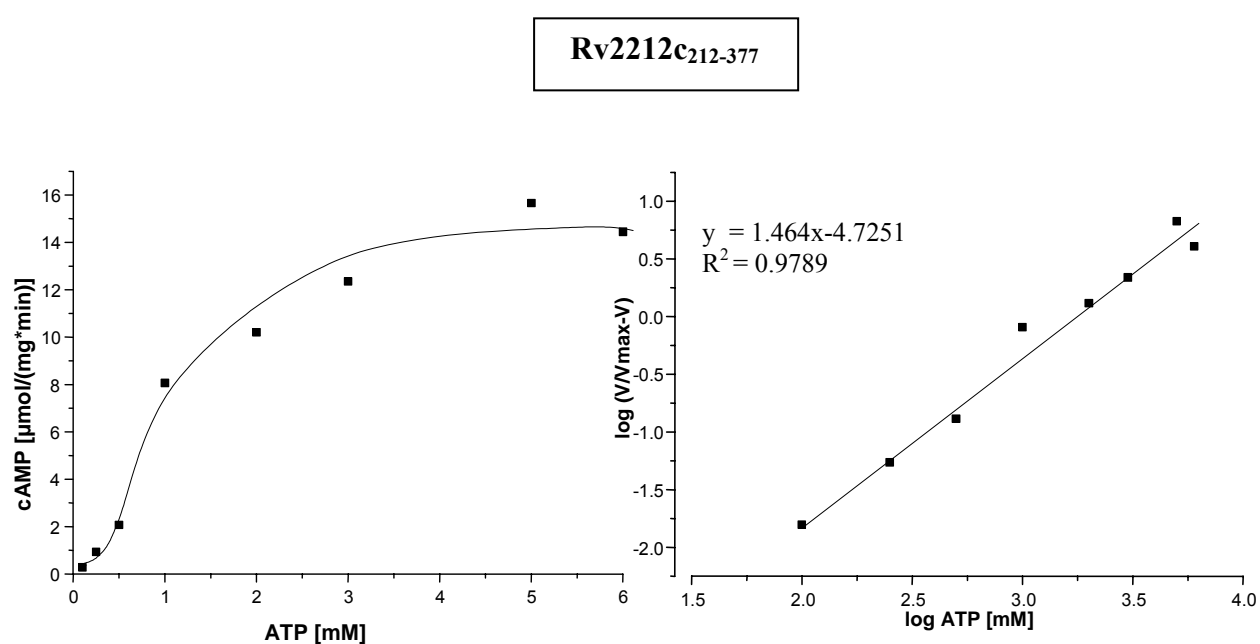
Table 4.5: MW and Ni^{2+} -NTA purified protein yield of C-terminally shortened constructs of Rv2212c₂₁₂₋₃₈₈

4.2.4.2 Enzyme kinetics

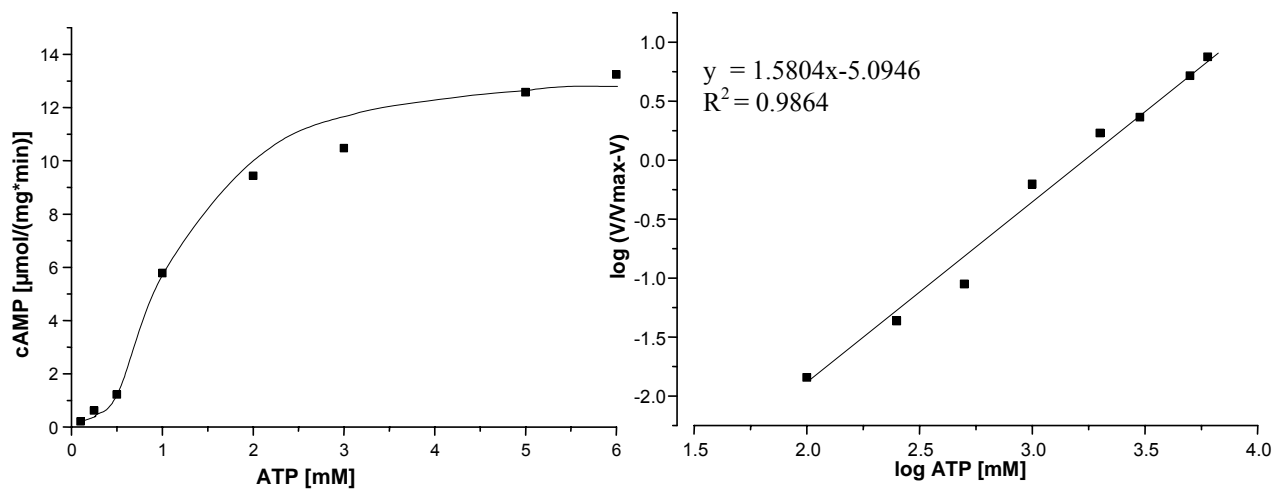
The kinetic properties of the six shortened constructs were determined using substrate concentrations ranging from 0.1 to 6.0 mM ATP and 10 mM Mn^{2+} (fig. 4.20). The V_{max} , K_m and Hill coefficient values of all constructs did not show a significant difference when compared to the wild type catalytic domain Rv2212_{c212-388} (table 4.6) denoting that these truncations did not affect protein folding. Rv2212_{c212-369} showed a specific activity of 10 pmol/mg*min using 7.5 μ g protein. No experiments were conducted on this construct.

Construct	V_{max} [μ mol/mg*min]	K_m [mM]	Hill coefficient	Specific activity [μ mol/mg*min]
Rv2212 _{c212-388} (wild type)	26	2.1	1.4	3.1
Rv2212 _{c212-377}	18	1.6	1.4	2.1
Rv2212 _{c212-374}	15	1.6	1.5	1.2
Rv2212 _{c212-373}	17	1.9	1.1	2.4
Rv2212 _{c212-372}	10	1.9	1.1	1.5
Rv2212 _{c212-371}	30	1.8	1.2	3.8
Rv2212 _{c212-370}	32	1.9	1.4	3.3

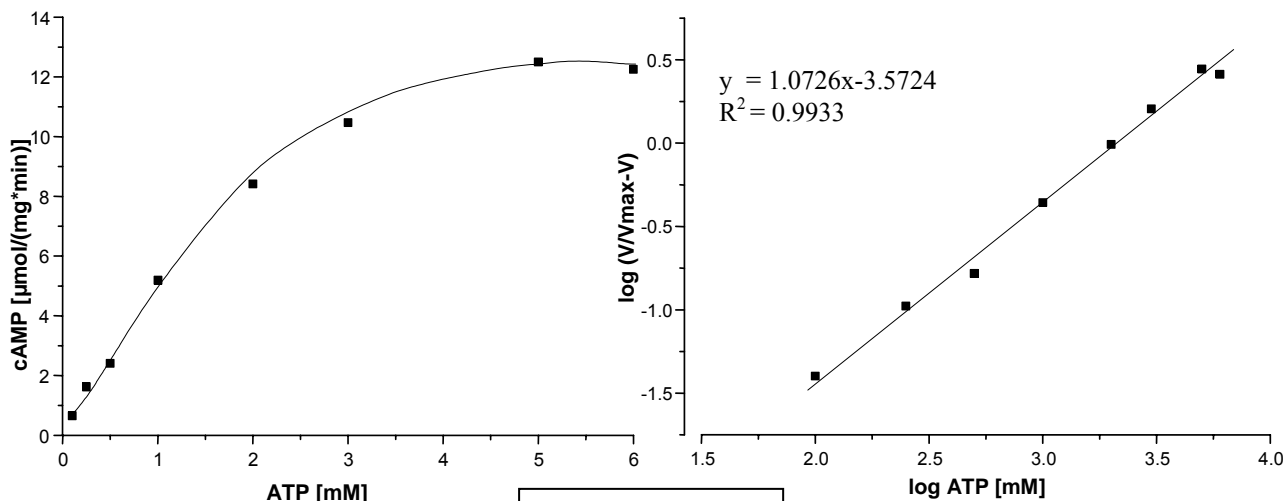
Table 4.6: Kinetic characterization and specific activities of the C-terminally shortened constructs of Rv2212_{c212-388}. Assays were carried out for 10 min at 37°C using BIS-TRIS/HCl, pH 6.5.



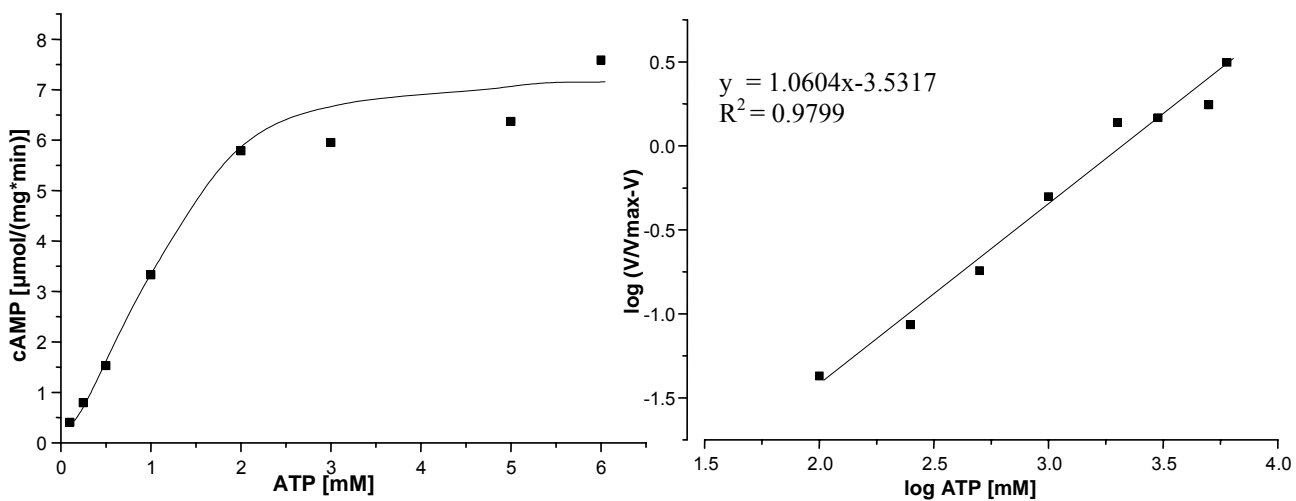
Rv2212c₂₁₂₋₃₇₄



Rv2212c₂₁₂₋₃₇₃



Rv2212c₂₁₂₋₃₇₂



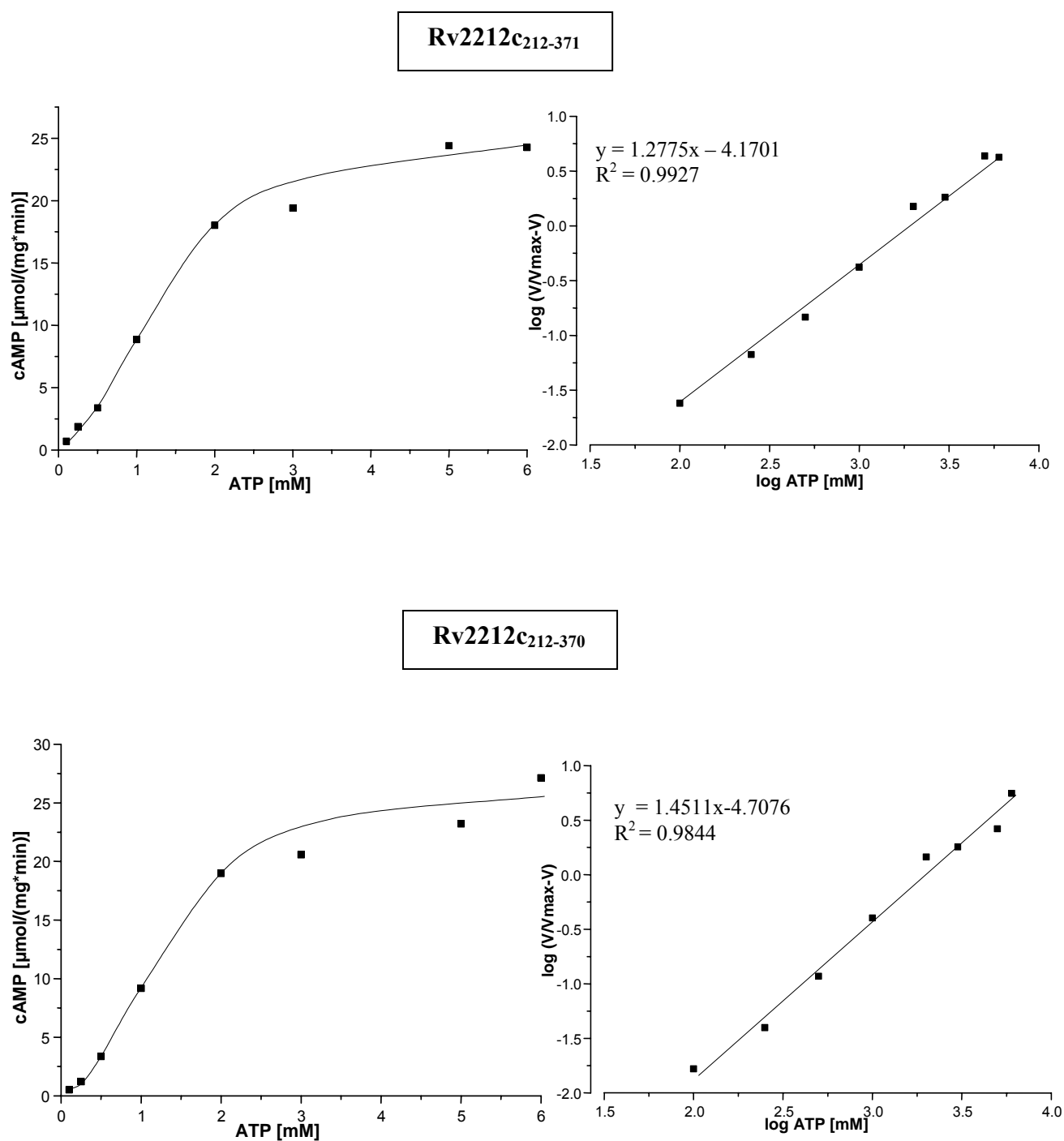


Fig. 4.20: Kinetics of the six C-terminally shortened constructs of Rv2212c₂₁₂₋₃₈₈ showing Michaelis-Menten curves and corresponding Hill-Plots. The assays were conducted using 0.15 μg protein, BIS-TRIS/HCl, pH 6.5, 37°C, 10 min.

4.2.4.3 Crystallization of Rv2212_{c212-377}, Rv2212_{c212-374} and Rv2212_{c212-370}

These three catalytic domains displayed a good activity, besides having comparable kinetic parameters when compared to wild type Rv2212_{c212-388}. This encouraged crystallization. Rv2212_{c212-377} (16 mg/ml) was screened using kits CS and CS2. It was incubated at 16°C and after 7 days transferred to 12°C, but no crystals were observed. Rv2212_{c212-374} (13 mg/ml) was screened with CS, CS2 and the Wizard kit I and II at 16°C. Coffin lid-like crystals (75 X 125 μ) probably of magnesium ammonium phosphate were grown, in about 7 days, in nearly all buffer systems containing ammonium phosphate: CS # 3, 11; Wizard I # 9, 34; Wizard II #10, 33, 46. Also 8 mg/ml of Rv2212_{c212-374} was incubated with 1 mM ATP overnight on ice before setting the plates for crystallization. No protein crystals were obtained, only the same salt crystals with (NH₄)₂HPO₄ buffers were observed. As with Rv2212_{c212-370}, crystallization trials were made using 13.7 mg/ml (without 10% glycerol) with CS, CS2 and Wizard I and 9.6 mg/ml (with 10% glycerol) with CS and Wizard II at 16°C. Only those coffin lid-like crystals were obtained as with Rv 2212_{c212-374}.

4.2.5 Expression and characterization of the mutants L370V, L370A and L370G

Successive C-terminal truncations in Rv2212_{c212-388} resulted in active constructs until the deletion of L₃₇₀ which abolished the activity. Here I investigated by a mutational approach the importance of this residue for the catalytic domain activity. L₃₇₀ in Rv2212_{c212-370} was mutated to V, A and G yielding L370V, L370A and L370G, respectively.

4.2.5.1 Expression and purification

The three mutants were expressed in E.coli with 60 μM IPTG at 16°C overnight. Cells were lysed with a French Press and the protein was purified by Ni²⁺-NTA affinity chromatography. The yield of proteins were 150 μg, 120 μg and 117 μg (per 400 ml culture) for L370V, L370A and L370G respectively. Proteins appeared as faint bands with a lot of impurities on 15% SDS-PAGE, therefore a Western-Blot was carried out to detect the mutants in the supernatants, pellets and in the Ni²⁺-NTA purified fractions. L370A was detected only in the pellets (fig. 4.21).

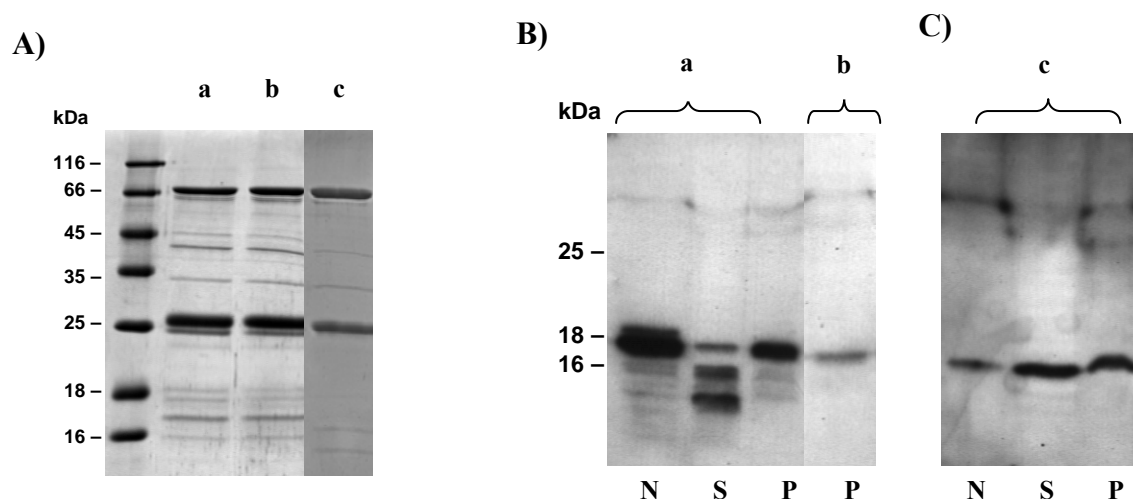


Fig. 4.21: A) 15% SDS-PAGE. **a** = 2.6 μ g L370V, **b** = 2 μ g L370A and **c** = 4 μ g L370G. B) and C) Western blots from a 15% SDS-PAGE using the RGS-His₄ antibody as primary antibody and the goat anti-mouse IgG-F_c peroxidase conjugated antibody as secondary antibody. 5 μ g and 4 μ g of Ni²⁺-NTA purified L370V and L370G were applied and 10 μ l of the impure supernatants. The pellets (about 20 mg) were suspended in 50 μ l H₂O, mixed with 50 μ l SDS-buffer and, after centrifugation, 10 μ l from the supernatants were loaded on the gel. The supernatant of L370V shows two thick bands below the original protein band (at 18.48 kDa), probably indicating degradation. Film exposure time is 60 sec (B) and 4 min (C). **a** = L370V, **b** = L370A, **c** = L370G, N= Ni²⁺-NTA purified protein, S = supernatant, P = pellet.

4.2.5.2 Adenylyl cyclase activity

The AC activity of the mutants was assayed using purified fractions, supernatants and pellets. The assays were conducted using 500 μ M ATP, 3 mM Mn²⁺, BIS-TRIS/HCl pH 6.5 at 37°C and for 10 min. The three mutants showed no activity denoting the importance of L₃₇₀ for folding, stability and, potentially, catalysis.

4.2.6 Expression and characterization of N-terminally shortened constructs

of Rv2212c₂₁₂₋₃₇₀

Truncations were carried out at the N-terminus of Rv2212c₂₁₂₋₃₇₀ to determine the shortest possible catalytically active form of Rv2212c. Five truncations were made and three active constructs (Rv2212c₂₁₃₋₃₇₀, Rv2212c₂₁₄₋₃₇₀, Rv2212c₂₁₅₋₃₇₀) were characterized (fig. 4.22).

```

Rv2212    212 : S A S V T C G I G F A D L S S F T A L T Q A L
Rv1264    211 : P G A R Q V T V A F A D L V G E T Q L G E V V

```

Fig. 4.22: Alignment of the N-terminal ends of the CHDs of Rv2212c and Rv1264. Sites of N-terminal truncations in Rv 2212c are indicated by dotted lines.

Results

4.2.6.1 Expression and purification

The constructs were expressed in E.coli with 60 μM IPTG at 16°C overnight. Cells were lysed with a French Press and proteins were purified by Ni²⁺-NTA affinity chromatography. The yields and the MWs of the constructs are shown in table 4.7. Proteins were stored at -20 °C with 20% glycerol. They were analyzed on an SDS-PAGE where all showed a single band except for Rv2212c₂₁₆₋₃₇₀ and Rv2212c₂₁₇₋₃₇₀ which were further analyzed on a Western blot to confirm expression (fig. 4.23).

Construct	MW (kDa)	Protein yield /400 ml culture
Rv2212c ₂₁₃₋₃₇₀	18.37	1 mg
Rv2212c ₂₁₄₋₃₇₀	18.26	1 mg
Rv2212c ₂₁₅₋₃₇₀	18.15	480 μg
Rv2212c ₂₁₆₋₃₇₀	18.00	810 μg
Rv2212c ₂₁₇₋₃₇₀	17.93	255 μg

Table 4.7: MW and Ni²⁺-NTA purified protein yields of N-terminally shortened constructs of Rv2212c₂₁₂₋₃₇₀.

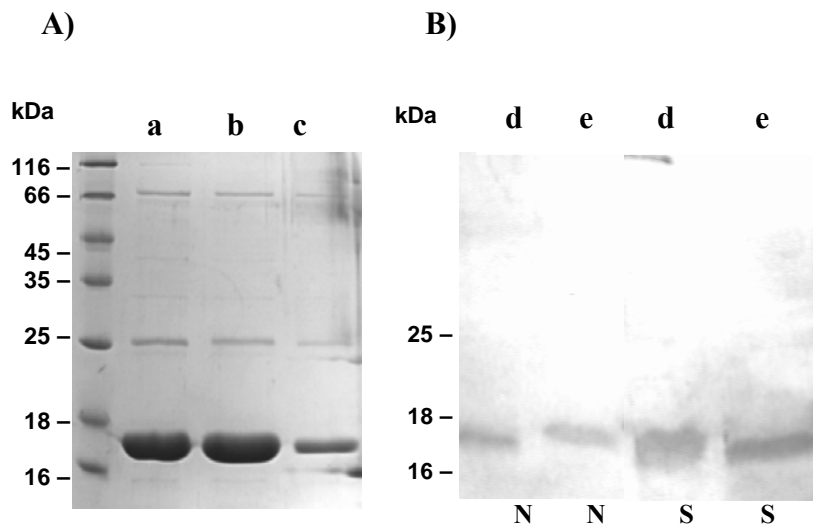


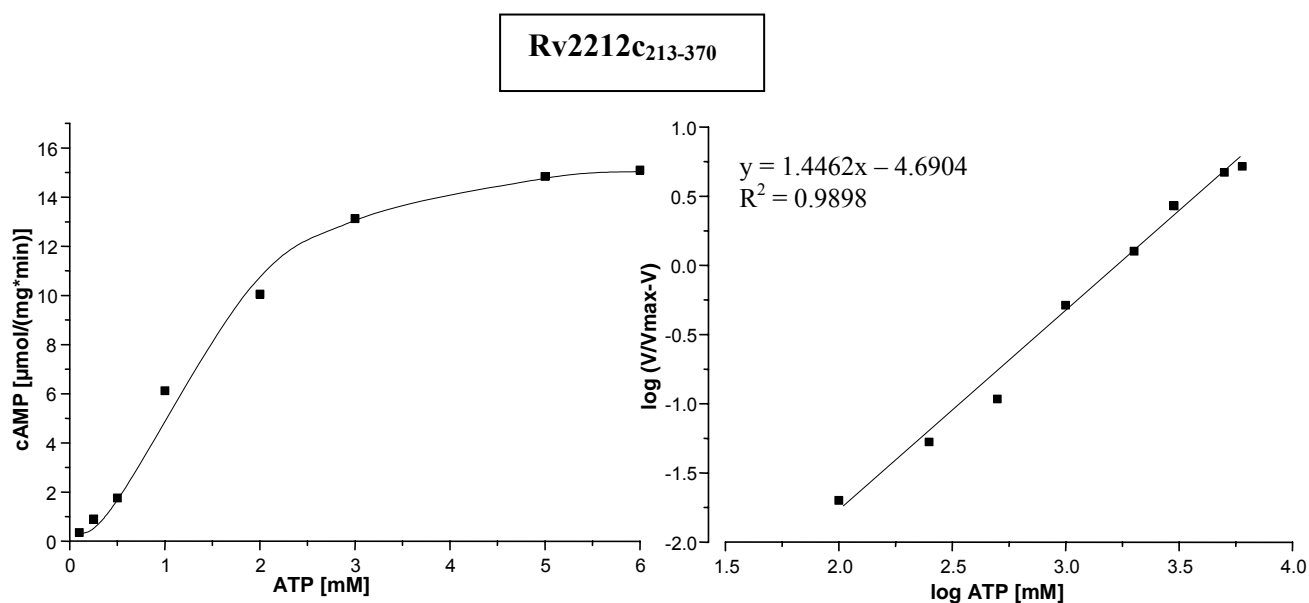
Fig. 4.23 : **A)** 15% SDS-PAGE showing Ni²⁺-NTA purified proteins of: 6.8 μg Rv2212c₂₁₃₋₃₇₀ (**a**) 7.6 μg Rv2212c₂₁₄₋₃₇₀ (**b**) and 0.96 μg Rv2212c₂₁₅₋₃₇₀ (**c**). **B)** Western blot from a 15% SDS-PAGE using the RGS-His₆ antibody as primary antibody and the goat anti-mouse peroxidase conjugated antibody as secondary antibody. 4 μg of purified proteins and 15 μl of the supernatants were applied per lane. Exposure time of the film is 2 sec. **d** = Rv2212c₂₁₆₋₃₇₀ **e** = Rv2212c₂₁₇₋₃₇₀, **N**= Ni²⁺-NTA purified protein, **S**= supernatant.

4.2.6.2 Enzyme kinetics

The kinetic properties of the three active shortened constructs were investigated using substrate concentrations ranging from 0.1 to 6.0 mM ATP (fig. 4.24). Comparing the V_{\max} , K_m and Hill coefficient (table 4.8) to the C-terminally shortened construct and the wild type, we can see that substrate affinity and cooperativity were not largely affected by N-terminal truncations.

Construct	V_{\max} [$\mu\text{mol}/\text{mg}\cdot\text{min}$]	K_m [mM]	Hill coefficient	Specific activity [$\mu\text{mol}/\text{mg}\cdot\text{min}$]
Rv2212c ₂₁₂₋₃₈₈ (wild type)	26	2.1	1.4	3.1
Rv2212c ₂₁₂₋₃₇₀	32	1.9	1.4	3.3
Rv2212c ₂₁₃₋₃₇₀	18	1.7	1.4	1.7
Rv2212c ₂₁₄₋₃₇₀	15	2.7	1.5	0.8
Rv2212c ₂₁₅₋₃₇₀	16	1.3	1.9	1.3

Table 4.8: Kinetic characterization and specific activities of the N-terminally shortened constructs of Rv2212c₂₁₂₋₃₇₀. Assays were carried out for 10 min at 37°C using BIS-TRIS/HCl, pH 6.5.



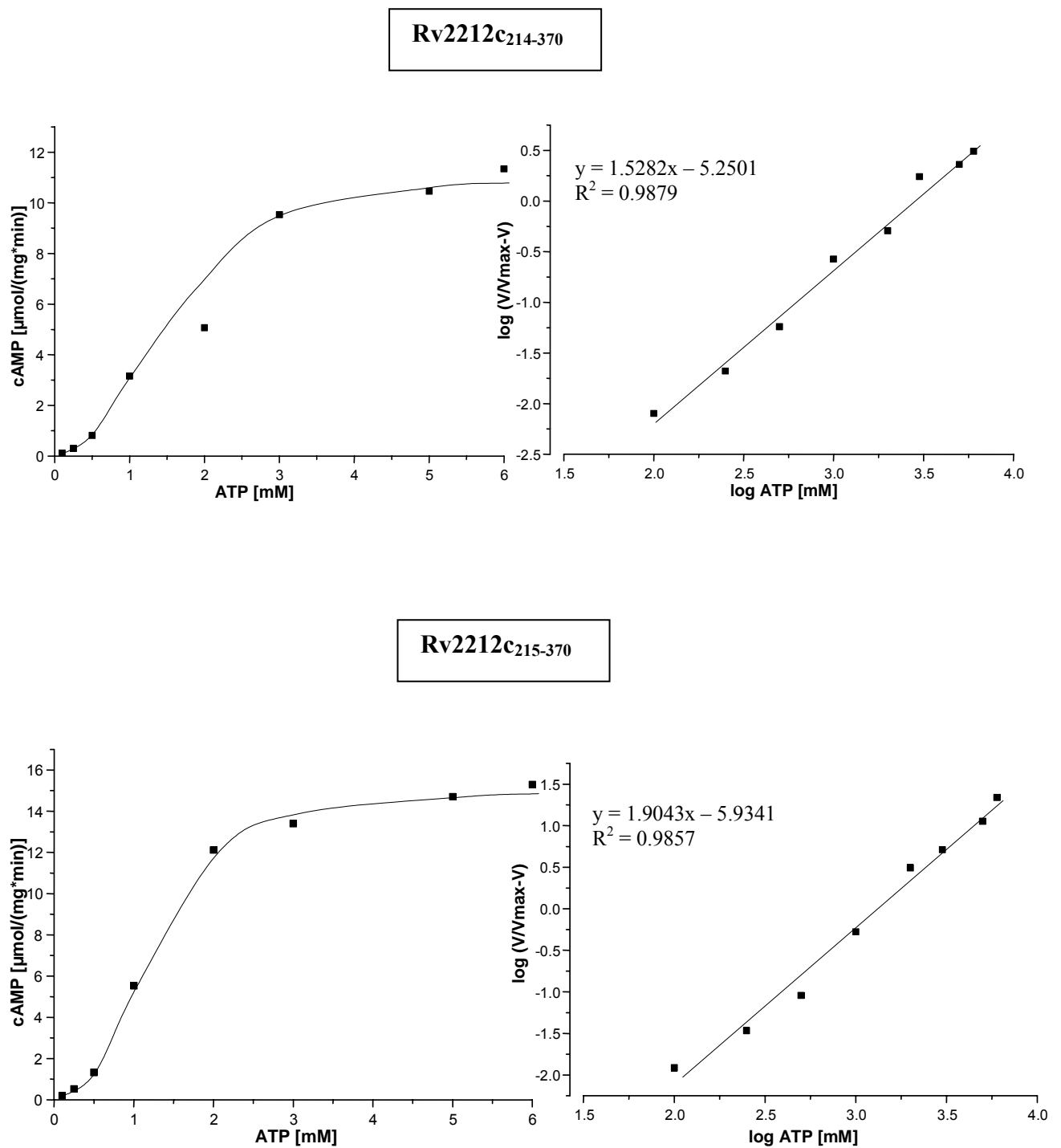
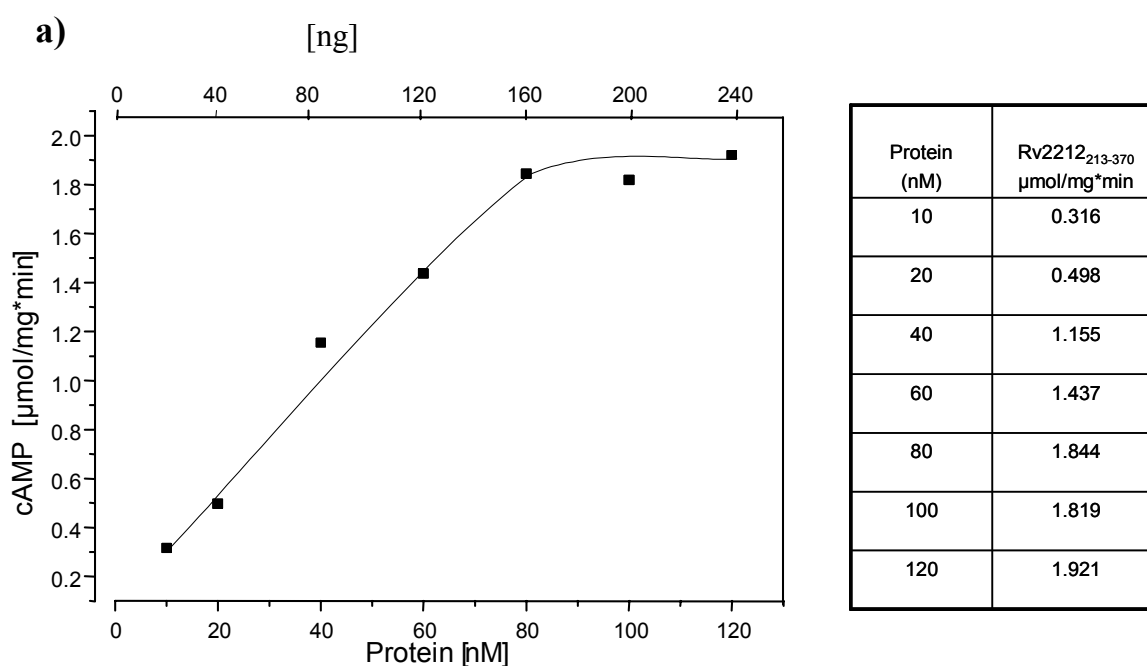


Fig. 4.24: Kinetics of the three active N-terminally shortened constructs of Rv2212c₂₁₂₋₃₇₀ showing Michaelis-Menten curves and corresponding Hill-Plots. The assays were conducted using 0.15 μg protein, BIS-TRIS/HCl pH 6.5, 10 mM Mn²⁺, 37°C, 10 min.

4.2.6.3 Protein dependence of Rv2212c₂₁₃₋₃₇₀ and Rv2212c₂₁₅₋₃₇₀

The specific activities of both proteins were dependent on the protein concentration just like the wild type catalytic domain (see section 4.2.3.2). Protein concentrations from 5 to 120 nM for Rv2212c₂₁₃₋₃₇₀ (10 - 240 ng) and 7 to 160 nM for Rv2212c₂₁₅₋₃₇₀ (14 - 320 ng) were tested. The specific activity increased linearly up to 80 nM for Rv2212c₂₁₃₋₃₇₀ and up to 60 nM for Rv2212c₂₁₅₋₃₇₀, suggesting the formation of homodimers (fig. 4.25). Further increments in protein concentration of Rv2212c₂₁₅₋₃₇₀ (> 60 nM) resulted in a gradual decrease in specific activity which may be attributed to formation of less productive multimers. Half maximal activities for Rv2212c₂₁₃₋₃₇₀ and Rv2212c₂₁₅₋₃₇₀ were attained at 30 and 20 nM, respectively, which are more or less similar to the K_{diss} value of the wild type (20 nM).



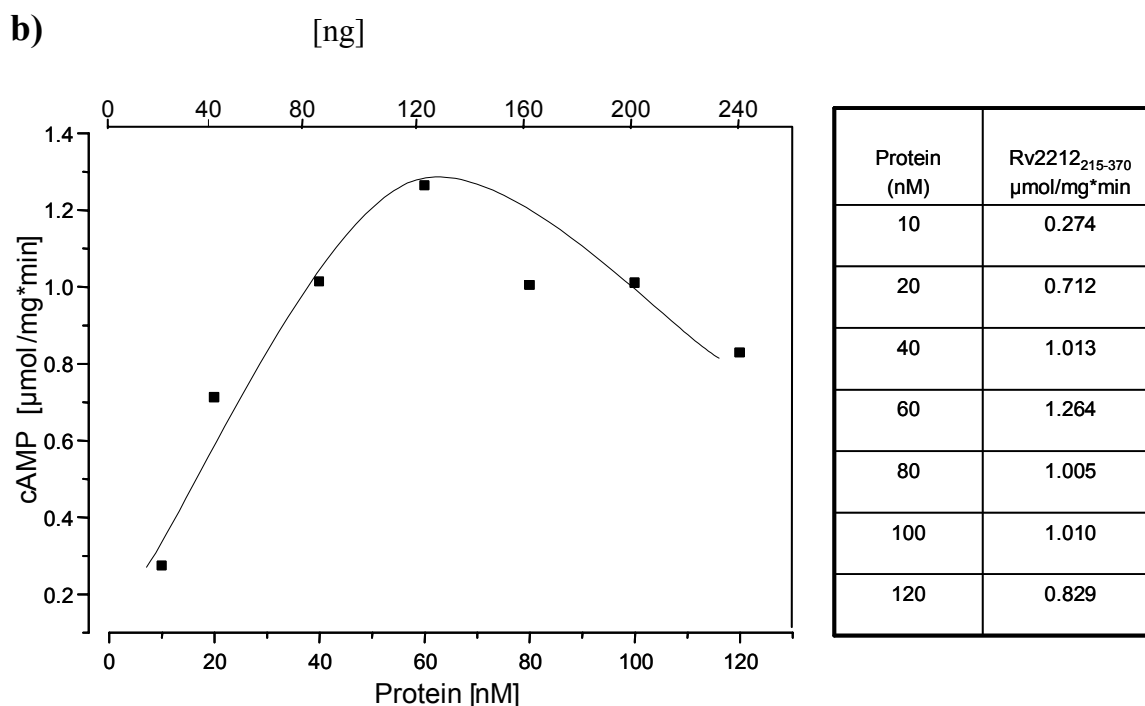


Fig. 4.25: Protein dependence of Rv2212c₂₁₃₋₃₇₀ (**a**) and Rv2212c₂₁₅₋₃₇₀ (**b**). Assay conditions were 500 μM ATP, 3 mM Mn²⁺, BIS-TRIS/HCl pH 6.5, 37°C, 10 min. Only protein concentrations from 10-120 nM were plotted for clarity.

4.2.6.4 Gel filtration of Rv2212c₂₁₃₋₃₇₀

Chromatography on the Superose 12 HR 10/30 column was used to detect whether Rv2212c₂₁₃₋₃₇₀ is a mono- or multimer. A single large peak was obtained (fig. 4.26, A). The protein fractions had AC activity (fig. 4.26, A). The protein eluted at 14.5 ml corresponded to a size of approximately 40 kDa which is about the size of a homodimer. This was expected as the K_{diss} for Rv2212c₂₁₃₋₃₇₀ is 30 nM (see above). Similarly 200 μg (in 250 μl) of Rv2212c₂₁₂₋₃₈₈ were chromatographed. It displayed the same protein profile, a large peak appeared at 14.3 ml corresponding to fractions 27-33 which had AC activity when tested (fig. 4.26, B). 4.7 mg Rv2212c₂₁₃₋₃₇₀ were purified in three runs on the column (250 μl portions) under the same conditions. Fractions 28-33 were collected (fig. 4.26, A), united and concentrated (see section 3.3.5). The buffer was then exchanged to crystallization buffer.

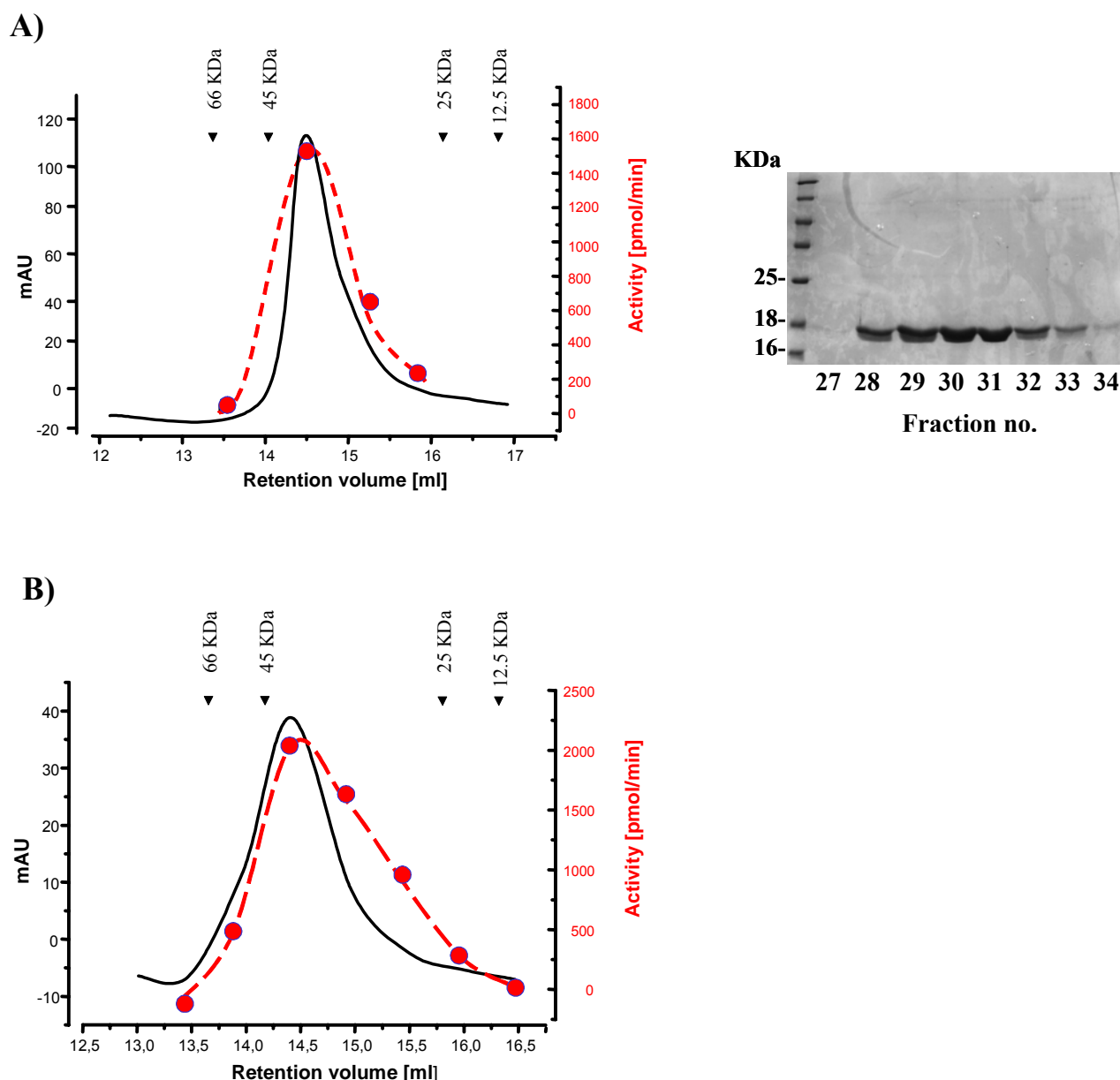


Fig. 4.26: **A)** Gel filtration chromatography of Rv2212_{c213-370} (250 μ l containing 530 μ g protein were loaded) on Superose 12 HR 10/30. Flow rate was 0.5 ml/min using FPLC buffer (see 2.3.2). The calibration proteins (marked by the inverted triangles) were cytochrome C (12.5 kDa), chymotrypsinogen A (25 kDa), ovalbumine (45 kDa) and BSA (66 kDa) (250 μ l each). Fractions 27-34 were collected (500 μ l each) and AC activity tested for fractions 28, 30, 32 and 33 (500 μ M ATP, 3 mM Mn²⁺, BIS-TRIS/HCl buffer pH 6.5, 37°C, 10 min) and an activity curve was plotted (.....). The protein was detected at 280 nm (—). 15% SDS-PAGE showing fractions (27-34) of Rv2212_{c213-370} collected from Superose 12 HR 10/30. 10 μ l from each fraction was applied on the gel.

B) Gel filtration chromatography of Rv2212_{c212-388} (250 μ l containing 200 μ g protein) on Superose 12 HR 10/30. Fractions 27-33 were collected (500 μ l each) and AC activity for each fraction was tested. Same conditions as above were applied.

4.2.6.5 Crystallization of Rv2212_{c213-370}

Although Rv2212_{c215-370} is the shortest active CHD, Rv2212_{c213-370} was better suited for crystallization because of its better protein yield. Ni²⁺-NTA purified Rv2212_{c213-370} (7.7 mg/ml) was crystallized using CS and CS2 at 16°C. Also the gel filtrated protein (9.3 mg/ml) was tried with Wizard I and II kits at the same temperature. No crystals were obtained in both cases.

4.2.7 Expression and characterization of adenylyl cyclase Rv2212c

Holoenzyme

4.2.7.1 Expression and purification

The clone for this protein was obtained from Stephan Zeibig (2003) in pQE-30 vector in BL21 cells. It was expressed in E.coli with 60 µM IPTG at 22°C for 5 hours. Cells were lysed by sonication, treated with lysozyme and DNaseI, and the protein was purified to homogeneity by Ni²⁺-NTA affinity chromatography (fig. 4.27). From a 200 ml culture 840 µg protein were obtained. Recovery was 1.9 mg from a 400 ml culture after an overnight expression at 16 °C and French Press lysis. The protein was stored at -20 °C with 20% glycerol.

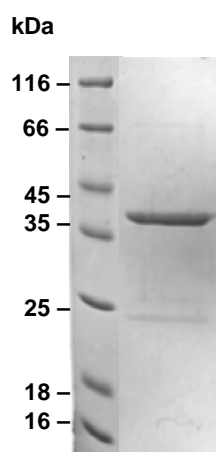


Fig. 4.27: 15% SDS-PAGE showing a single band of 2.8 µg Ni²⁺-NTA purified Rv2212_{c1-388} MW = 43.67 kDa, pI = 4.5.

4.2.7.2 Protein dependence

The specific activity was independent of the protein concentration over the tested range (fig. 4.28). Comparing this result to that of the catalytic domain (see section 4.2.3.2), it seems that the N-terminal domain of Rv2212c plays an important role in dimerization as it shifts the equilibrium completely towards the dimer side already at very low protein concentrations.

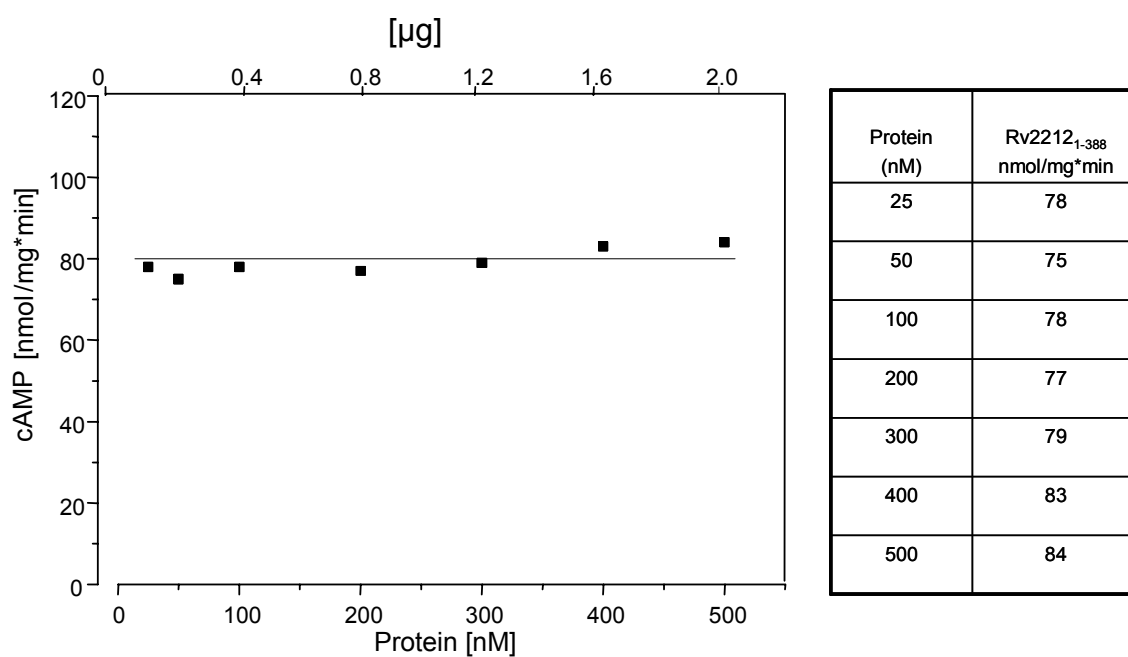


Fig. 4.28: Protein dependence of Rv2212c₁₋₃₈₈. Assay was conducted using 500 μ M ATP, 3 mM Mn²⁺, BIS-TRIS/HCl pH 6.5, 37°C, 10 min.

4.2.7.3 Time dependence

The activity of 100 nM protein (0.4 μg) was tested at 2 min. time intervals. The curve (fig. 4.29) shows linearity up to 14 min. Afterwards the activity went down probably due to the inhibiting effect of the increasing amounts of pyrophosphate.

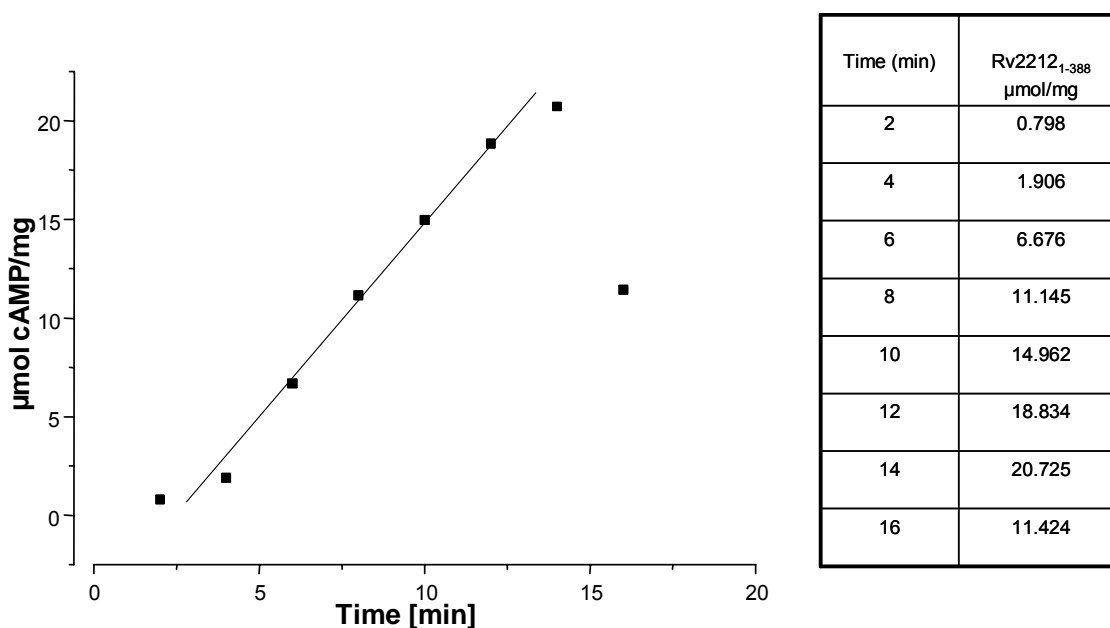


Fig. 4.29: Time dependence of Rv2212c₁₋₃₈₈. Assay conditions were 500 μM ATP, 3 mM Mn^{2+} , BIS-TRIS/HCl pH 6.5 at 37°C .

4.2.7.4 pH dependence

100 nM (0.4 μg) protein was tested from pH 4.6 to 8.0 using 3 different buffer systems (fig. 4.30). The pH strongly affected the specific activity. The pH optimum was at pH 6.5 (BIS-TRIS/HCl), as for the catalytic domain (see section 4.2.3.5). This demonstrated that the N-terminal domain was not operating as a pH sensor as in Rv1264 (Tews *et al.*, 2005). At alkaline pH (8.0), the activity increases clearly once again to 0.245 ± 0.01 $\mu\text{mol}/\text{mg} \cdot \text{min}$ ($n = 8$), due to unknown reasons.

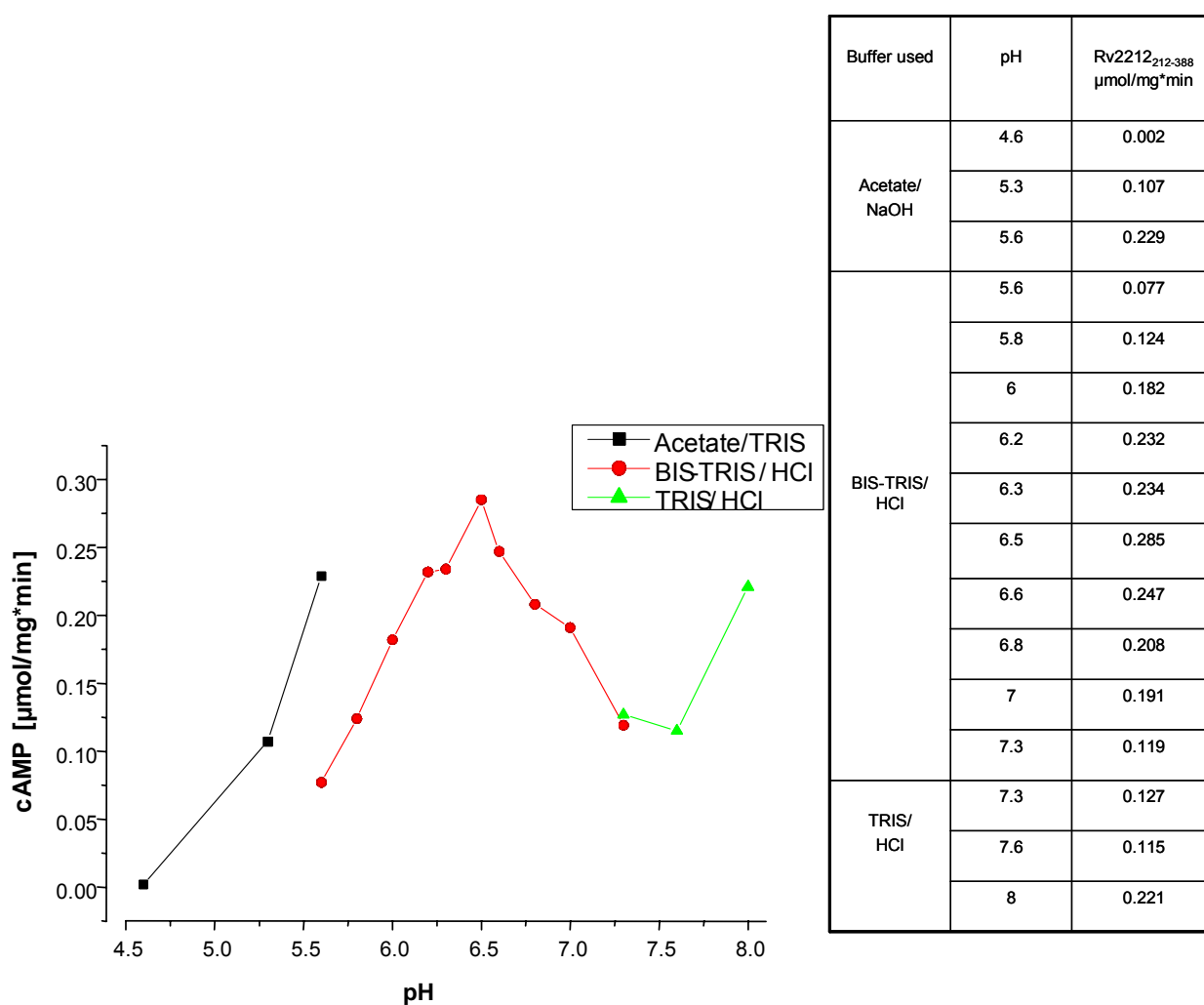


Fig. 4.30: pH dependence of Rv2212c₁₋₃₈₈. Assay conditions were 0.4 μg protein, 500 μM ATP, 3 mM Mn²⁺ at 37°C for 10 min.

4.2.7.5 Effect of chemical compounds on AC activity

I wanted to find out how is Rv2212c holoenzyme regulated and what is the function of its regulatory N-terminal domain. *Mycobacterium tuberculosis* differs radically from other bacteria in that a very large portion of its coding capacity (about 30%) is devoted to production of enzymes involved in lipogenesis and lipolysis (Cole *et al.*, 1998). Therefore among other compounds lipids were studied to see whether any of them would have a regulatory effect on enzyme activity.

4.2.7.5.1 Effect of sugars

The activity was tested in the presence of 1 mM of: D-galactose, D-mannose, L-arabinose, L-rhamnose, D-glucose, D-fructose, fructose-1,6-bisphosphate and glucose-6-phosphate. None of them affected AC activity (table 4.9).

Compound tested (1mM)	% of corresponding basal activity	Specific activity ($\mu\text{mol}\cdot\text{mg}^{-1}\cdot\text{min}^{-1}$)
D-galactose	123	2.1
D-mannose	100	1.7
L-arabinose	105	1.8
L-rhamnose	100	1.7
D-glucose	105	1.8
D-fructose	123	2.1
Fructose-1,6-bisphosphate	111	1.9
Glucose-6-phosphate	105	1.8

Table 4.9: Effect of monosaccharides on Rv2212c₁₋₃₈₈ AC activity. Assay conditions: 100 nM enzyme, 500 μM ATP, BIS-TRIS/HCl pH 6.5, 10 mM Mn^{2+} , 37°C, 10 min. Basal activity (without additives) was 1.7 $\mu\text{mol}\cdot\text{mg}^{-1}\cdot\text{min}^{-1}$.

4.2.7.5.2 Effect of amino acids

The effect of 1 mM of: DL-threonine, L-isoleucine, L-valine, L-asparagine, L-histidine, L-aspartic acid, D-alanine, L-alanine, L-cysteine, L-leucine and glycine, on AC activity of the holoenzyme was tested. None had a significant effect on enzyme activity (table 4.10). There is a clear drop in the basal activity of the enzyme compared to table 4.9. This reflects the instability in the enzyme activity which is referred to in the discussion (section 5.8).

Compound tested (1mM)	% of corresponding basal activity	Specific activity (nmol·mg ⁻¹ ·min ⁻¹)
DL-threonine	108	81
L-isoleucine	113	85
L-valine	126	95
L-asparagine	134	101
L-histidine	125	94
L-aspartic acid	110	83
D-alanine	96	72
L-alanine	82	62
L-cysteine	77	58
L-leucine	80	60
Glycine	82	62

Table 4.10: Effect of different amino acids on Rv2212c₁₋₃₈₈ AC activity. Assay conditions were as in table 4.9. Basal activity (without additives) was 75 nmol·mg⁻¹·min⁻¹.

4.2.7.5.3 Effect of salts and other miscellaneous compounds

Sodium chloride, potassium chloride, sodium citrate, sodium acetate, sodium bicarbonate, NADH, glyoxylic acid, α -ketoglutarate, pyruvate and phosphoenolpyruvate were tested with Rv 2212c₁₋₃₈₈ at 1 mM concentration. AC activity was not remarkably affected by any of these compounds (table 4.11).

Compound tested (1mM)	Specific activity nmol·mg ⁻¹ ·min ⁻¹	Basal activity (without additives) nmol·mg ⁻¹ ·min ⁻¹
Sodium chloride	32	34
Potassium chloride	41	34
Sodium citrate	32	34
Sodium acetate	35	34
Sodium bicarbonate	40	34
NADH	50	34
Glyoxylic acid	44	75
α -ketoglutarate	1600	1786
Pyruvate	1374	1786
Phosphoenolpyruvate	1545	1786

Table 4.11: Effect of salts and other miscellaneous compounds on Rv2212c₁₋₃₈₈ AC activity. Assay conditions were the same as in table 4.9. Compounds were tested in three different tests.

4.2.7.5.4 Effect of phospholipids

A 10 mM solution in 10% alcohol/water of phosphatidyl ethanolamine and phosphatidyl choline was prepared. Further dilutions were with H₂O. A concentration range of 1 μ M-1 mM of each was tested with 100 nM Rv2212c₁₋₃₈₈. 70 μ M phosphatidyl ethanolamine caused a 70% decrease in the specific activity while the same concentration of phosphatidyl choline caused a 50% decrease (table 4.12). No further tests were done with these phospholipids due to the difficulty in getting a reproducible dose-response curve probably due to the effect of alcohol which had to be used as a solvent. 1 mM of each was also tested with the holoenzymes of Rv1264 and Rv1625c as a control, but no significant effects were detected (table 4.12).

Holoenzyme	Compound tested	Specific activity nmol·mg ⁻¹ ·min ⁻¹	Specific activity (without additives) nmol·mg ⁻¹ ·min ⁻¹
Rv2212c	70 μM phosphatidyl ethanolamine	64.7	204
	70 μM phosphatidyl choline	103	204
Rv1264	1 mM phosphatidyl ethanolamine	88	109
	1 mM phosphatidyl choline	82	109
Rv1625c	1 mM phosphatidyl ethanolamine	541	313
	1 mM phosphatidyl choline	421	313

Table 4.12: Effect of phospholipids on AC activities of each of Rv2212c, Rv1264 and Rv1625c holoenzymes. Assay conditions were 500 μM ATP, 3 mM Mn²⁺, BIS-TRIS/HCl buffer pH 6.5, 37°C, 10 min for Rv2212c. The same conditions were applied except for a different buffer system (MES/TRIS pH 5.7) for Rv1264 and a different buffer and reaction temperature (TRIS/HCl pH 7.5 at 30°C) for Rv1625c.

4.2.7.5.5 Effect of fatty acids

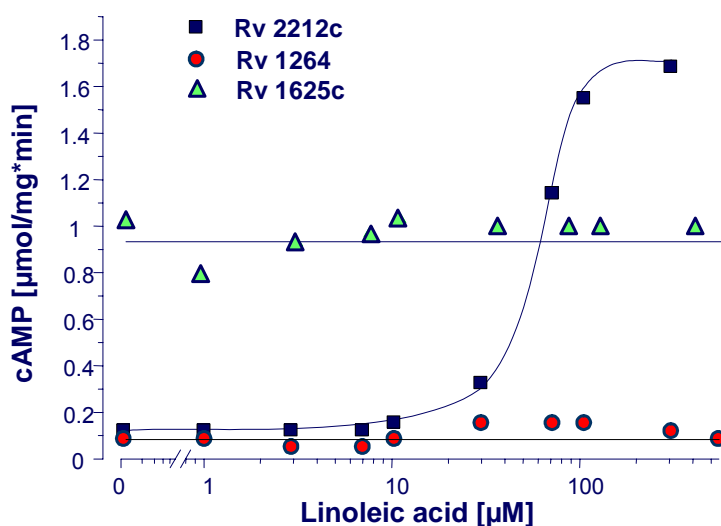
5 mM solutions of unsaturated FAs (except for arachidonic acid) were prepared in 1 mM TRIS. Further dilutions were done in BIS-TRIS/HCl, pH 6.5 for Rv2212c, in MES/TRIS, pH 5.7 for Rv1264 (from Dr. Linder) and in TRIS/HCl, pH 7.5 for Rv1625c (from Dr. Guo). Arachidonic acid was obtained as a 328 mM alcohol solution from Prof. Laufer's laboratory, diluted to 5 mM in 1 mM TRIS and further diluted in the buffers indicated above. Palmitic acid was dissolved in alcohol (300 mM), diluted to 5 mM in 1 mM TRIS and further diluted as above.

FAs were tested at 1 to 500 μM with 100 nM Rv2212c₁₋₃₈₈, Rv1625c and 600 nM Rv1264 holoenzyme. Testing with Rv1625c and Rv1264 was done as a control to see whether any effect is specific to Rv2212c or it is generalized among other mycobacterial ACs. Linoleic acid (300 μM) caused a 13-fold increase in Rv2212c₁₋₃₈₈ activity, while oleic and arachidonic acid (500 μM and 70 μM, respectively) stimulated 9-fold (fig. 4.31 a, b and c). V_{max} was unaffected by the presence of 100 μM of any of these FA, K_m decreased slightly and the Hill coefficient decreased indicating a loss in cooperativity in substrate binding (table 4.14). On the other hand, this effect was not detected with the other two mycobacterial ACs, Rv1264 and Rv1625c (fig. 4.31, a and b). Rv1625c activity was not affected at all up to a concentration of 500 μM (linoleic and oleic), and Rv1264 was only 2-fold stimulated by linoleic acid (100 μM). Linolenic acid (300 μM) stimulated Rv2212c₁₋₃₈₈ 4-fold (fig. 4.31, d)

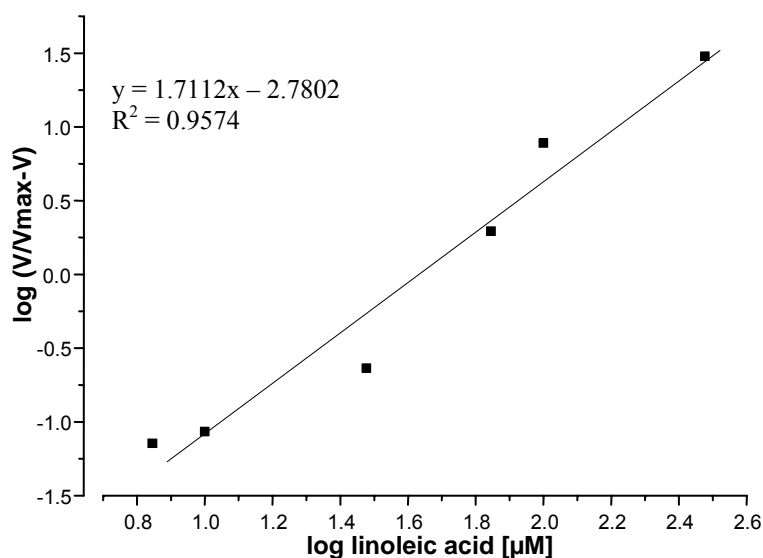
Results

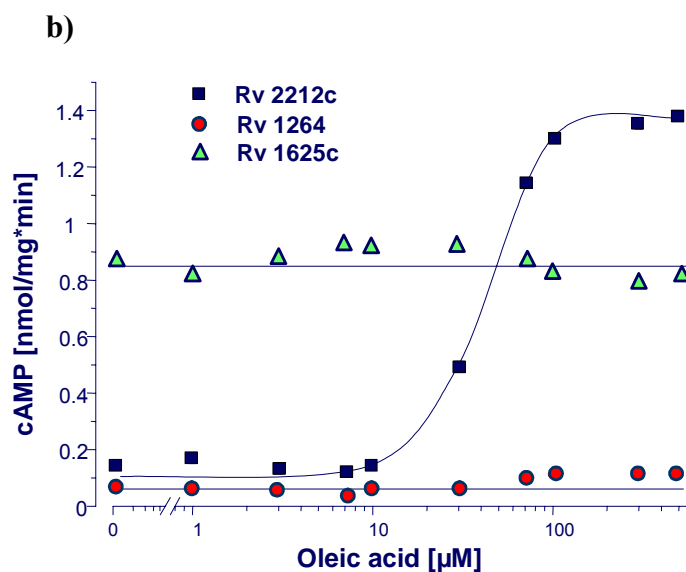
and palmitic acid (100 μM) 3-fold. While linolenic acid (30 and 300 μM), arachidonic acid (10 and 70 μM) and palmitic acid (100 and 300 μM) did not affect Rv1264 activity. The Hill coefficients of linoleic, oleic and arachidonic acid stimulation were 1.6 to 1.7 (table 4.13), denoting a cooperative binding of these fatty acids to Rv2212c₁₋₃₈₈. Arachidonic acid was most active ($\text{EC}_{50} = 10 \mu\text{M}$), (table 4.13). Comparing these results to those in section 4.2.3.7, we can see that the effects of linoleic, oleic and arachidonic acid on Rv2212c₂₁₂₋₃₈₈ are less than half of that on Rv2212c₁₋₃₈₈. Also the Hill coefficients of 1.0 (table 4.2), show no cooperativity in binding of these FAs to Rv2212c₂₁₂₋₃₈₈.

a)

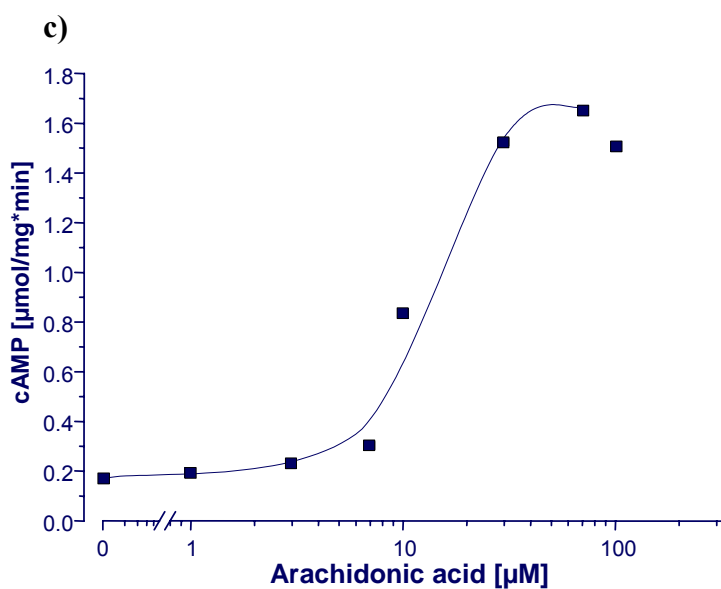
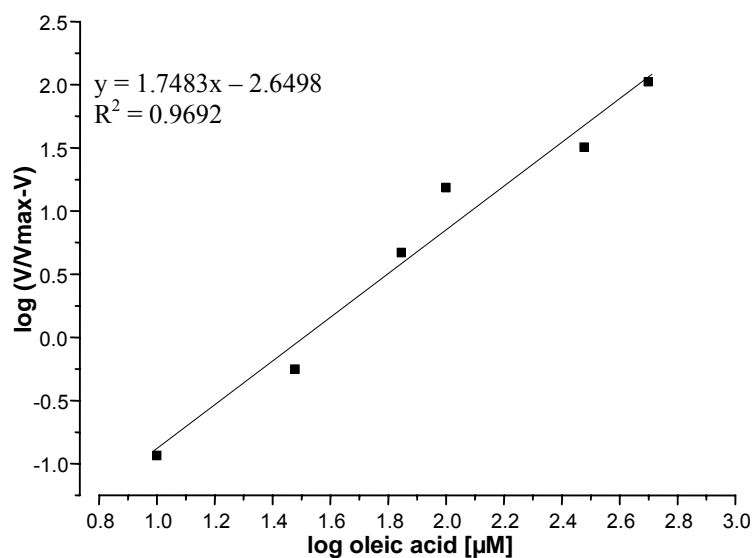


Linoleic acid (μM)	Rv2212 ₁₋₃₈₈ ($\mu\text{mol}/\text{mg}\cdot\text{min}$)	Rv1264 ($\mu\text{mol}/\text{mg}\cdot\text{min}$)	Rv1625 ($\mu\text{mol}/\text{mg}\cdot\text{min}$)
0	0.132	0.084	1.021
1	0.124	0.080	0.804
3	0.116	0.067	0.940
7	0.117	0.051	0.977
10	0.139	0.102	1.036
30	0.329	0.131	0.990
70	1.160	0.160	0.987
100	1.551	0.160	0.997
300	1.694	0.121	0.990
500	1.424	0.101	0.851





Oleic acid (µM)	Rv2212 ₁₋₃₈₈ µmol/mg*min	Rv1264 µmol/mg*min	Rv1625 µmol/mg*min
0	0.149	0.069	0.897
1	0.165	0.061	0.830
3	0.128	0.052	0.884
7	0.127	0.039	0.931
10	0.145	0.065	0.905
30	0.499	0.065	0.923
70	1.146	0.109	0.865
100	1.305	0.113	0.837
300	1.348	0.120	0.804
500	1.377	0.113	0.806



Arachidonic acid (µM)	Rv2212 ₁₋₃₈₈ µmol/mg*min
0	0.191
1	0.196
3	0.229
7	0.304
10	0.834
30	1.525
70	1.649
100	1.504
300	0.933

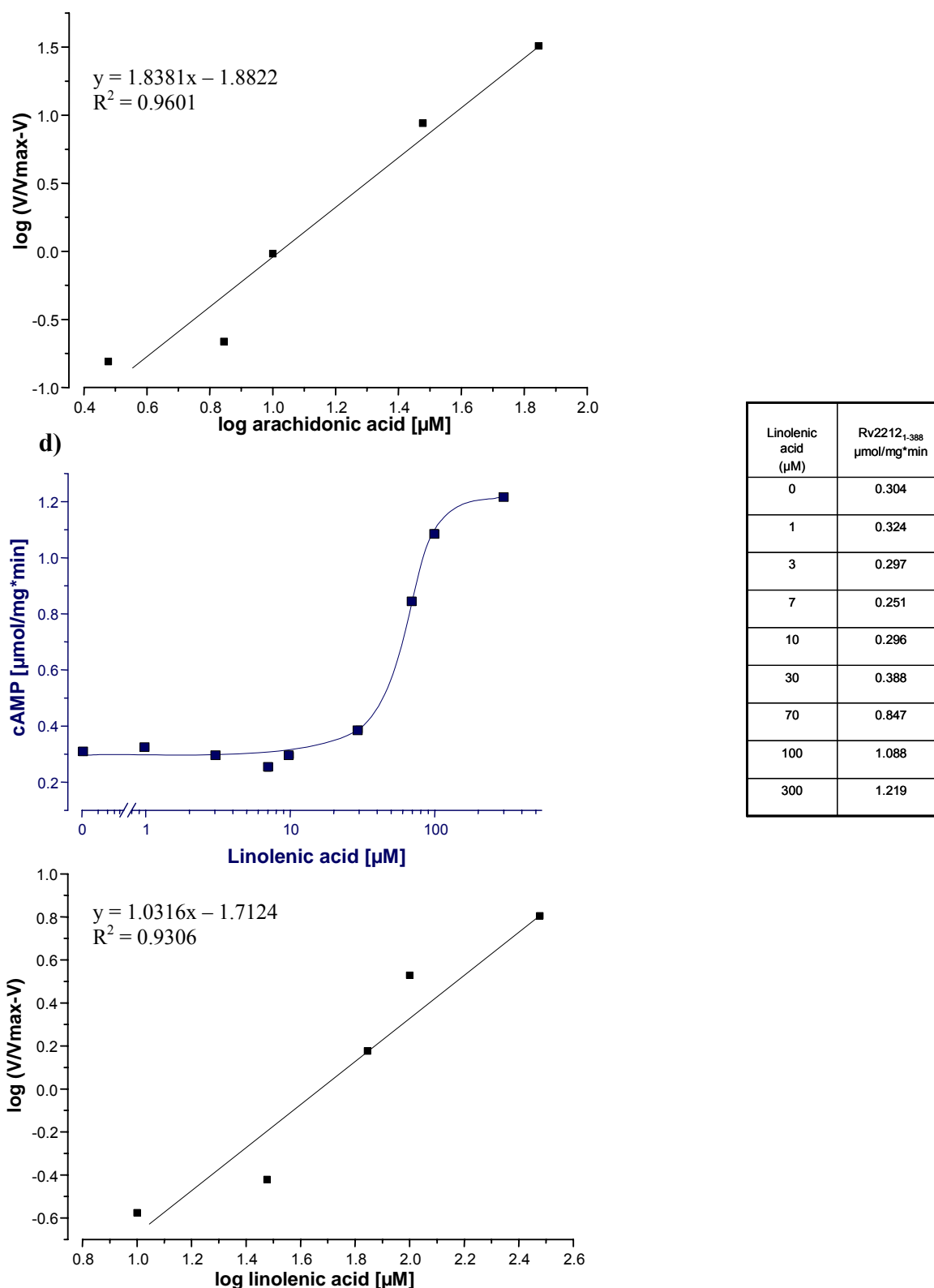


Fig. 4.31: Dose–response curves of linoleic, oleic, arachidonic and linolenic acid stimulation of Rv2212c₁₋₃₈₈ activity (**a**, **b**, **c** and **d**), and of linoleic and oleic acids on activities of Rv1264 and Rv1625c (**a** and **b**). The corresponding Hill plots for Rv2212c₁₋₃₈₈ are shown. Assay conditions were 500 μM ATP, 3 mM Mn^{2+} , BIS-TRIS/HCl, pH 6.5, 37°C, 10 min for Rv2212c. The same conditions were applied except for a different buffer system (MES/TRIS, pH 5.7) for Rv1264 and a different buffer and reaction temperature (TRIS/HCl, pH 7.5 at 30°C) for Rv1625c. For each fatty acid dilution, a control sample consisting of the solvent system free from FA was tested to exclude the solvent effect.

Fatty acid	EC ₅₀ [μM]	Hill coefficient
Linoleic	56 ± 4 (2)	1.7 ± 0.1 (2)
Oleic	41 ± 3 (2)	1.6 ± 0.1 (2)
Arachidonic	10 ± 0.2 (4)	1.7 ± 0.1 (4)
Linolenic	63 ± 0.8 (4)	1.3 ± 0.04 (4)

Table 4.13: EC₅₀ values and Hill coefficients for FAs tested with Rv2212c₁₋₃₈₈. EC₅₀ values were derived by Origin 6.0 program and the Hill coefficients from the Hill plots above (fig. 4.31). Standard errors of the mean are shown (number of experiments in brackets).

Kinetic parameter	Rv2212c ₁₋₃₈₈	Rv2212c ₁₋₃₈₈ + 100 μM linoleic	Rv2212c ₁₋₃₈₈ + 100 μM oleic	Rv2212c ₁₋₃₈₈ + 70 μM arachidonic
V _{max} (μmol/mg*min)	3.6 ± 0.1 (6)	3.8 ± 0.1 (6)	4.1 ± 0.0 (2)	3.6 ± 0.05 (2)
K _m (mM)	2.2 ± 0.2 (6)	0.9 ± 0.02 (6)	1.2 ± 0.01 (2)	1.1 ± 0.1 (2)
Hill coefficient	1.8 ± 0.0 (6)	1.2 ± 0.02 (6)	1.0 ± 0.03 (2)	0.9 ± 0.01 (2)

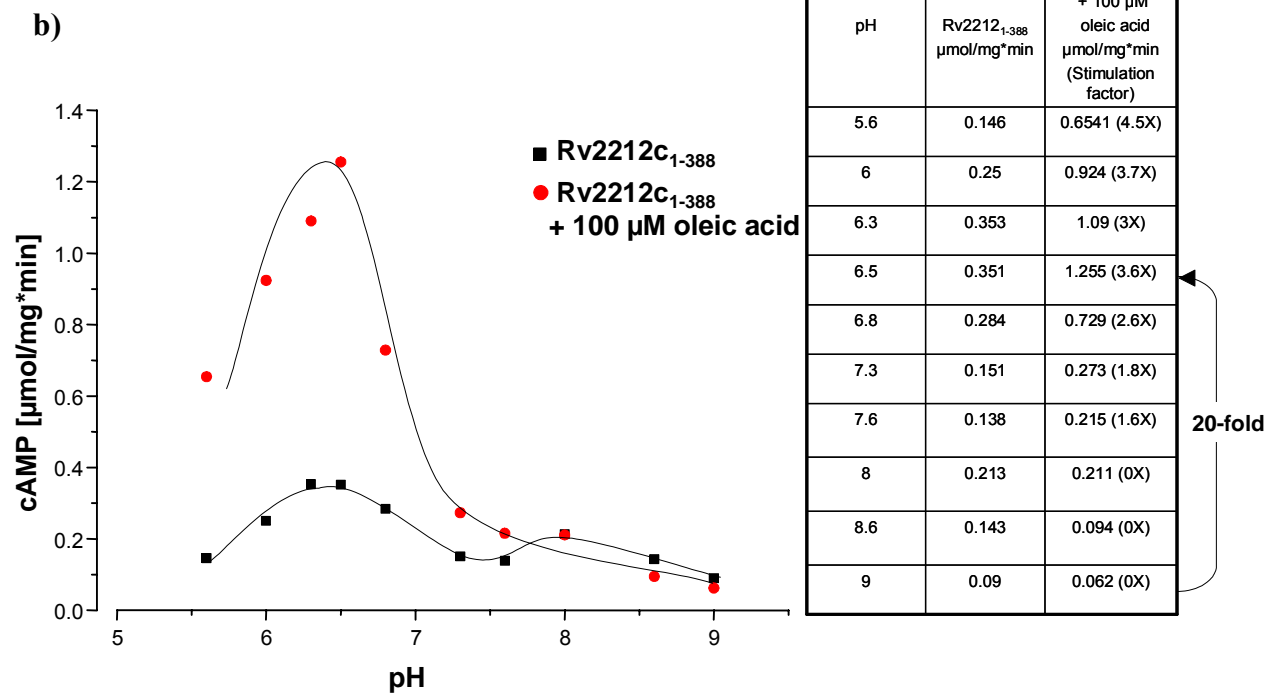
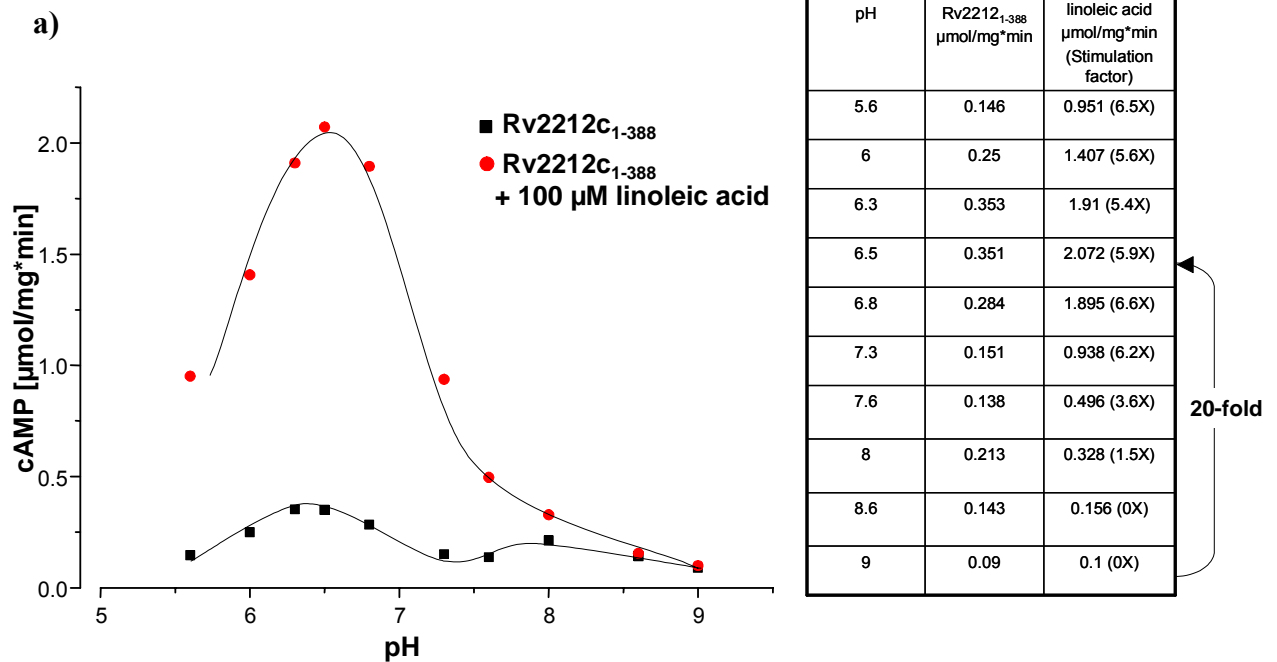
Table 4.14: Kinetic characterization of Rv2212c₁₋₃₈₈ alone and in the presence 100 μM of linoleic and oleic acids, and 70 μM arachidonic. Assay conditions were 10 mM Mn²⁺, BIS-TRIS/HCl, pH 6.5, 37°C, 10 min. An ATP range of 0.1-6 mM was used. Standard errors of the mean are shown (number of experiments in brackets).

4.2.7.5.6 pH dependence of fatty acids effect

100 μM linoleic, oleic and arachidonic acid were tested with 100 nM Rv2212c₁₋₃₈₈ at different pH (5-9). The three fatty acids showed a significant stimulation of the enzymatic activity starting at pH 5.6 to pH 7.6, while above that hardly any stimulation was detected (fig. 4.32). Also the increase in specific activity usually observed at pH 8 was lost in presence of the FA. The specific activity increased 20-25 fold at pH 6.5 compared to that at pH 9, in the presence of FAs (fig. 4.32). This points to a pH-sensory effect in presence of these FAs. V_{max} values and Hill coefficients remained unaffected at pH 6.5 and 9, in the presence of 100 μM linoleic acid (table 4.15). While the K_m value increased almost 25-fold from 0.9 ± 0.02 mM ATP at

Results

pH 6.5 to 23 ± 0.5 mM at pH 9 (table 4.15). The effect of linoleic (100 μ M) and arachidonic (70 μ M) acid was also tested on Rv1264 at different pH values (5.5, 6.5 and 7.5) as a control. A 4-fold increase in activity was shown by linoleic at pH 7.5, while arachidonic acid caused a 2-fold stimulation.



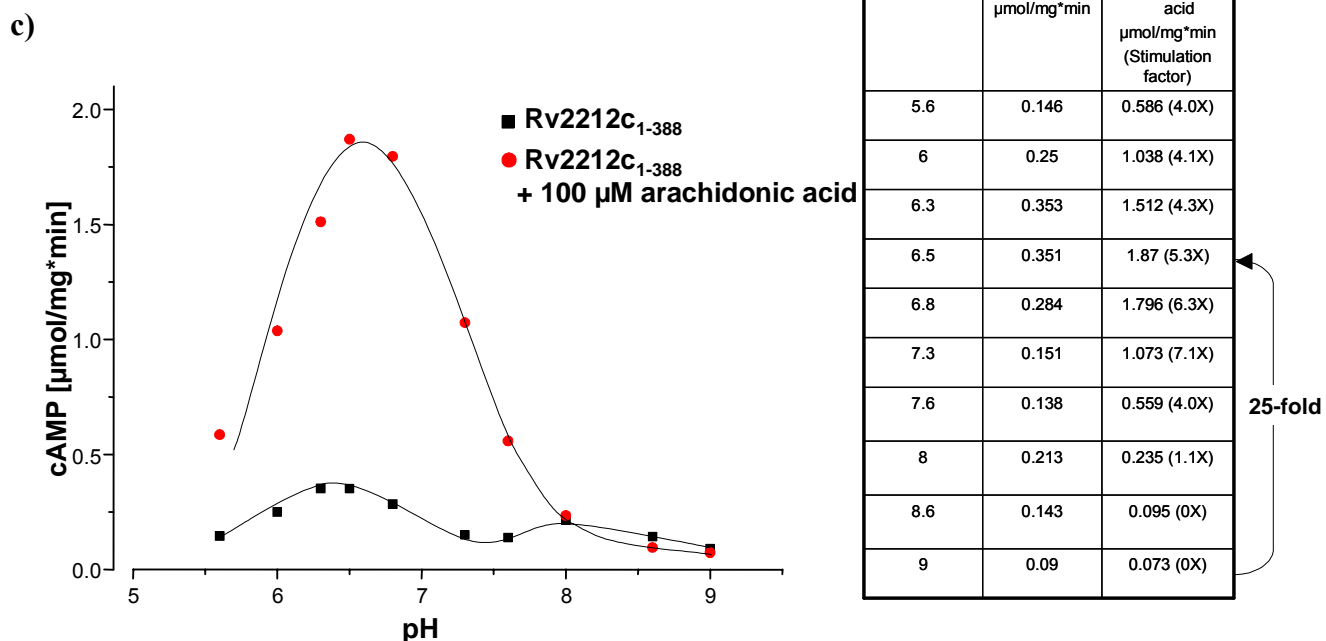


Fig. 4.32: pH dependence curves of Rv2212c₁₋₃₈₈ ± 100 μM of linoleic, oleic and arachidonic acids (a,b and c). Assay conditions were 500 μM ATP, 3 mM Mn²⁺, 37°C, 10 min. Buffer systems used: Acetate/NaOH (pH 5 and 5.6), BIS-TRIS/HCl (pH 5.6-7.3) and TRIS/HCl (pH 7.3-9).

Kinetic parameter	Rv2212c ₁₋₃₈₈ (pH=6.5)	Rv2212c ₁₋₃₈₈ + 100 μM linoleic (pH=6.5)	Rv2212c ₁₋₃₈₈ + 100 μM linoleic (pH=9)
V _{max} (μmol/mg*min)	3.6 ± 0.1 (6)	3.8 ± 0.1 (6)	3.9 ± 0.1 (6)
K _m (mM)	2.2 ± 0.2 (6)	0.9 ± 0.02 (6)	23 ± 0.5 (6)
Hill coefficient	1.8 ± 0.0 (6)	1.2 ± 0.02 (6)	1.3 ± 0.01 (6)

Table 4.15: Kinetic characterization of Rv2212c₁₋₃₈₈ ± 100 μM linoleic acid at pH 6.5 and with 100 μM linoleic acid at pH 9. Assay conditions were 10 mM Mn²⁺, BIS-TRIS/HCl, pH 6.5 and TRIS/HCl, pH 9 at 37°C for 10 min. An ATP range of 0.1-6 mM was used at pH 6.5 and a range of 0.1-8 mM at pH 9. Kinetic parameters of Rv2212c₁₋₃₈₈ at pH 9 without any additives were not determined.

4.2.7.5.7 Effect of linoleic acid on the time dependence

100 μM of linoleic acid was tested with 100 nM holoenzyme at 2 min. time intervals. The velocity was linear up to 12 min \pm linoleic acid (fig. 4.33). This could be due to the inhibiting effect of increasing amounts of the outcoming pyrophosphate. The stimulation factor of linoleic acid decreased gradually over time.

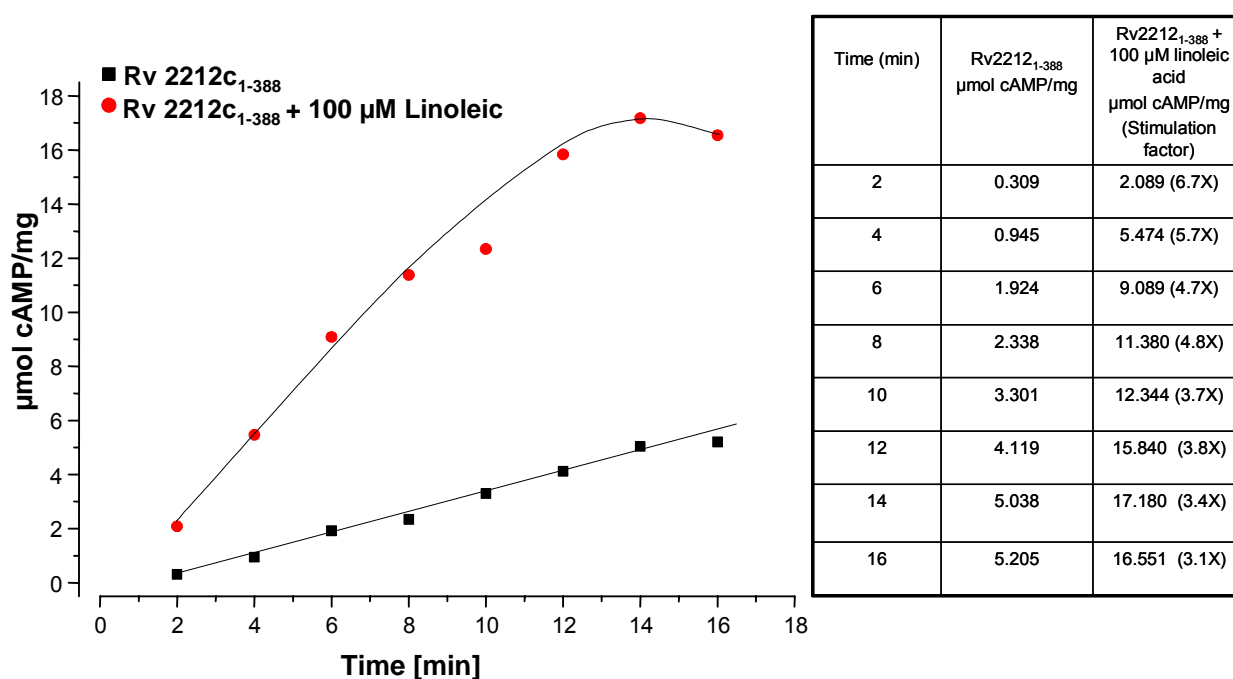


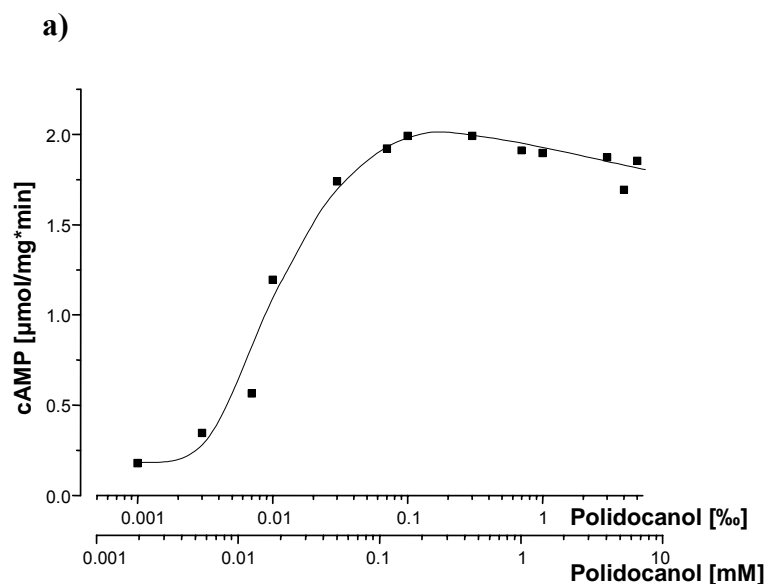
Fig. 4.33: Time dependence of Rv2212c₁₋₃₈₈ \pm 100 μM linoleic acid. Assay conditions were 100 nM enzyme, 500 μM ATP, 3 mM Mn^{2+} , BIS-TRIS/HCl, pH 6.5, 37°C .

4.2.7.5.8 Effect of detergents

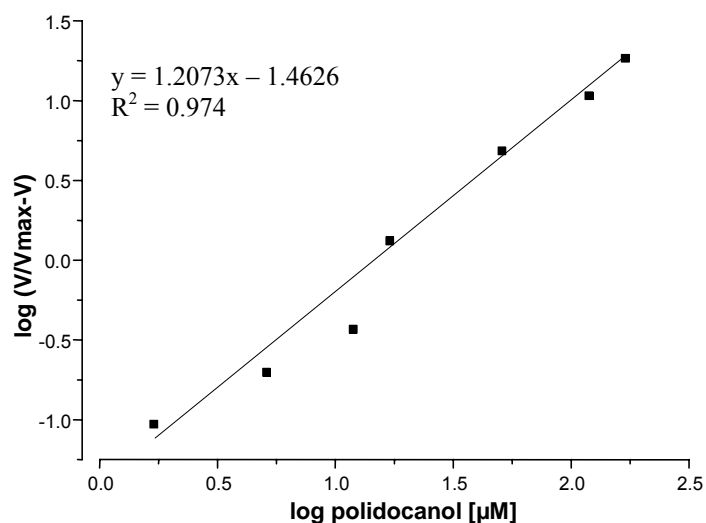
To examine whether these stimulatory effects are just due to the detergent-like (hydrophilic/hydrophobic) properties of FA, the effect of different detergents on 100 nM Rv2212c₁₋₃₈₈ activity was tested.

Detergents were prepared as a 10% solution in BIS-TRIS/HCl, pH 6.5, and further dilutions were made in the same buffer. A concentration range of 0.001 – 3‰ was tested. Polidocanol (0.1‰ = 170 μM) increased the activity 12-fold, while Triton X-100 and Nonidet P40 caused 5- and 4-fold increase respectively at 0.07‰ (fig. 4.34). V_{max} was not changed by 170 μM Polidocanol, while K_m decreased about 8-fold from 2.2 ± 0.2 mM ATP to 0.3 ± 0.05 mM

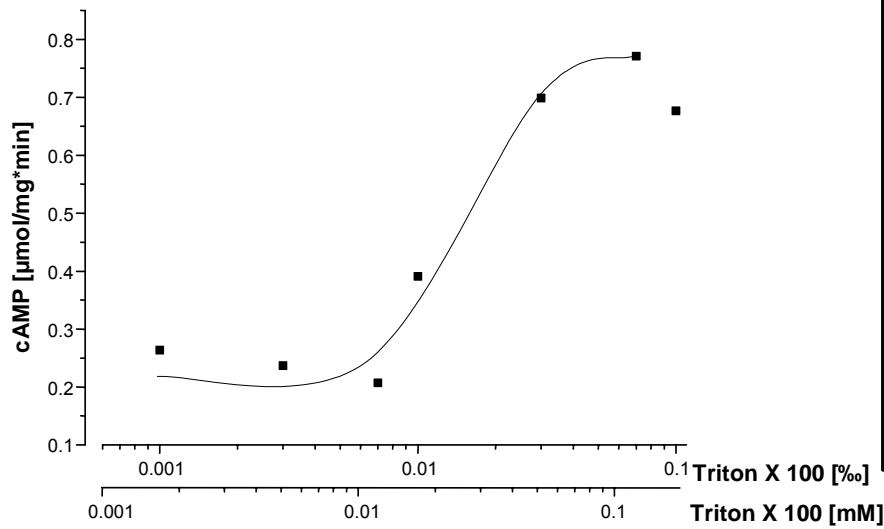
(table 4.17). The Hill coefficient decreased from 1.8 ± 0.0 to 1.1 ± 0.1 . CHAPS (2‰) stimulated Rv2212c₁₋₃₈₈ only 3-fold, while PEG (200, 400, 1000, 8000) did not show an effect up to 1%. As a control, the activity of Rv1264 AC was tested in the presence of Polidocanol (0.1 and 0.01‰), Triton X-100, Nonidet P40 and CHAPS (0.2 and 2‰ each). None affected AC activity significantly. Detergents were prepared as above for this test but using MES/TRIS, pH 5.5 (optimum pH for Rv1264). Assay conditions were as in legend of fig. 4.34, except for the MES/TRIS, pH 5.5.



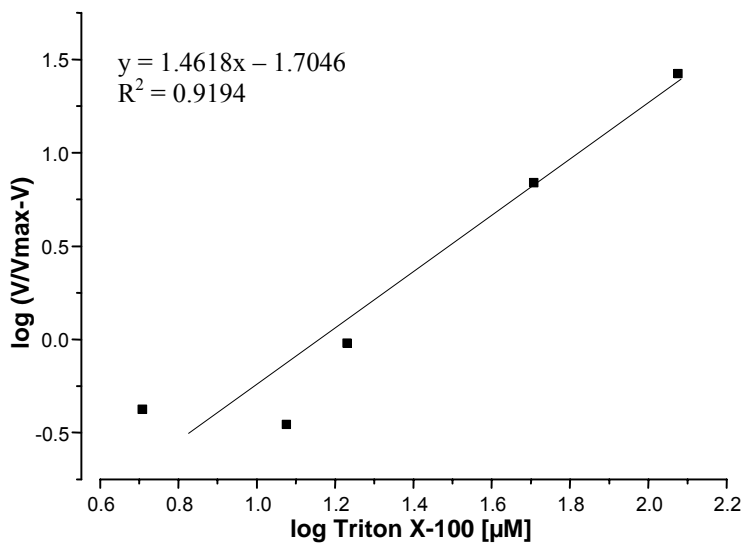
Polidocanol (mM)	Rv2212 ₁₋₃₈₈ $\mu\text{mol}/\text{mg}\cdot\text{min}$
0	0.173
0.0017	0.18
0.0051	0.348
0.0119	0.566
0.017	1.195
0.051	1.74
0.119	1.921
0.17	1.992
0.51	1.992
1.19	1.911
1.7	1.896
5.1	1.87
6.8	1.694
8.5	1.85



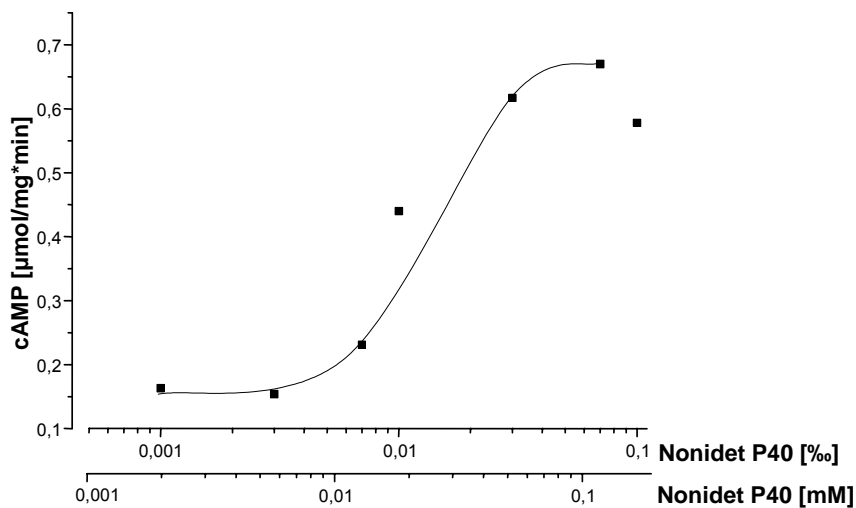
b)



Triton X-100 (mM)	Rv2212 ₁₋₃₈₈ µmol/mg*min
0	0.157
0.0015	0.264
0.0045	0.237
0.0105	0.207
0.015	0.391
0.045	0.699
0.105	0.771
0.15	0.677



c)



Nonidet P40 (mM)	Rv2212 ₁₋₃₈₈ µmol/mg*min
0	0.157
0.0017	0.163
0.0051	0.154
0.0119	0.231
0.017	0.44
0.051	0.617
0.119	0.67
0.17	0.578

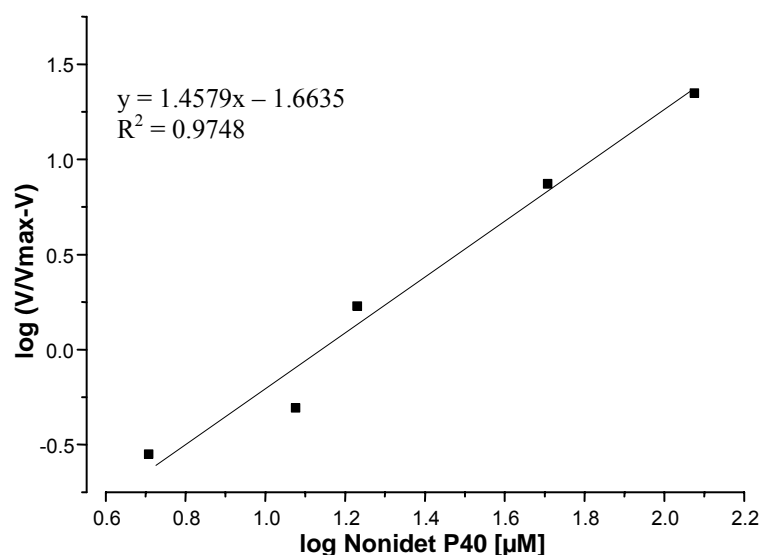


Fig. 4.34: Dose–response curves of Polidocanol, Triton X-100 and Nonidet P40 stimulation of Rv2212c₁₋₃₈₈ (a, b and c). The corresponding Hill plots are shown. Assay conditions were 100 nM protein, 500 µM ATP, 3 mM Mn²⁺, BIS-TRIS/HCl, pH 6.5, 37°C, 10 min.

Detergent	EC ₅₀ [µM]	Hill coefficient
Polidocanol	16 ± 0.6 (2)	1.2 ± 0.04 (2)
Triton X-100	16 ± 0.05 (2)	1.5 ± 0.2 (2)
Nonidet P40	15 ± 0.2 (2)	1.5 ± 0.1 (2)

Table 4.16: EC₅₀ values and Hill coefficients of detergents tested with Rv2212c₁₋₃₈₈. Assay conditions (see legend of fig. 4.34). Standard errors of the mean are shown (number of experiments in brackets).

Kinetic parameter	Rv2212c ₁₋₃₈₈	Rv2212c ₁₋₃₈₈ + 170µM Polidocanol
V _{max} (µmol/mg*min)	3.6 ± 0.1 (6)	3.8 ± 0.1 (2)
K _m (mM)	2.2 ± 0.2 (6)	0.3 ± 0.05 (2)
Hill coefficient	1.8 ± 0.0 (6)	1.1 ± 0.1 (2)

Table 4.17: Kinetic characterization of Rv2212c₁₋₃₈₈ ± 170 µM (0.1%) Polidocanol. Assay conditions were: 100 nM protein, 10 mM Mn²⁺, BIS-TRIS/HCl, pH 6.5, 37°C, 10 min. An ATP range of 0.1-6 mM was used. Standard errors of the mean are shown (number of experiments in brackets).

4.2.7.5.9 pH dependence of the polidocanol effect

100 nM of Rv2212c₁₋₃₈₈ was tested with 0.2‰ (340 μM) Polidocanol at a pH range of 5-9. Polidocanol significantly stimulated the activity at all pH values. It maintained a more or less constant specific activity from pH 6 till pH 8.6 thus displaying a pH-independent stimulation of the holoenzyme (fig. 4.35). Polidocanol (340 μM) did not show an enzymatic stimulation when tested with Rv1264 at pH-values 5.5, 6.5 and 7.5 (table 4.18).

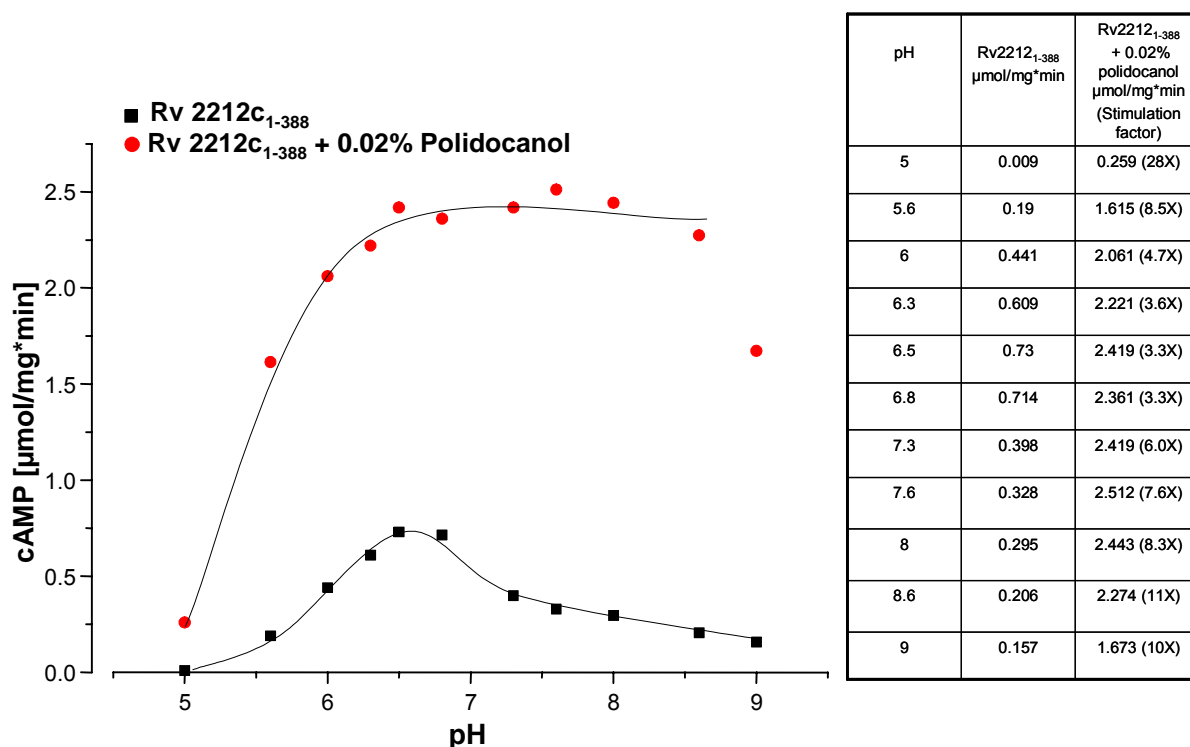


Fig. 4.35: pH dependence curve of Rv2212c₁₋₃₈₈ ± 0.2‰ polidocanol. Assay conditions were 100 nM protein, 500 μM ATP, 3 mM Mn²⁺, 37°C, 10 min. Buffer systems used: Acetate/NaOH (pH 5 and 5.6), BIS-TRIS/HCl (pH 5.6-7.3) and TRIS/HCl (pH 7.3-9).

pH	Rv1264 (nmol·mg ⁻¹ ·min ⁻¹)	Rv1264 + 340 μM polidocanol (nmol·mg ⁻¹ ·min ⁻¹)
5.5	71	45
6.5	25	15
7.5	2	2.8

Table 4.18: Specific activities of Rv1264 ± 0.2‰ polidocanol at different pH. Assay conditions were 600 nM protein, 500 μM ATP, 3 mM Mn²⁺, 37°C, 10 min. Buffer systems used: MES/TRIS (pH 5.5), BIS-TRIS/HCl (pH 6.5) and TRIS/HCl (pH 7.5).

4.2.7.5.10 Effect of Polidocanol on the time dependence

Polidocanol (0.2%) caused a 14.5 X stimulation in activity of Rv2212c₁₋₃₈₈. This stimulation factor decreased gradually with time. The same as with 100 μ M linoleic acid (fig. 4.33), a linearity was displayed up to 12 min \pm 0.2% Polidocanol, then the activity decreased slightly along with time (fig. 4.36).

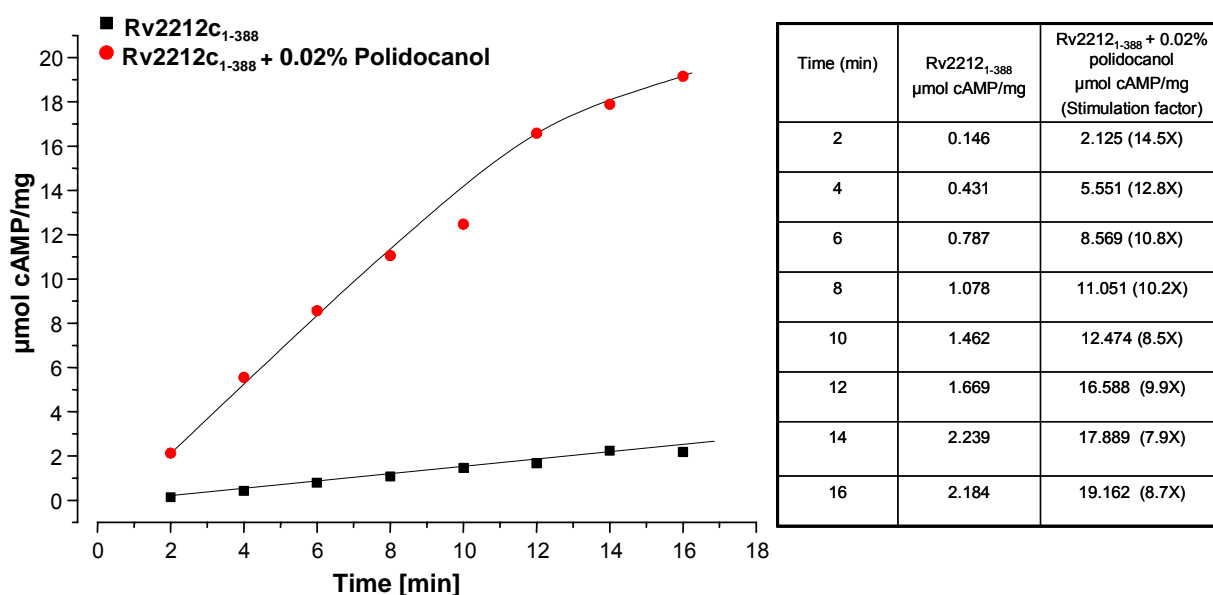


Fig. 4.36: Time dependence of Rv2212c₁₋₃₈₈ \pm 0.2% polidocanol. Assay conditions were 100 nM protein, 500 μ M ATP, 3 mM Mn²⁺, BIS-TRIS/HCl, pH 6.5, 37°C .

4.2.7.6 Crystallization of Rv2212c₁₋₃₈₈

The Ni²⁺-NTA purified protein was prepared in two different concentrations. 7.1 mg/ml was used with buffers from CS and CS2 kits at 12°C. A 12.9 mg/ml solution was tried with buffers from CS2 and CS Lite and left at 16°C, then transferred to 12°C after 17 days. Rv 2212c₁₋₃₈₈ had a high tendency to precipitate and no crystals grew.

4.2.8 Expression and characterization of C-terminally His-tagged

constructs of adenylyl cyclase Rv2212c

These constructs were cloned in pQE-60 and expressed to be used for crystallization. Transferring the His-tag to the C-terminus has been useful for crystallization as in the case of the CHD of Rv0386 (Castro, L.I., 2004).

4.2.8.1 Expression and purification of Rv2212c₁₋₂₀₂ C-His, Rv2212c₂₁₂₋₃₈₈ C-His and

Rv2212c₁₋₃₈₈ C-His

The constructs were expressed in E.coli at 16°C overnight, using 60 µM IPTG for Rv2212c₁₋₂₀₂ and 100 µM for Rv2212c₂₁₂₋₃₈₈ and Rv2212c₁₋₃₈₈. Cells were lysed by sonication, treated with lysozyme and DNAaseI, and proteins were purified to homogeneity by Ni²⁺-NTA affinity chromatography. Protein yield was about 45 µg, 52 µg and 18 µg per 200 ml culture for each of Rv2212c₁₋₂₀₂, Rv2212c₂₁₂₋₃₈₈ and Rv2212c₁₋₃₈₈ respectively. The proteins were stored at -20 °C with 20% glycerol. They were analysed on a 12.5% SDS-PAGE where only Rv2212c₁₋₂₀₂ and Rv2212c₂₁₂₋₃₈₈ were detected, Rv2212c₁₋₃₈₈ was detected by a Western blot (fig. 4.37, A and B). A Dot-blot was also carried out to assure detection of the proteins because of the faint bands observed on the SDS-PAGE (fig. 4.37, C).

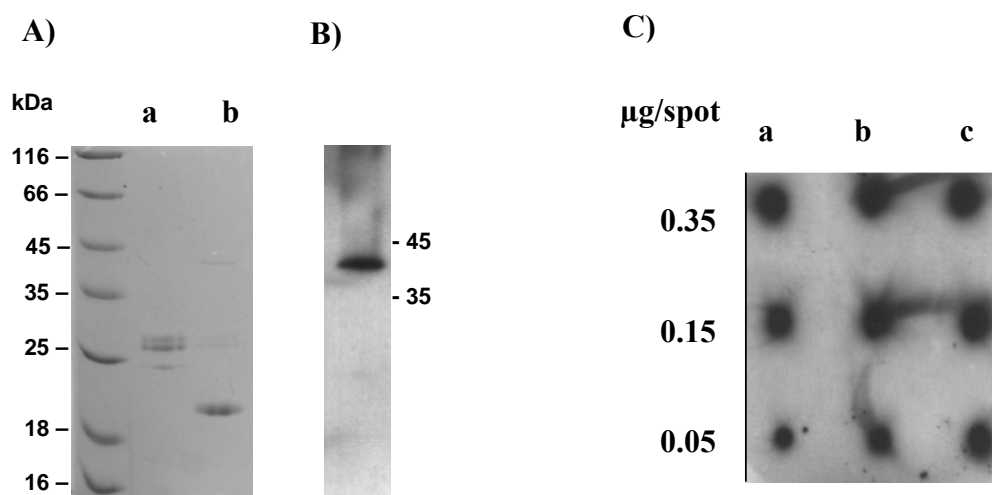


Fig. 4.37: **A)** 12.5 % SDS-PAGE of Ni^{2+} -NTA purified proteins of: 2.2 μg Rv2212c₁₋₂₀₂ C-His (**a**) and 2.5 μg Rv2212c₂₁₂₋₃₈₈ C-His (**b**). Note that in lane (**a**) the lower faint band of about 23.43 kDa is that of the purified protein. **B)** Western blot showing a single band at about 43 kDa of Rv2212c₁₋₃₈₈ C-His, from a 12.5 % SDS-PAGE using Tetra-His antibody as primary antibody and the goat anti-mouse IgG-F_c peroxidase conjugated antibody as secondary antibody. Exposure time of the film is 4 sec. **C)** Dot-blot using the same antibodies as in (**B**). (**a**) Rv2212c₁₋₂₀₂ C-His, (**b**) Rv2212c₂₁₂₋₃₈₈ C-His and (**c**) Rv2212c₁₋₃₈₈ C-His. Protein concentrations of 0.05-0.035 μg per spot were applied. Film exposure was 1 min.

4.2.8.2 Adenylyl cyclase activity

The specific activity of Rv2212c₂₁₂₋₃₈₈ C-His was 332.4 nmol/mg*min which is only 10 % of the corresponding N-terminally His-tagged construct. While that of Rv2212c₁₋₃₈₈ C-His was 563.5 nmol/mg*min which is 78 % of the corresponding N-terminally His-tagged holoenzyme. The assays were conducted using 500 μM ATP, 3 mM Mn^{2+} , BIS-TRIS/HCl, pH 6.5, 37°C, 10 min. 3.4 and 2.4 μg of Rv2212c₂₁₂₋₃₈₈ and Rv2212c₁₋₃₈₈ were used in test. The constructs were not further used in crystallization experiments because of the poor yield and comparatively low activity.

5 Discussion

5.1 Mycobacterial Rv2435c

In the completed genome of *M. tuberculosis* H37Rv 15 open reading frames were identified which probably code for functional class III ACs, implying that the resulting signal transduction modalities using cAMP as a second messenger are of great importance to the tubercle bacillus (Cole *et al.*, 1998; McCue *et al.*, 2000). Two of these genes, Rv1625c and Rv2435c, code for proteins that are grouped with the mammalian ACs on a branch separate from other prokaryotic cyclases. This prompted further analysis of their protein sequences. Recent work concentrated on the membrane-bound Rv1625c (Guo *et al.*, 2001, 2005; Reddy *et al.*, 2001; Shenoy *et al.*, 2003), while Rv2435c remained enigmatic. Seven predicted mycobacterial cyclase genes contain variations at canonical positions of the catalytic centre; one is Rv2435c belonging to class IIIa and six class IIIc genes. Four class IIIb cyclases contain a threonine variant at the substrate binding aspartate (Linder and Schultz, 2003). So the pressing question was whether this non-canonical predicted AC, Rv2435c, is capable of converting ATP into cAMP in spite of having four deviations from the conserved hexad of catalytic residues. And if active, does it function as a homodimer like the similar mammalian-type Rv1625c? What is the real function of its unique extracellular domain? Actually two main points encouraged the expression and biochemical characterization of Rv2435c at that time. First, the significant sequence similarity of its CHD to the catalytically active Rv1625c CHD (55%) as well as several eukaryotic ACs such as the C₂ segment of rat type II (IIC2) and C_{1a} of canine type V (VC1) (49 % and 48 %, respectively). Second, the rather unexpected enzymatic activities observed for unorthodox class IIIc mycobacterial ACs (Rv0386 and Rv1900c) which were investigated in parallel in this laboratory.

5.2 Characterization of Rv2435c₅₁₁₋₇₃₀

The recombinant Rv2435c₅₁₁₋₇₃₀ was successfully expressed in *E.coli* BL21 cells and purified to be utilized in answering the first two of the former questions. It is a soluble protein having a molecular mass of 25 kDa. Activity was tested with different protein concentrations, substrate concentrations and pH values. Both Mn²⁺ and Mg²⁺ were tested as a metal cofactor. The GC activity was also tested at 0.1 mM GTP. Unfortunately all these trials were in vain. This does not necessarily mean that the four variations in the six canonical residues are the only reason behind the inactivity of this CHD. Recently, mycobacterial ACs showing variations in these canonical residues appeared to be utilizing alternate mechanisms of catalysis or substrate-binding for the conversion of ATP to cAMP. For example, in the variant

AC Rv1900c both a histidine residue which substitutes the canonical transition-state stabilizing asparagine, and an asparagine-aspartate couple which replaces the usual substrate-specifying lysine-aspartate pair appeared to be dispensable for catalysis. So the preference of Rv1900c for ATP over GTP is probably governed by other determinants as general steric constraints of the purine-binding pocket (Sinha *et al.*, 2005). On the other hand, the unorthodox Rv0386 class IIIc AC revealed a completely novel mechanism of substrate binding where the glutamine-asparagine couple was specifically needed for catalysis (Castro *et al.*, 2005).

5.3 Characterization of Rv2435c holoenzyme

Failure with Rv2435c CHD led to the transition to the next point and trying with the holoenzyme. Rv2435c holoenzyme seemed to be an interesting protein in terms of its domain composition. It is the only mycobacterial AC which possesses a C-terminal CHD preceded by an extracellular domain anchored by two transmembrane helices (fig. 4.1). Through a sequence alignment with Rv1625c three different starts were chosen for the predicted Rv2435c AC holoenzyme. The three holoenzymes were detected by a Western blot in both supernatants and pellets. It is most likely that the main portion of the protein was degraded in all three constructs yielding a fragment corresponding to nearly the size of the CHD (25 kDa) to which the C-terminal His-tag is attached. It could be speculated that the folding of these holoenzymes was defective and that the most probable site for rupture was an interdomain, before the CHD. One hypothesis might be that a certain ligand for the Rv2435c extracellular domain exists in *M. tuberculosis* and not in *E. coli* which might be responsible for preserving the protein's native conformation and stability. As it was recently reported that the transcription factor TraR of *Agrobacterium tumefaciens* must bind its inducing ligand to acquire its native conformation and protease resistance when expressed in *E. coli* cells (Zhu and Winans, 2001). It is worth saying that such phenomenon of holoenzyme degradation during expression was observed before with mycobacterial ACs Rv0386, Rv1319c and Rv1318c (Castro L.I., 2004; Hammer A., 2004).

Inability of Rv2435c to function as an active AC could be attributed to one of several reasons: (i) Redundancy of functional ACs in *M. tuberculosis* which could have led to an evolutionary deterioration of its activity. (ii) The need for a ligand that could initiate the enzymatic activity through the extracellular domain by inducing certain conformational changes under certain environmental conditions in the host. (iii) The comparatively high deviation from the canonical

residues (4 out of 6) could lead us to the assumption that Rv2435c serves a different biological function in the mycobacterium, especially due to the similarity between its extracellular domain and the methyl accepting chemotaxis proteins. Replacing the odd residues with the canonical ones might give clues in this issue.

5.4 Mycobacterial Rv2212c

Attention was focused to Rv2212c after the discovery of the autoinhibitory and pH-sensing functions of the N-terminal domain of AC Rv1264 which has a similar domain organization (Linder *et al.*, 2002; Tews *et al.*, 2005). The Rv2212c CHD has a specific activity of $3.1 \mu\text{mol cAMP}\cdot\text{mg}^{-1}\cdot\text{min}^{-1}$, and this belongs to the high activity CHDs of *M. tuberculosis* such as Rv1625c ($2 \mu\text{mol cAMP}\cdot\text{mg}^{-1}\cdot\text{min}^{-1}$; Guo *et al.*, 2001), Rv1264 ($1 \mu\text{mol cAMP}\cdot\text{mg}^{-1}\cdot\text{min}^{-1}$; Linder *et al.*, 2002), Rv1900c ($1 \mu\text{mol cAMP}\cdot\text{mg}^{-1}\cdot\text{min}^{-1}$; Sinha *et al.*, 2005) and Rv1647 ($3 \mu\text{mol cAMP}\cdot\text{mg}^{-1}\cdot\text{min}^{-1}$; Shenoy *et al.*, 2005). Being one of the most active mycobacterial ACs, the pressing question was how is it regulated.

When Stephan Zeibig (2003) started working on Rv2212c, he expressed both Rv2212c₂₁₂₋₃₈₈ and Rv2212c₁₋₃₈₈ and his main issue was to answer two questions: (i) Does the N-terminal domain of Rv2212c regulate the activity in a pH-dependent manner analogous to Rv1264? (ii) Does the N-terminal domain of Rv1264 retain its pH-sensing function when linked to the CHD of Rv2212c?

Both Rv2212c₁₋₃₈₈ and Rv2212c₂₁₂₋₃₈₈ had optimal activities at the same pH (6.5). An activation of the Rv2212c₁₋₃₈₈ by an acidic milieu was not observed. While Rv1264 holoenzyme was activated 40-fold at acidic pH (6) (Tews *et al.*, 2005). This gave a clear negative answer to the first of the two questions above.

Two chimeras were built connecting the N-terminal domain of Rv1264 and the CHD of Rv2212c in a trial to investigate the second question (Zeibig, 2003). The linker region between the two domains in these chimeras was taken once from Rv2212c sequence and once from Rv1264 as shown in fig. 5.1.



Fig. 5.1: Sequence alignment showing the linker region between the CHD and the N-terminal domain in Rv2212c and Rv1264. The triangles mark the beginnings and the ends of the linker regions chosen in the two chimeras (Zeibig, 2003). Residues H₁₉₂ and E₁₉₅ in the α -N₁₀ switch, identified by mutagenesis to be important for the interaction between the regulatory and catalytic domains in Rv1264, are indicated by black dots (Tews *et al.*, 2005).

Both chimeras displayed similar pH-dependence to that of Rv2212c₁₋₃₈₈. Thus it is clear that the Rv1264 N-terminal domain did not confer its pH-sensing function to Rv2212c₂₁₂₋₃₈₈. However a significant drop in the activities of these chimeras compared to that of Rv2212c₁₋₃₈₈ indicated a rather similar autoinhibition. This could argue for a structural similarity of the protein surfaces of the CHDs of both enzymes at the regions of contact between the regulatory and catalytic domains. For example, the conservation of a certain epitope which plays an important role in the autoinhibition mechanism (Zeibig, 2003). After the elucidation of the X-ray structure of Rv1264 in both the active and inhibited states (Tews *et al.*, 2005), two residues in the α N₁₀-switch helix were identified by mutagenesis to be important in the interaction between the regulatory and catalytic domains. H₁₉₂ which is conserved in Rv2212c whereas E₁₉₅ is not. Both were included in the N-terminal domain of Rv1264 in the above mentioned chimeras (fig. 5.1). In the inhibited state, H₁₉₂ interacts with the conserved canonical K₂₆₁ and D₃₁₂ via hydrogen bonds, holding them away from their respective positions in the active state. Such an interaction might have occurred to some extent in the chimeras yielding the observed autoinhibition. E₁₉₅ interacts, together with D₆₂ and Y₆₆, with R₃₀₉ in the CHD. R₃₀₉ is not conserved in Rv2212c CHD which probably disrupts the second site of interaction rendering the holoenzyme active and unregulated, as the R309A mutant in Rv1264 (Tews *et al.*, 2005) (fig. 4.6). It is noteworthy that R₃₀₉ is conserved in similar ACs from *Brevibacterium liquefaciens* and *Streptomyces*, but not in Rv2212c from *M. tuberculosis* and its ortholog from *M. smegmatis* (Linder *et al.*, 2002).

Such an assumption could only be proven by an elucidation of the X-ray structure of Rv2212c. So we are left with the question: what is the function of the N-terminal domain and does it at all possess a role in regulating the Rv2212c₁₋₃₈₈?

5.5 Rv2212c₁₋₂₀₂

The dimer of N-terminal domains of Rv1264 was previously determined to 1.6 Å resolution (F.Findeisen *et al.*, unpublished data). This encouraged the idea of expression and purification of Rv2212c₁₋₂₀₂ for crystallization. It was successfully purified in large quantities. The first crystals were obtained with buffer CS#19 of the Hampton research kit in four days at 16°C at a protein concentration of 19.7 mg/ml. Optimization of the size and quality of the obtained crystals was then carried out through variation of the crystallization conditions and buffer concentrations. Suitable styloid crystals 50×100 μ were obtained with 30% isopropanol, 0.22 M CH₃COO NH₄, 0.1 M Tris/HCl pH 8.5 in seven days. But unfortunately these crystals did not diffract. Actually due to the presence of 30% isopropanol, the crystals had to be frozen and mounted at the beamline which might have disturbed the crystals. Due to the high crystallization potential of this domain, crystallization is continued in collaboration with the Biochemistry Centre in Heidelberg. Moving the His-tag to the C-terminal position was not tolerated by the Rv2212c₁₋₂₀₂, because of a 96 % reduction in protein yield. Moreover the protein was not sufficiently purified for crystallization.

5.6 Rv2212c₂₁₂₋₃₈₈

The recombinant Rv2212c₂₁₂₋₃₈₈ displayed high AC activity (3.1 μmol cAMP·mg⁻¹·min⁻¹) at 0.5 mM ATP using Mn²⁺ as a cofactor, whereas Mg²⁺-mediated catalysis was not detected. A preference for Mn²⁺ was shown by all mycobacterial ACs examined so far. GTP was not accepted as a substrate irrespective of the metal cation employed (Zeibig, 2003). The amount of cAMP increased linearly with time. Operating as a symmetric homodimer with two identical catalytic centres is likely due to the conservation of the six canonical amino acids. The Hill coefficient of 1.4 ± 0.02 indicated a pronounced cooperativity for ATP, consistent with the presence of two catalytic sites. This is supported by the increase in specific activity with increasing protein concentrations. The specific activity tripled by increasing protein concentration from 5 to 80 nM. The apparent association constant of 20 nM indicated a high affinity of the monomers to each other. The apparent V_{max} of 26 ± 0.5 μmol cAMP·mg⁻¹·min⁻¹ derived from a Hill-plot is very high compared to other mycobacterial ACs. Rv2212c₂₁₂₋₃₈₈ had a relatively high K_m (2.1 ± 0.01 mM) as the K_m values observed for purified membrane-bound and soluble ACs is within the range of 30-400 μM (Tang and Hurley, 1998). In comparison to the other mycobacterial CHDs (K_m of Rv1264 = 0.3 mM; Rv1625c = 0.15 mM; Rv0386 = 0.6 mM; Rv1900c = 0.3 mM; Rv1319c = 0.057 mM; Rv3645 = 1.2 mM)

(Castro *et al.*, 2005; Guo *et al.*, 2001; Linder *et al.*, 2002, 2004; Sinha *et al.*, 2005), Rv2212c₂₁₂₋₃₈₈ had a rather low affinity for ATP which might be of a biological significance. Truncations at the C-terminus of Rv2212c₂₁₂₋₃₈₈ were possible and not detrimental up to L₃₇₀. Therefore crystallization was attempted with Rv2212c₂₁₂₋₃₇₇, Rv2212c₂₁₂₋₃₇₄ and Rv2212c₂₁₂₋₃₇₀. On the other hand, removing L₃₇₀ or mutating it to V, A or G abolished AC activity. Also removal of the first three residues at the N-terminus of Rv2212c₂₁₂₋₃₇₀ up to V₂₁₅ did not affect kinetic properties of the CHD. Deleting L₃₇₀ at the C-terminus or V₂₁₅ at the N-terminus probably caused important conformational changes affecting the catalytic fold and hence reducing activity besides leading to a drop in the expression. It is noteworthy that L₃₇₀ is conserved in the Rv2212c ortholog in *M. smegmatis* (Linder *et al.*, 2002). Both Rv2212c₂₁₃₋₃₇₀ and Rv2212c₂₁₅₋₃₇₀ showed similar protein-dependence profiles as the wild type CHD. Rv2212c₂₁₃₋₃₇₀ was chosen for crystallization because of its higher yield. Rv2212c₂₁₄₋₃₇₀ was not considered because of its low specific activity. Gel filtration for both wild type Rv2212c₂₁₂₋₃₈₈ and Rv2212c₂₁₃₋₃₇₀ gave a single peak at 14.5 ml corresponding to approximately 40 kDa which is about the size of a homodimer.

Transferring the His-tag to the C-terminus caused a 90% drop in the specific activity of Rv2212c₂₁₂₋₃₈₈ accompanied by an extremely poor protein yield. Therefore it was impossible to use this construct for crystallization or any other experiments.

5.7 Rv2212c₁₋₃₈₈

An autoinhibitory effect of the N-terminal domain of Rv2212c₁₋₃₈₈ analogous to that of Rv1264 was not observed as Rv2212c₁₋₃₈₈ showed a specific activity of 0.72 $\mu\text{mol cAMP}\cdot\text{mg}^{-1}\cdot\text{min}^{-1}$ at 0.5 mM ATP using 10 mM Mn²⁺. This is about 4.5-fold less than that of its CHD using identical assay conditions. The Rv2212c N-terminal domain displayed an important role in the dimerization and hence stabilization of the catalytically active dimer. This is demonstrated by the protein-dependence of Rv2212c₁₋₃₈₈ where the equilibrium is shifted towards the active dimer already at 12 nM, whereas the CHD required a protein concentration of at least 80 nM to achieve maximal specific activity. The property of the holoenzyme to tolerate higher temperatures (over 43°C) and NaCl addition more than the CHD was further proof of the role played by the N-terminal domain in structurally stabilizing the holoenzyme. The activation energy for Rv2212c₁₋₃₈₈ was 46 kJ/mol and for Rv2212c₂₁₂₋₃₈₈ it was 65 kJ/mol (Zeibig, 2003). Also transferring the His-tag to the C-terminus was much more tolerated by Rv2212c₁₋₃₈₈ as it caused a drop of only 22% in specific activity compared to a 90% drop in case of Rv2212c₂₁₂₋₃₈₈.

5.8 The effect of chemicals on Rv2212c activity

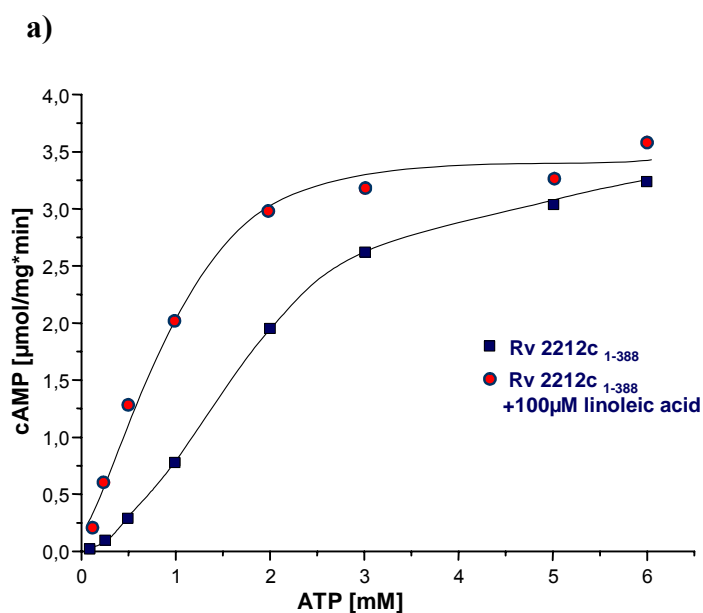
The function of the regulatory domain remained unclear. Random testing of different compounds, involved in *M. tuberculosis* metabolism, on enzymatic activity was used.

The distinct stimulatory effect of the unsaturated fatty acids (arachidonic, oleic, linoleic, and linolenic) on Rv2212c was surprising, particularly because such an effect was neither observed with Rv1264 nor with Rv1625c (fig. 4.31, a and b). Detection of an oleic acid molecule embedded in the N-terminal domain of Rv1264 by X-ray analysis (confidential information) made it appear even more interesting. Linoleic, oleic and arachidonic acids demonstrated a significant stimulatory effect on Rv2212c₁₋₃₈₈, whereas only 30-40 % of this effect was observed with Rv2212c₂₁₂₋₃₈₈. Polidocanol was the only detergent that exhibited a comparable stimulatory effect on the holoenzyme. Probably due to structural similarities to FAs, having a long alkyl chain devoid of any aromatic rings (see appendix section 8.4). It also affected the Rv2212c₂₁₂₋₃₈₈ (67% of the stimulatory effect). Furthermore, the FAs showed a significant cooperativity in binding to the holoenzyme not shown with the CHD as denoted from their corresponding Hill coefficients (tables 4.2 and 4.13), whereas Polidocanol showed a similar cooperativity in binding to both, the holoenzyme and CHD. The most striking was the change in the pH-dependence of the holoenzyme in presence of 100 μ M of any of these FAs (fig. 4.32). The specific activity increased 20-25 fold at pH 6.5 compared to that at pH 9. This was clearly different in case of the CHD as only a 4-fold increase in the specific activity was detected going from pH 9 to pH 6.5 in presence of 100 μ M linoleic acid (fig. 4.15). Also polidocanol did not demonstrate this effect as it maintained a pH-independent stimulation of the holoenzyme (fig. 4.35).

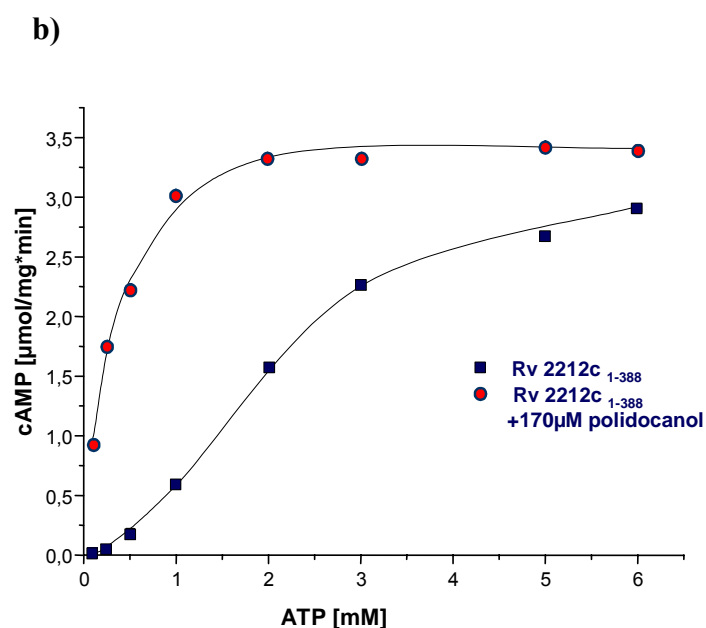
Taken together one may assume that the FAs possess a dual effect on Rv2212c. (i) A regulatory effect through the N-terminal domain, stimulating and conferring a pH-sensing function to the holoenzyme demonstrated by its pH-dependency in presence of 100 μ M FA, somehow akin to the pH-sensing function of Rv1264 although there was a 40-fold increase in activity going from pH 8 to pH 6 accompanied with a 12-fold increase in V_{\max} and about a 2-fold decrease in K_m (Tews *et al.*, 2005). The fact that V_{\max} of Rv2212c remained unaltered and the apparent K_m value decreased 25-fold from 23 ± 0.5 mM at pH 9 to 0.9 ± 0.02 mM at pH 6.5 in presence of 100 μ M linoleic acid, one could argue for a different mechanism in pH-sensing. At the same time this raises questions concerning the role played by the embedded oleic acid molecule in the N-terminal domain of Rv1264, as whether it has a physiological function in pH-sensing. (ii) A detergent-like side effect, as manifested by polidocanol

stimulation which is pH-independent. Activation by detergents was also recently reported for the mycobacterial class IIIc AC Rv1647 (Shenoy *et al.*, 2005).

The presence of 100 μM of these FAs did not affect V_{max} of the Rv2212c₁₋₃₈₈ but slightly increased its substrate affinity at pH 6.5. In other words the stimulation factor of the FAs significantly decreased by increasing substrate concentrations up to 5 mM ATP where hardly any stimulation by FA could be observed. This drop in the stimulation factor by increasing ATP concentrations was barely visible with the CHD (see fig.5.2, a and c for comparison).



ATP (mM)	Rv2212 ₁₋₃₈₈ $\mu\text{mol/mg*min}$	Rv2212 ₁₋₃₈₈ + 100 μM linoleic $\mu\text{mol/mg*min}$ (Stimulation factor)
0.1	0.016	0.207 (13X)
0.25	0.092	0.601 (6.5X)
0.5	0.295	1.297 (4X)
1	0.783	2.027 (2.5X)
2	1.948	2.979 (1.5X)
3	2.619	3.17 (1.2X)
5	3.031	3.264 (1X)
6	3.233	3.595 (1X)



ATP (mM)	Rv2212 ₁₋₃₈₈ $\mu\text{mol/mg*min}$	Rv2212 ₁₋₃₈₈ + 170 μM polidocanol $\mu\text{mol/mg*min}$ (Stimulation factor)
0.1	0.008	0.932 (116.5X)
0.25	0.053	1.759 (33X)
0.5	0.190	2.233 (11.7X)
1	0.597	2.994 (5X)
2	1.571	3.333 (2X)
3	2.274	3.340 (2X)
5	2.661	3.427 (1.2X)
6	2.910	3.404 (1.1X)

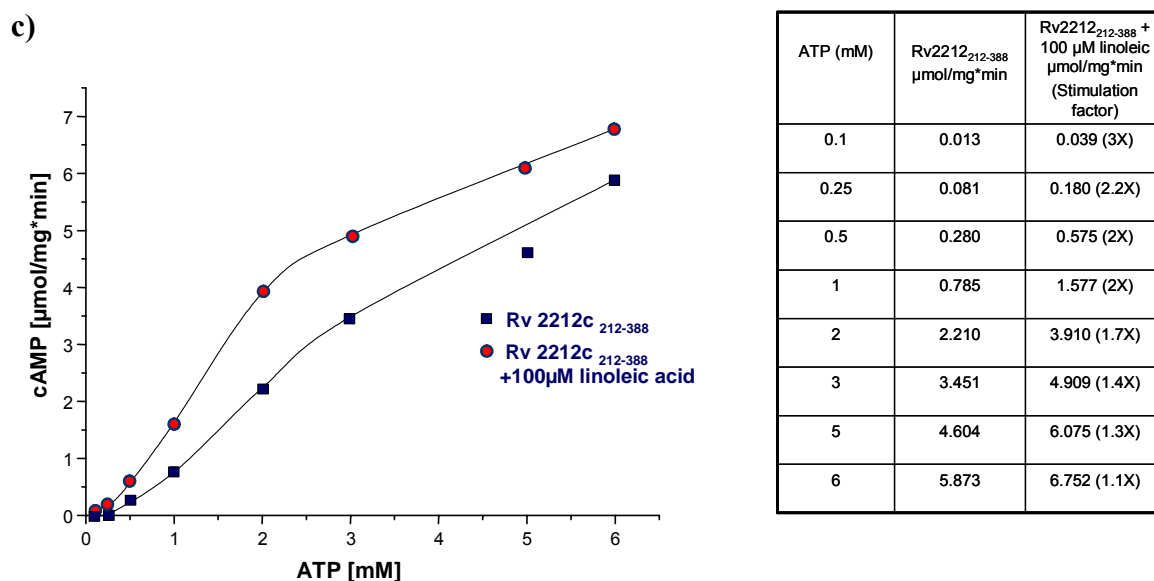


Fig. 5.2: Michaelis-Menten curves of Rv2212c₁₋₃₈₈ ± 100µM linoleic acid (a), 170 µM polidocanol (b) and of Rv2212c₂₁₂₋₃₈₈ ± 100 µM linoleic acid (c). Assay conditions were 10 mM Mn²⁺, BIS-TRIS/HCl, pH 6.5, 37°C, 10 min. Rv2212c₁₋₃₈₈ concentration was 100 nM and that of Rv2212c₂₁₂₋₃₈₈ was 200 nM. An ATP range of 0.1-6 mM was used.

This could lead us to the hypothesis that Rv2212c has two interconvertible states; an active state and an inhibited state in a way similar to Rv1264 (Tews *et al.*, 2005). But in case of Rv2212c, either the FAs or high concentrations of ATP could shift the equilibrium towards the active state, by certain conformational changes, thus increasing the affinity towards the substrate and consequently the activity without affecting V_{max} . It is the conformation to which the FA is bound, which is capable of sensing pH changes and hence be regulated accordingly. This also might be a good explanation for the instability in activity observed with Rv2212c₁₋₃₈₈ and Rv2212c₂₁₂₋₃₈₈ throughout this work. The enzymatic activity is higher when more of the enzyme molecules are bound to FAs thus shifting the equilibrium more towards the active state. Another reason could be the reversibility in binding of these FAs causing continuous conformational interconversions leading to the observed instability.

Yet the detergent-like effect of these FAs cannot be ignored as 170 µM of polidocanol did not change the V_{max} of Rv2212c₁₋₃₈₈, infact decreased the K_m value about 8-fold (fig. 5.2 b). This implies that still a lot is left to be known about the actual role of FAs in Rv2212c stimulation and regulation.

5.9 Outlook

The real biological function of Rv2435c in the tubercle bacillus is still an open question. Also exploring the mysterious task of its extracellular domain might lead to novel regulatory mechanisms in bacteria in general.

As for the Rv2212c, unsaturated FAs had quite a clear role in stimulating and regulating this enzyme. How these FAs affect AC activity in such a regulatory mechanism remains a question for future studies. Success in structural elucidation of the N-terminal domain through X-ray crystallography would be of great help in answering this question. Also site directed mutagenesis in the region corresponding to the determined oleic acid binding site in Rv1264 N-terminal domain, and testing these mutants in the presence of FAs could give clues to the way these FAs bind to and regulate Rv2212c.

6 Summary

The *Mycobacterium tuberculosis* genome has 15 open reading frames for class III adenylyl cyclases. Here I report on two structurally different ACs belonging to two different subclasses; the mammalian-like Rv2435c classified as class IIIa, and Rv2212c belonging to class IIIc. Rv2435c is unique in possessing an extracellular domain, two transmembrane helices as a membrane anchor and a C-terminal catalytic domain. Having four deviations from the canonical hexad in the catalytic centre raised theoretical questions concerning AC activity. Three different holoenzyme constructs were expressed and were mostly degraded. Both the catalytic domain and these unstable holoenzymes did not display enzymatic activity. Rv2212c is composed of two distinct protein modules; a C-terminal CHD and an N-terminal regulatory domain, the occurrence of which is restricted to several adenylyl cyclases present in Gram-positive bacteria including the mycobacterial Rv1264. All six amino acids annotated to be participating in catalysis are conserved. The expressed CHD was shown to function as a homodimer. Its specific activity ($3.1 \mu\text{mol cAMP}\cdot\text{mg}^{-1}\cdot\text{min}^{-1}$) and V_{max} were high compared to other mycobacterial ACs, whereas substrate affinity was quite low. GC activity was absent. The holoenzyme had a specific activity 4.5-fold lower than the CHD, arguing against the idea of an autoinhibitory N-terminal domain. Also the function of a pH-sensing N-terminal domain was excluded as both CHD and holoenzyme demonstrated a pH-optimum at pH 6.5. Nevertheless the N-terminal domain had a role in dimerization and enzyme stabilization. Unsaturated FAs (arachidonic, oleic and linoleic) caused a significant stimulation of the enzyme by increasing its substrate affinity but without altering V_{max} and conferring an increased pH-sensitivity to the protein. The effect of the FAs did not only involve the N-terminal domain because the CHD was similarly affected but to a much lesser extent. In particular, a pH-regulation in presence of FAs was not shown for the CHD, which makes the regulatory role played by the N-terminal domain in presence of FAs more relevant. Deciphering the molecular structure of this protein is required to be able to figure out how the FAs exert these effects and how exactly they interact with the enzyme.

7 Zusammenfassung

Das Genom von *M. tuberculosis* enthält 15 Klasse III Adenylatcyclasen. Im Rahmen der vorliegenden Arbeit wurden zwei Adenylatcyclasen mit unterschiedlichen strukturellen Eigenschaften untersucht: die Mammalia-ähnliche Rv2435c aus Klasse IIIa und Rv2212c aus Klasse IIIc. Rv2435c ist die einzige mycobakterielle AC, die aus einer extrazellulären Domäne, zwei transmembranären Helices als Membrananker und einer C-terminalen katalytischen Domäne (CHD) besteht. Sie besitzt vier Abweichungen von den sechs kanonischen Aminosäuren im katalytischen Zentrum, was theoretische Fragen über die AC Aktivität aufgeworfen hat. Drei verschiedene Holoenzym-Konstrukte wurden exprimiert. Allerdings wurden größtenteils Abbruchprodukte gebildet. Sowohl die katalytische Domäne, als auch diese instabilen Holoenzyme zeigten keine enzymatische Aktivität. Rv2212c besteht aus zwei unterschiedlichen Domänen, einer C-terminalen CHD und einer N-terminalen regulatorischen Domäne, die auch in anderen Adenylatcyclasen aus Gram-positiven Bakterien (Rv1264 inbegriffen) gefunden wurde. Alle sechs kanonischen Aminosäuren sind konserviert. Die exprimierte CHD funktioniert als Homodimer. Ihre spezifische Aktivität ($3.1 \mu\text{mol cAMP} \cdot \text{mg}^{-1} \cdot \text{min}^{-1}$) und V_{max} waren hoch im Vergleich zu anderen mycobakteriellen Adenylatcyclasen, die Substrataffinität war allerdings gering. GC Aktivität wurde nicht gefunden. Die spezifische Aktivität des Holoenzym war 4,5-fach niedriger als die der CHD, was gegen eine mögliche autoinhibitorische Funktion der N-terminalen Domäne spricht. Auch eine Funktion als pH-Sensor kann ausgeschlossen werden, da CHD und Holoenzym ihr pH-Optimum bei pH 6,5 haben. Dennoch spielt die N-terminale Domäne eine Rolle bei der Dimerisierung und der Enzymstabilität. Ungesättigte Fettsäuren (Arachidonsäure, Ölsäure und Linolsäure) stimulierten das Enzym signifikant durch eine Erhöhung der Substrataffinität aber ohne eine Änderung von V_{max} und verliehen dem Protein eine hohe pH- Empfindlichkeit. Diese Effekte betreffen allerdings nicht nur die N-terminale Domäne, denn auch die CHD wurde durch die Fettsäuren stimuliert in geringerem Ausmaß. Die Tatsache, dass eine pH-Regulation durch die CHD in Anwesenheit der Fettsäuren nicht beobachtet werden konnten, spricht für die Bedeutung der N-terminalen Domäne bei der Regulation in Gegenwart von Fettsäuren. Durch die Aufklärung der molekularen Struktur des Proteins könnten der Einfluss der Fettsäuren und die Interaktionen mit dem Protein genauer untersucht werden.

8 Appendix

8.1 DNA and protein sequences of Rv2435c

Gene name MT2509, UniProtKB/TrEMBL accession number P71914.

bp = base pairs, **aa** = amino acids.

	bp	aa
TTGACGTCGGGTGAGGCACTGGACTCGGTAGCCGAGAGTGAATCCACCCCGGCTAAGAAG	60	
L T S G E A L D S V A E S E S T P A K K		20
CGCCATAAGAATGTGCTCCGGCGTCGGCCGCGTTTCCGGGCCAGCATCCAGTCCAAGCTC	120	
R H K N V L R R R P R F R A S I Q S K L		40
ATGGTGCTGCTGCTGTTGACGAGTATCGTGTCCGTCGCGGCGATTGCGGCCATTGTCTAT	180	
M V L L L L T S I V S V A A I A A I V Y		60
CAATCTGGTCGCACTTCGCTAAGAGCAGCCGCTACGAGCGGTTGACCCAGTTGCGCGAG	240	
Q S G R T S L R A A A Y E R L T Q L R E		80
TCGCAGAAGCGGGCAGTTGAGACACTATTTTCTGACCTGACGAATTCGCTGGTCATTTAC	300	
S Q K R A V E T L F S D L T N S L V I Y		100
GAACGTGGACTCACGGTTGTCGATGCCGTCGTGCGGTTACGGCCGGCTTTGACCAGCTG	360	
E R G L T V V D A V V R F T A G F D Q L		120
GCTGACGCCACGATCAGCCCCGCCAACACAGGCGATCGTCAACTACTACAACAACGAA	420	
A D A T I S P A Q Q Q A I V N Y Y N N E		140
TTCATCACACCCGTCGAACGCACGACCGGCGATAAACTCGACATCACCGCGCTGCTGCCG	480	
F I T P V E R T T G D K L D I T A L L P		160
ACTTCTCCGGCCAAAGGTATCTTCAGGCGTACTACACGACCATTCACGTCGGACCAA	540	
T S P A Q R Y L Q A Y Y T A P F T S D Q		180
GATGCGATGCGGC TGGAC GATGC CGGCGACGGCAGTGC ATGGTC GGCCGCCAACGCGCAA	600	
D A M R L D D A G D G S A W S A A N A Q		200
TTC AACAGCTATT TCCGGGAAATCGTCACCCGGTTCGATTACGACGACGCGGTATTGCTG	660	
F N S Y F R E I V T R F D Y D D A V L L		220
GACACCCGGGGCAATATCGTCTATACCC TGAGCAAGGACCCCGACCTCGGTACCAACATT	720	
D T R G N I V Y T L S K D P D L G T N I		240
CTGACCGGGCCGATATCGCAATCCAATC TGC GTGACGCCTACCTTAAAGCGTTGGGCGCC	780	
L T G P Y R E S N L R D A Y L K A L G A		260
AACGCCGTGCACTTACCTGGATTACCGACTTCAAGCCGTATCAGCCTCAACTCGGCGTG	840	
N A V D F T W I T D F K P Y Q P Q L G V		280

CCGACCGCGTGGTTGGTGGCACCGGTCTGAAGCGGGCGGCAAAAC TCAGGGCGTTTGGCG 900
P T A W L V A P V E A G G K T Q G V L A 300
CTGCCGTTGCCGATCGACAAGATCAATAAGATCATGACCGCCGACAGGC AATGGCAAGCG 960
L P L P I D K I N K I M T A D R Q W Q A 320
GCTGGCATGGGTAGTGGGACGGAAACCTATCTCGCCGGTCCGGACAGTCTGATGCGGTCC 1020
A G M G S G T E T Y L A G P D S L M R S 340
GATTCTCGGCTCTTCTGCAAGACCCGGAGGAA TACCGAAACAGGTTGTGGCAGCAGGC 1080
D S R L F L Q D P E E Y R K Q V V A A G 360
ACGTCACTTGATGTGGTCAACAGAGCGATCCAGTTCGGTGGGACGACGC TGCTGCAGCCT 1140
T S L D V V N R A I Q F G G T T L L Q P 380
GTTGCGACCGAAGGACTGCGCGCCGCCAACGCGGACAGACCGGAACCGTCACCTCCACC 1200
V A T E G L R A A Q R G Q T G T V T S T 400
GACTACACGGGTAGCAGGGAAC TGGAGGCCTACGCGCCGCTGAATGTGCGGAC TCCGAT 1260
D Y T G S R E L E A Y A P L N V P D S D 420
CTGCACTGGTCGATCCTGGCAACGCGGAACGAT TCTGAGGCGTTGCGGGCCGTCGCGTCG 1320
L H W S I L A T R N D S E A F A A V A S 440
TTCAGCAGGGCGCTTGTGCTGGT TACAGTTGGCATCATTGTCGT CATCTGTGTGGCGTCG 1380
F S R A L V L V T V G I I V V I C V A S 460
ATGCTGATCGCCCATGCGATGGT GCGGCCAATCGGCGGCTCGAGGTTGGCACCCAGAAG 1440
M L I A H A M V R P I R R L E V G T Q K 480
ATCAGCGCAGGCGACTACGAAGTCAACATTCGGTAAAGT CACGCGACGAAATCGGTGAT 1500
I S A G D Y E V N I P V K S R D E I G D 500
CTTACAGCCGCTTTCAACGAGATGAGTCGGAATCTGCAAACCAAAGAGGAGCTGCTCAAC 1560
L T A A F N E M S R N L Q T K E E L L N 520
GAGCAACGCAAGGAAAACGACCGGTTAT TGCTATCGATGATGCCCGAGCCAGTTGTCGAG 1620
E Q R K E N D R L L L S M M P E P V V E 540
CGGTACCGCCTTGGGGAGCAGACCATTGCGCAGGAGCACCAAGATGTCACCGTCCTGTTT 1680
R Y R L G E Q T I A Q E H Q D V T V L F 560

GCCGACATCCTGGGTGTCGACGAGATTTCCAGCGGCTGTGGGTAACGAACTGGTCAA 1740
 A D I L G V D E I S S G L S G N E L V K 580
 ATTGTCGACGAGCTGGTCCGCCAGTTCGATTCGGCCGCCGAACACCTTGGTGTGGAACGC 1800
 I V D E L V R Q F D S A A E H L G V E R 600
 ATTCGCACGCTGCACAATGGCTATCTCGCCGTTGCGGGGTAACCACGCCACGGCTGGAC 1860
 I R T L H N G Y L A G C G V T T P R L D 620
 AATATTCCCGAACCGTGCACCTCGCCCTAGAGATGCGGCGCATCGTCGATCGGTTCAAT 1920
 N I P R T V D F A L E M R R I V D R F N 640
 TGCCAAACCGGTAACGATCTGCACCTGCGAGTCGGTATCAACACCGGGGACGTCATTAGC 1980
 C Q T G N D L H L R V G I N T G D V I S 660
 GGGCTGGTCGGCAGATCAAGTGTGCTACGACATGTGGGGCGCGCAGTGAGTCTGGCC 2040
 G L V G R S S V V Y D M W G A A V S L A 680
 TACCAAATGCACAGCGTTTACCACAGCCCGGCATCTATGTCACCTCGCAGGTGTATGAG 2100
 Y Q M H S G S P Q P G I Y V T S Q V Y E 700
 GCGATGCGAGACGTGTGGCAGTTCACGGCTGCGGGCACGATTTCTGTCGGAGGGTTAGAA 2160
 A M R D V W Q F T A A G T I S V G G L E 720
 GAGCCGATCTACCGATTGTCGGAGCGATCATGAACCTGCTCGAC TCGACATGGT TCTACT 2220
 E P I Y R L S E R S . T C S T R H G S T 740
 GGGCCGTTGGCATTGCATCGGATTGCCGGCCGGGCTAATCGTTCTCACCGAAC TGCACA 2280

8.2 DNA and protein sequences of Rv2212c

Gene name MT2268, UniProtKB/Swiss-Prot accession number P64265.

bp = base pairs, **aa** = amino acids.

	bp	aa
ATGGGCGTCCCTGCTGGCACACTTAGGCAGGTGTACGATTCCTTGGACTTCGACGCCCTC	60	
M G V P A G T L R Q V Y D S L D F D A L		20
GAGGCCGCGGAATTGCCAACCCACGCGAGCGGGCCGGCTTGTCTACCTACCTGGATGAG	120	
E A A G I A N P R E R A G L L T Y L D E		40
CTTGGCTTACGGTTCGAAGAGATGGTGC AAGCCGAACGCCGCGGGCCGGTTGTTCGGGCTG	180	
L G F T V E E M V Q A E R R G R L F G L		60
GCCGGTGACGTCTGCTATGGTCCGGGCCCCCGATCTACACCTGGCGACCGGGCTGAC	240	
A G D V L L W S G P P I Y T L A T A A D		80
GAACTGGGGTTGTCTAGCCGACGACGTTCGCACGCGCGTGGAGTTTGTCTCGGCCTCACCGTC	300	
E L G L S A D D V A R A W S L L G L T V		100
GCGGGTCCGACGTTCCCACGCTGAGCCAGGCCGACGTTCGCACGCCCTGGCGACCTGGGTC	360	
A G P D V P T L S Q A D V D A L A T W V		120
GCACTGAAGGCGCTGGTGGGTGAGGACGGCGCATTCGGCCTGCTGCGAGTGCTCGGCACT	420	
A L K A L V G E D G A F G L L R V L G T		140
GCCATGGCCCGACTCGCCGAGGCCGAGTCGACCATGATCCGCGCCGGGTACCGAACATC	480	
A M A R L A E A E S T M I R A G S P N I		160
CAAATGACGCACCCACGACGAACCTGCCACGGCACGGGCTATCGCGCGGCTGCGGAG	540	
Q M T H T H D E L A T A R A Y R A A A E		180
TTCGTCCCCGGATCGGTGCGCTGATCGACACCGTCCACCGTCACCACC TGGCCAGCGCA	600	
F V P R I G A L I D T V H R H H L A S A		200
CGAACCTACTTTGAAGGCGTCATTGGCGACACGTTCGGCAAGCGTGACGTGCGGTATCGGC	660	
R T Y F E G V I G D T S A S V T C G I G		220
TTTGCGGATCTGTCCAGCTTACCGCGTTGACCCAGGCGCTCACCCCCGCGCAGTTGCAG	720	
F A D L S S F T A L T Q A L T P A Q L Q		240
GACCTGCTCACCGAATTCGACGCCGCCGTCACCGACGTGGTGCATGCCGACGGTGGCCGG	780	
D L L T E F D A A V T D V V H A D G G R		260
TTGGTGAAGTTTCATCGGCCGACCCGTGATGTGGGTGAGCTCGTCCGCCAACGACTGGTG	840	
L V K F I G D A V M W V S S S P E R L V		280

CGGGCGGCGGTGGATCTCGTCGATCATCCGGGTGCGCGCGCGGCCGAACGCAGGTCCGT 900
R A A V D L V D H P G A R A A E L Q V R 300
GCCGGTCTGCCTATGGCACGGTGCTGGCCCTAACGGTGACTACTTCGGCAACCCGGTC 960
A G L A Y G T V L A L N G D Y F G N P V 320
AACCTGGCTGCGCGCCTGGTGGCGGCCGAGCGCCAGGGCAGATCCTGGCCGAGCGCAA 1020
N L A A R L V A A A A P G Q I L A A A Q 340
CTCCGCGACATGTTGCCAGACTGGCCTGCCCTCGCCATGGCCATTGACGCTCAAGGGG 1080
L R D M L P D W P A L A H G P L T L K G 360
TTTGACGCCCCGGTGATGGCCTTCGAACTGCACGACAACCCTCGTGCGAGGGATGCTGAC 1140
F D A P V M A F E L H D N P R A R D A D 380
ACGCCAAGCCCCGCCGCCAGTGATTAGGGTGGTTGCCCGTGACCACCGAACCGGGTTACC 1200
T P S P A A S D . G G C P . P P N R V T 400

8.3 Sequence alignment of Rv2435c with *Desulfovibrio vulgaris*

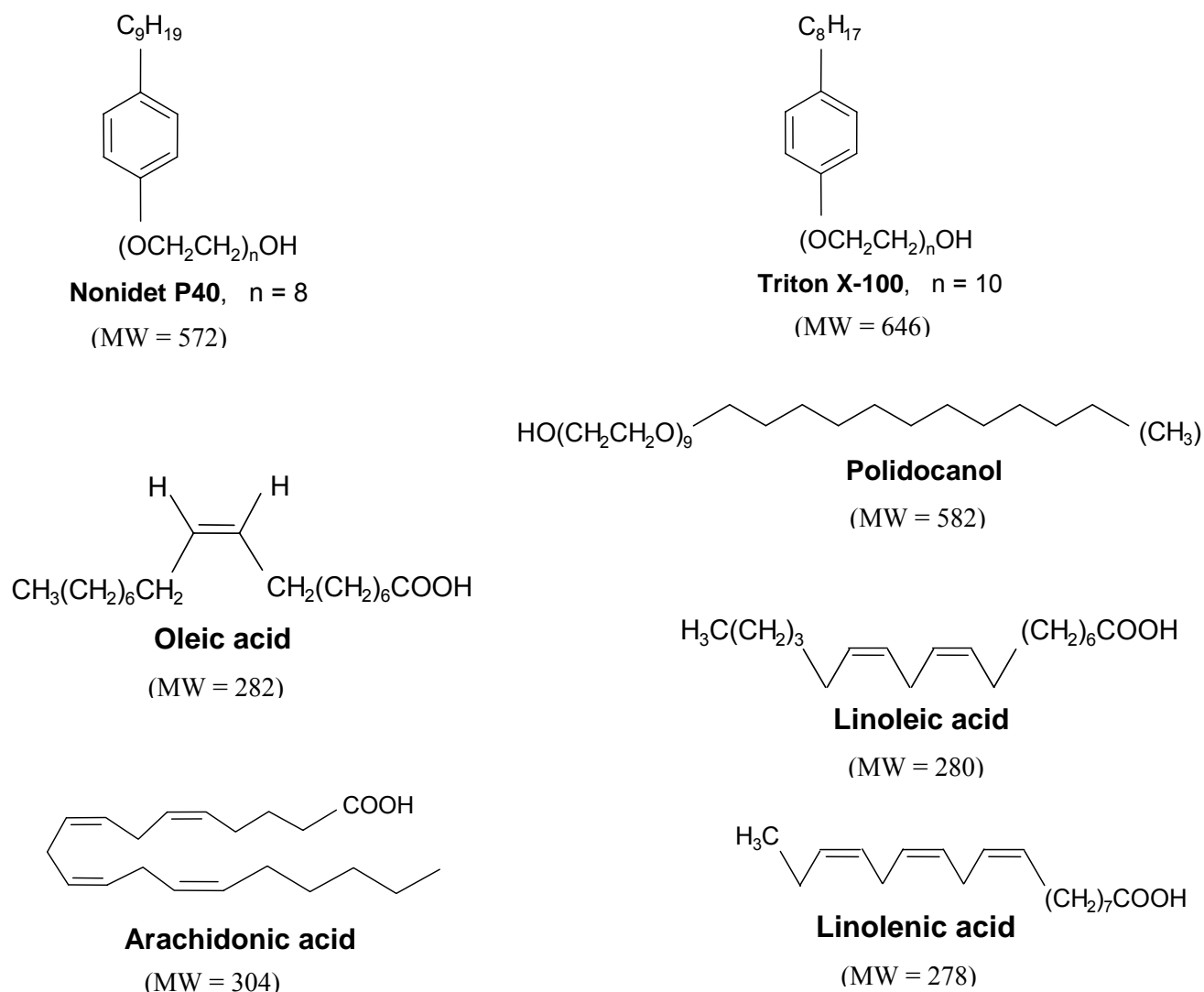
Rv2435c	1 :	LTSGEALDSVAESESTPAKKRHKNVLRRRPRFRASIQSKLMVLLLLTSTIV
DcrH	1 :	MT-----LKR-----KLMVGFLLALFW
Rv2435c	51 :	SVAAATAAT-----VYQSGRTSLRAAAYERLTQLRESQKRAVETL
DcrH	18 :	TCTLIAGVNWYFAHDGMNGIGDTAVEAMKDRARGQLSIRSASAKALHIEDL
Rv2435c	90 :	FSDLTNSLVIYERGLTVVDAVVRFTAGFDQLADATLSPAQQQAIIV----
DcrH	68 :	FQIRIRNQRTRTLAESLTVREAATLSAAMFTVQGETGALDAKALRGKLTE
Rv2435c	135 :	NYYNNEFTTPVERTIGDKLD-----ITALLPTSPAQRYLQAYYTAPFT
DcrH	118 :	DYAGANYLANPTFAHARTAKGYAPRPAETYLPKDANGIILQAMYVHP--S
Rv2435c	178 :	SDQDAM---RLDDAGDGSAMSAANAQNSYFREIVTRFDYDDAVLLDIT-
DcrH	167 :	GNNPPLGEKHRLDANPLASTYNTLHRKHPILRNYLTFGGYDIFIIDAA
Rv2435c	223 :	RGNIIVYTLISKDPDLCTNILTGPYRESNLRDAYLKALGANAV---DFTWIT
DcrH	217 :	SGVIVYTVKEKDYATSLLTGPYRDTGLGAVFREAVENGRKGRRDVAVLS
Rv2435c	270 :	DFKPYQPQLGVPTAWLVAPV-EAGGKTQGVLAALPLPIDKINKIMTADROW
DcrH	267 :	DFAPYEPSYNAPAAFTAAPVFDDRGTCAVLAFAQMPVDNIDRIMTSNGRW
Rv2435c	319 :	QAAGMGSGETETYLAGEPDSLMSRDSRFLQDPEEYRKQVVAAGTSLDVVNR
DcrH	317 :	QEVGLGTGETETYLVGPD--MHERSKL-----RAASGASDEVV--
Rv2435c	369 :	AIQFGGTLLQPVALEGRLAAQRGQTGTVISTDYTGSRLEAYAPLNVPD
DcrH	352 :	-----VDSEAARKALGGESGTATIRDYRCKNVLAAWQPLRL--
Rv2435c	419 :	SDLHWSLLATRNDSEAFAAVASFRA-----LVLVIVGIIIVVI
DcrH	388 :	EGLHYGLIAEIDIDEALLAASKITAAARQGAERTLWGTLLVLAALGTTLLGS
Rv2435c	457 :	CVASMLIAHAMVRPIRRLEVGTQKISAGDYEVNIPVKSRLDEIGDITAAFN
DcrH	438 :	GIATIALVG-ALSRPLQRLQVYAGDVAAGNLDARPEGQYPAELDAMRHSIE

Alignment of the N-terminal region of Rv2435c (including the extracellular domain, and the two transmembrane helices marked by top bars) with the ligand binding N-terminal domain of the chemotaxis receptor H (DcrH) in *Desulfovibrio vulgaris* UniProtKB/TrEMBL accession number Q726F3. Both domains show a 27% identity and a 47% similarity.

8.4 Fatty acids and detergents tested with Rv2212c

Compound	Chemical name
Linoleic acid	9,12-Octadecadienoic acid
Oleic acid	9-Octadecenoic acid
Arachidonic acid	5,8,11,14-Eicosatetraenoic acid
Linolenic acid	9,12,15-Octadecatrienoic acid
Palmitic acid	Hexadecanoic acid
Polidocanol	Dodecyl nonaethylene glycol
Triton X-100	Octylphenol-polyethyleneglycol ether
Nonidet P 40	Nonylphenyl-polyethyleneglycol
CHAPS	3-(3-Cholamidopropyl)-dimethylammonio-1-propane sulfonate

Chemical names of different fatty acids and detergents tested with mycobacterial Rv2212c.



Chemical structures of some fatty acids and detergents tested with mycobacterial Rv2212c.

9 References

- Altschul, S.F., Madden, T.L., Schaffer, A.A., Zhang, J., Zhang, Z., Miller, W. and Lipman, D.J. (1997) Gapped BLAST and PSI-BLAST: a new generation of protein database search programs. *Nucleic Acids Res*, **25**, 3389-3402.
- Barzu, O. and Danchin, A. (1994) Adenylyl cyclases: a heterogeneous class of ATP-utilizing enzymes. *Prog Nucleic Acid Res Mol Biol*, **49**, 241-283.
- Botsford, J.L. and Harman, J.G. (1992) Cyclic AMP in prokaryotes. *Microbiol Rev*, **56**, 100-122.
- Bradford, M.M. (1976) A rapid and sensitive method for the quantitation of microgram quantities of protein utilizing the principle of protein-dye binding. *Anal Biochem*, **72**, 248-254.
- Castro, L.I. (2004) Mycobacterial adenylyl cyclases Rv1625c and Rv0386: orthodox vs. unorthodox catalysis. Dissertation der Universität Tübingen.
- Castro, L.I., Hermsen, C., Schultz, J.E. and Linder, J.U. (2005) Adenylyl cyclase Rv0386 from *Mycobacterium tuberculosis* H37Rv uses a novel mode for substrate selection. *FEBS J*, **272**, 3085-3092.
- Cohen, S.N., Chang, A.C. and Hsu, L. (1972) Nonchromosomal antibiotic resistance in bacteria: genetic transformation of *Escherichia coli* by R-factor DNA. *Proc Natl Acad Sci USA*, **69**, 2110-2114.
- Cole, S.T., Brosch, R., Parkhill, J., Garnier, T., Churcher, C., Harris, D., Gordon, S.V., Eiglmeier, K., Gas, S., Barry, C.E., 3rd, Tekaiia, F., Badcock, K., Basham, D., Brown, D., Chillingworth, T., Connor, R., Davies, R., Devlin, K., Feltwell, T., Gentles, S., Hamlin, N., Holroyd, S., Hornsby, T., Jagels, K., Krogh, A., McLean, J., Moule, S., Murphy, L., Oliver, K., Osborne, J., Quail, M.A., Rajandream, M.A., Rogers, J., Rutter, S., Seeger, K., Skelton, J., Squares, R., Squares, S., Sulston, J.E., Taylor, K., Whitehead, S. and Barrell, B.G. (1998) Deciphering the biology of *Mycobacterium tuberculosis* from the complete genome sequence. *Nature*, **393**, 537-544.
- Cotta, M.A., Whitehead, T.R. and Wheeler, M.B. (1998) Identification of a novel adenylate cyclase in the ruminal anaerobe, *Prevotella ruminicola* D31d. *FEMS Microbiol Lett*, **164**, 257-260.
- Deckers, H.M. and Voordouw, G. (1996) The *dcr* gene family of *Desulfovibrio*: implications from the sequence of *dcrH* and phylogenetic comparison with other *mcp* genes. *Antonie Van Leeuwenhoek*, **70**, 21-29.
- Ducruix, A. and Giegé, R. (1999) Crystallization of nucleic acids and proteins. *Oxford University Press*.
- D'Souza, C.A. and Heitman, J. (2001) Conserved cAMP signaling cascades regulate fungal development and virulence. *FEMS Microbiol Rev*, **25**, 349-364.

References

- Gazdik, M.A. and McDonough, K.A. (2005) Identification of cyclic AMP-regulated genes in *Mycobacterium tuberculosis* complex bacteria under low-oxygen conditions. *J Bacteriol*, **187**, 2681-2692.
- Gross, A., Bouaboula, M., Casellas, P., Liautard, J.P. and Dornand, J. (2003) Subversion and utilization of the host cell cyclic adenosine 5'-monophosphate/protein kinase A pathway by *Brucella* during macrophage infection. *J Immunol*, **170**, 5607-5614.
- Gueirard, P., Druilhe, A., Pretolani, M. and Guiso, N. (1998) Role of adenylate cyclase-hemolysin in alveolar macrophage apoptosis during *Bordetella pertussis* infection in vivo. *Infect Immun*, **66**, 1718-1725.
- Guo, Y.L., Kurz, U., Schultz, A., Linder, J.U., Dittrich, D., Keller, C., Ehlers, S., Sander, P. and Schultz, J.E. (2005) Interaction of Rv1625c, a mycobacterial class IIIa adenylyl cyclase, with a mammalian congener. *Mol Microbiol*, **57**, 667-677.
- Guo, Y.L., Seebacher, T., Kurz, U., Linder, J.U. and Schultz, J.E. (2001) Adenylyl cyclase Rv1625c of *Mycobacterium tuberculosis*: a progenitor of mammalian adenylyl cyclases. *EMBO J*, **20**, 3667-3675.
- Hammer, A. (2004) Klonierung und Charakterisierung von fünf Adenylatcyclasen aus *Stigmatella aurantiaca* und *Mycobacterium tuberculosis*. Dissertation der Universität Tübingen.
- Kanacher, T., Schultz, A., Linder, J.U. and Schultz, J.E. (2002) A GAF-domain-regulated adenylyl cyclase from *Anabaena* is a self-activating cAMP switch. *EMBO J*, **21**, 3672-3680
- Kasahara, M., Unno, T., Yashiro, K. and Ohmori, M. (2001) CyaG, a novel cyanobacterial adenylyl cyclase and a possible ancestor of mammalian guanylyl cyclases. *J Biol Chem*, **276**, 10564-10569.
- Kaur, H. and Khuller, G.K. (1995) Role of cyclic adenosine monophosphate in phospholipid synthesis in *Mycobacterium smegmatis* ATCC 607. *Lipids*, **30**, 345-349.
- Khelef, N., Zychlinsky, A. and Guiso, N. (1993) *Bordetella pertussis* induces apoptosis in macrophages: role of adenylate cyclase-hemolysin. *Infect Immun*, **61**, 4064-4071.
- Krupinski, J., Coussen, F., Bakalyar, H.A., Tang, W.J., Feinstein, P.G., Orth, K., Slaughter, C., Reed, R.R. and Gilman, A.G. (1989) Adenylyl cyclase amino acid sequence: possible channel- or transporter-like structure. *Science*, **244**, 1558-1564.
- Laemmli, U.K. (1970) Cleavage of structural proteins during the assembly of the head of bacteriophage T4. *Nature*, **227**, 680-685.
- Linder, J.U., Hammer, A. and Schultz, J.E. (2004) The effect of HAMP domains on class IIIb adenylyl cyclases from *Mycobacterium tuberculosis*. *Eur J Biochem*, **271**, 2446-2451.

- Linder, J.U., Schultz, A. and Schultz, J.E. (2002) Adenylyl cyclase Rv1264 from *Mycobacterium tuberculosis* has an autoinhibitory N-terminal domain. *J Biol Chem*, **277**, 15271-15276.
- Linder, J.U. and Schultz, J.E. (2003) The class III adenylyl cyclases: multi-purpose signalling modules. *Cell Signal*, **15**, 1081-1089.
- Lowrie, D.B., Aber, V.R. and Jackett, P.S. (1979) Phagosome-lysosome fusion and cyclic adenosine 3':5'-monophosphate in macrophages infected with *Mycobacterium microti*, *Mycobacterium bovis* BCG or *Mycobacterium lepraemurium*. *J Gen Microbiol*, **110**, 431-441.
- McCue, L.A., McDonough, K.A. and Lawrence, C.E. (2000) Functional classification of cNMP-binding proteins and nucleotide cyclases with implications for novel regulatory pathways in *Mycobacterium tuberculosis*. *Genome Res*, **10**, 204-219.
- McKinney, J.D., Honer zu Bentrup, K., Munoz-Elias, E.J., Miczak, A., Chen, B., Chan, W.T., Swenson, D., Sacchettini, J.C., Jacobs, W.R., Jr. and Russell, D.G. (2000) Persistence of *Mycobacterium tuberculosis* in macrophages and mice requires the glyoxylate shunt enzyme isocitrate lyase. *Nature*, **406**, 735-738.
- Padh, H. and Venkitasubramanian, T.A. (1976) Adenosine 3',5'-monophosphate in *Mycobacterium phlei* and *Mycobacterium tuberculosis* H37Ra. *Microbios*, **16**, 183-189.
- Padh, H. and Venkitasubramanian, T.A. (1977) Adenosine 3', 5'-monophosphate in mycobacteria. *Life Sci*, **20**, 1273-1280.
- Peterkofsky, A., Reizer, A., Reizer, J., Gollop, N., Zhu, P.P. and Amin, N. (1993) Bacterial adenylyl cyclases. *Prog Nucleic Acid Res Mol Biol*, **44**, 31-65.
- Petersen, S. and Young, G.M. (2002) Essential role for cyclic AMP and its receptor protein in *Yersinia enterocolitica* virulence. *Infect Immun*, **70**, 3665-3672.
- Pethe, K., Swenson, D.L., Alonso, S., Anderson, J., Wang, C. and Russell, D.G. (2004) Isolation of *Mycobacterium tuberculosis* mutants defective in the arrest of phagosome maturation. *Proc Natl Acad Sci USA*, **101**, 13642-13647.
- Raviglione, M.C. (2003) The TB epidemic from 1992 to 2002. *Tuberculosis (Edinb)*, **83**, 4-14.
- Reddy, S.K., Kamireddi, M., Dhanireddy, K., Young, L., Davis, A. and Reddy, P.T. (2001) Eukaryotic-like adenylyl cyclases in *Mycobacterium tuberculosis* H37Rv: cloning and characterization. *J Biol Chem*, **276**, 35141-35149.
- Salomon, Y., Londos, C. and Rodbell, M. (1974) A highly sensitive adenylate cyclase assay. *Anal Biochem*, **58**, 541-548.
- Shenoy, A.R., Sivakumar, K., Krupa, A., Srinivasan, N. and Visweswariah, S.S. (2004a) A survey of nucleotide cyclases in Actinobacteria: unique domain organization and

References

- expansion of the class III cyclase family in *Mycobacterium tuberculosis*. *Comp Funct Genom*, **5**, 17-38.
- Shenoy, A.R., Sreenath, N.P., Mahalingam, M. and Visweswariah, S.S. (2005) Characterization of phylogenetically distant members of the adenylate cyclase family from mycobacteria: Rv1647 from *Mycobacterium tuberculosis* and its orthologue ML1399 from *M. leprae*. *Biochem J*, **387**, 541-551.
- Shenoy, A.R., Srinivasan, N., Subramaniam, M. and Visweswariah, S.S. (2003) Mutational analysis of the *Mycobacterium tuberculosis* Rv1625c adenylyl cyclase: residues that confer nucleotide specificity contribute to dimerization. *FEBS Lett*, **545**, 253-259.
- Sinha, S.C., Wetterer, M., Sprang, S.R., Schultz, J.E. and Linder, J.U. (2005) Origin of asymmetry in adenylyl cyclases: structures of *Mycobacterium tuberculosis* Rv1900c. *EMBO J*, **24**, 663-673.
- Sismeiro, O., Trotot, P., Biville, F., Vivares, C. and Danchin, A. (1998) *Aeromonas hydrophila* adenylyl cyclase 2: a new class of adenylyl cyclases with thermophilic properties and sequence similarities to proteins from hyperthermophilic archaeobacteria. *J Bacteriol*, **180**, 3339-3344.
- Smith, R.S., Wolfgang, M.C. and Lory, S. (2004) An adenylate cyclase-controlled signaling network regulates *Pseudomonas aeruginosa* virulence in a mouse model of acute pneumonia. *Infect Immun*, **72**, 1677-1684.
- Sturgill-Koszycki, S., Schlesinger, P.H., Chakraborty, P., Haddix, P.L., Collins, H.L., Fok, A.K., Allen, R.D., Gluck, S.L., Heuser, J. and Russell, D.G. (1994) Lack of acidification in *Mycobacterium* phagosomes produced by exclusion of the vesicular proton-ATPase. *Science*, **263**, 678-681.
- Sunahara, R.K., Beuve, A., Tesmer, J.J., Sprang, S.R., Garbers, D.L. and Gilman, A.G. (1998) Exchange of substrate and inhibitor specificities between adenylyl and guanylyl cyclases. *J Biol Chem*, **273**, 16332-16338.
- Sunahara, R.K., Dessauer, C.W. and Gilman, A.G. (1996) Complexity and diversity of mammalian adenylyl cyclases. *Annu Rev Pharmacol Toxicol*, **36**, 461-480.
- Tang, W.J. and Gilman, A.G. (1995) Construction of a soluble adenylyl cyclase activated by G_{sa} and forskolin. *Science*, **268**, 1769-1772.
- Tang, W.J. and Hurley, J.H. (1998) Catalytic mechanism and regulation of mammalian adenylyl cyclases. *Mol Pharmacol*, **54**, 231-240.
- Taussig, R. and Zimmermann, G. (1998) Type-specific regulation of mammalian adenylyl cyclases by G protein pathways. *Adv Second Messenger Phosphoprotein Res*, **32**, 81-98.
- Tesmer, J.J., Sunahara, R.K., Gilman, A.G. and Sprang, S.R. (1997) Crystal structure of the catalytic domains of adenylyl cyclase in a complex with G_{sa} ·GTP γ s. *Science*, **278**, 1907-1916.

- Tesmer, J.J., Sunahara, R.K., Johnson, R.A., Gosselin, G., Gilman, A.G. and Sprang, S.R. (1999) Two-metal-ion catalysis in adenylyl cyclase. *Science*, **285**, 756-760.
- Tews, I., Findeisen, F., Sinning, I., Schultz, A., Schultz, J.E. and Linder, J.U. (2005) The structure of a pH-sensing mycobacterial adenylyl cyclase holoenzyme. *Science*, **308**, 1020-1023.
- Towbin, H., Staehelin, T. and Gordon, J. (1979) Electrophoretic transfer of proteins from polyacrylamide gels to nitrocellulose sheets: procedure and some applications. *Proc Natl Acad Sci USA*, **76**, 4350-4354.
- Tucker, C.L., Hurley, J.H., Miller, T.R. and Hurley, J.B. (1998) Two amino acid substitutions convert a guanylyl cyclase, RetGC-1, into an adenylyl cyclase. *Proc Natl Acad Sci USA*, **95**, 5993-5997.
- Windsor, W.T., Walter, L.J., Syto, R., Fossetta, J., Cook, W.J., Nagabhushan, T.L. and Walter, M.R. (1996) Purification and crystallization of a complex between human interferon gamma receptor (extracellular domain) and human interferon gamma. *Proteins*, **26**, 108-114.
- Wolfgang, M.C., Lee, V.T., Gilmore, M.E. and Lory, S. (2003) Coordinate regulation of bacterial virulence genes by a novel adenylate cyclase-dependent signaling pathway. *Dev Cell*, **4**, 253-263.
- Yan, S.Z., Huang, Z.H., Shaw, R.S. and Tang, W.J. (1997) The conserved asparagine and arginine are essential for catalysis of mammalian adenylyl cyclase. *J Biol Chem*, **272**, 12342-12349.
- Zeibig, S. (2003) Klonierung und Charakterisierung einer Adenylatcyclase aus *Mycobacterium tuberculosis*. Diplomarbeit der Fakultät für Chemie und Pharmazie der Universität Tübingen.
- Zhang, G., Liu, Y., Ruoho, A.E. and Hurley, J.H. (1997) Structure of the adenylyl cyclase catalytic core. *Nature*, **386**, 247-253.
- Zhu, J. and Winans, S.C. (2001) The quorum-sensing transcriptional regulator TraR requires its cognate signalling ligand for protein folding, protease resistance, and dimerization. *Proc. Natl. Acad. Sci. USA*, **98**, 1507-1512.

Meine akademischen Lehrer neben Herrn Prof. Dr. J. E. Schultz waren die Damen und Herren:

Abdel-Bari, A.	Pharmazeutische Industrie, Kairo, Ägypten
Abdel-Kawi, M.	Phytochemie, Kairo, Ägypten
Asem, M.	Pharmazeutische Industrie, Kairo, Ägypten
Attia, A.	Phytochemie und Spektroskopie, Kairo, Ägypten
El-Hefnawi, M.	Phytochemie und Spektroskopie, Kairo, Ägypten
El-Khayal, M.	Pharmakologie, Kairo, Ägypten
El-Meligy, M.	Pharmazeutische Industrie, Kairo, Ägypten
El-Samaligy, M.	Pharmazeutische Industrie, Kairo, Ägypten
El-Shami, A.	Pharmakognosie, Kairo, Ägypten
El-Sherei, M.	Pharmakognosie, Kairo, Ägypten
Hagag, M.	Phytochemie, Kairo, Ägypten
Hamdy, A.	Biochemie, Kairo, Ägypten
Mansour, K.	Organische Chemie, Kairo, Ägypten
Rashwan, O.	Phytochemie, Kairo, Ägypten
Tawakul, M.	Analytische Chemie, Kairo, Ägypten
Teema, M.	Pharmazeutische Mikrobiologie, Kairo, Ägypten

Lebenslauf

Persönliche Daten

Name: Amira Ahmed Abdallah Abdel Motaal

Geburtstag: 09.04.1972

Geburtsort: Alexandria, Ägypten

Ausbildung

1978-1980 Grundschule, Kuwait

1980-1984 Grundschule, Abu-Dhabi

1984-1986 Gymnasium, Alexandria, Ägypten

1986-1989 Abitur, Kairo, Ägypten

1989-1994 Bachelor in Pharmazeutische Naturwissenschaften an der
Fakultät für Pharmazie, Kairo Universität

1994-2001 Assistent in der Abteilung Pharmakognosie der Universität Kairo
Master in Pharmazeutische Naturwissenschaften (Pharmakognosie)

2002-2004 DAAD Stipendiatin zur Promotion an der Fakultät für Chemie und
Pharmazie der Universität Tübingen

2004-2006 Wissenschaftliche Angestellte mit Gelegenheit zur Promotion an der
Fakultät für Chemie und Pharmazie der Universität Tübingen. Der
experimentelle Teil der vorliegenden Arbeit wurde zwischen Oktober 2002
und Juli 2005 unter der Leitung von Herrn Prof. Dr. J. E. Schultz angefertigt

Curriculum vitae

Personal data

Name: Amira Ahmed Abdallah Abdel Motaal
Date of birth: 09.04.1972
Place of birth: Alexandria, Egypt

1978-1981 Primary school, Kuwait
1980-1984 Primary school, Abu-Dhabi
1984-1986 Secondary school, Alexandria, Egypt
1986-1989 General secondary education certificate, Cairo, Egypt
1989-1994 Bachelor degree of Pharmaceutical Sciences, Faculty of Pharmacy,
Cairo University
1994-2001 Assistant in the Pharmacognosy Department, Cairo University
Master of Pharmaceutical Sciences (Pharmacognosy)
2002-2004 DAAD scholarship for PhD studies at the Faculty of Chemistry and
Pharmacy, Tübingen University
2002-2006 Scientific employee for the purpose of PhD studies at the Faculty of
Chemistry and Pharmacy, Tübingen University. The experimental part of this
work was carried out in the period from October 2002 till July 2005 under the
supervision of Prof. Dr. J. E. Schultz